Design of High-Rise Hotel

Building in Los Angeles, California, USA

(Capstone project II)

Bachelor of Engineering

(Civil and Environmental Engineering)

Aikelbet Zhumagulova

Aruzhan Syndarova

Assanali Aldan

Bexultan Bazarbayev

Nurmukhammed Mukhtarzhanov

Yelnur Nurgali

2025

Declaration

We hereby declare that this report entitled “Design of High-rise Hotel building in Riverside, California, USA” is the result of our own project work except for quotations and citations which have been duly acknowledged. We also declare that it has not been previously or concurrently submitted for any other degree at Nazarbayev University.

Aikelbet Zhumagulova

Aruzhan Syndarova

Assanali Aldan

Bexultan Bazarbayev

Nurmukhammed Mukhtarzhanov

Yelnur Nurgali

Acknowledgment

We would like to thank Professor Mert Guney for helping us develop the work and providing us with the necessary theoretical knowledge. Our deepest gratitude to Professors Dichuan Zhang, Abid Nadeem, Ferhat Karaca, Sung-Woo Moon, Alfrendo Satyanaga, and Chang-Seon Shon for their invaluable guidance and supervision throughout the capstone project.

Table of contents

List of Tables

List of Figures

1. Introduction

High-rise building construction presents unique challenges and opportunities in urban areas, particularly in creating vibrant spaces. This capstone project focuses on the design of a 15-storey hotel with two levels of underground parking, strategically located in the bustling

downtown area of Los Angeles at 1030 S Hill Street. Situated in a seismic zone, the project must adhere to high standards of safety, sustainability, and functionality.

The project aims to develop a structure that addresses the city's demand for premium hospitality services while offering innovative solutions for optimizing urban space utilization, implementing sustainable practices, and ensuring compliance with local and international building codes. The goal is to enhance the urban landscape by providing an extraordinary yet environmentally sensitive lodging experience, leveraging modern architectural and engineering principles.

This report covers architectural planning, structural and geotechnical design, environmental considerations, and construction management. It explores the complex interplay of technical, environmental, and financial factors, offering detailed design guidance for a high-performance, sustainable building that aligns with the Los Angeles environment. Key objectives of this project include

- Ensuring compliance with local regulations, seismic safety, and environmental standards
- Conducting geotechnical analysis for optimal design
- Blending seamlessly with Los Angeles's urban environment
- Utilizing sustainable, energy-efficient systems
- Managing costs to maximize efficiency and guest satisfaction
- Enhancing operational efficiency and promoting sustainable profitability.

2. Structural Part

2.1. Architectural Design

2.1.1. Overview of the building

The hotel facility stands at 15 stories tall and includes a two-story parking area beneath the ground floor at 1030 South Hill Street in downtown Los Angeles California USA. The building fulfills the criteria for high-rise classification in its seismic region. The building's lowest floor accommodates both the hotel lobby and restaurant areas and dining spaces and features kitchens together with laundry services. General and service elevators comprise seven lifts in the facility together with three staircases for building access. The accompanying image showcases a 3D model of the hotel. Each room of the first story reaches a height of 5 meters but the remaining rooms from second through fifteenth floors rise to 3.3 meters. This building implements design features from the IBC 2024 (International Building Code).

Figure 1. 3D Model of the building

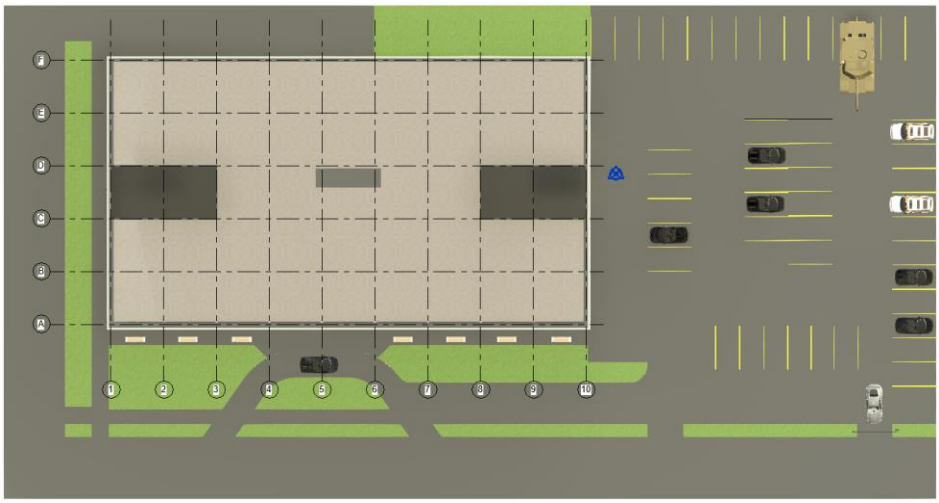

Figure 2. Site layout plan

2.1.2. Site selection

A building and commercial use history exists at this site from the beginning of the twentieth century. The site exists within an area undergoing redevelopment which manages to keep both contemporary buildings alongside historic architecture (Sharp, 2024). The location receives seamless sunlight from the south and southeast directions where shadows reach lengths near 0.75 meters while receiving 12 hours and 10 minutes of daily sunshine. The site gains natural ventilation due to Pacific Ocean breezes blowing from the southwest direction.

2.1.3. Design Conditions

Building is located in the high wind and seismic zone.

August serves as the hottest month for the site according to its seasonal patterns since summer highs rise to 38°C whereas January experiences the lowest temperatures at 2.5°C (US Department of Commerce, 2024). The site maintains a relative humidity of 60% which follows the standard climate range of 40-60% throughout the whole year in this area (Western Regional Climate Center, 2024). The area demonstrates a dry and warm environmental condition because it

fails to receive any snowfall throughout the year as documented by the US Department of Commerce in 2024. The soil environment supports durable construction since chloride levels remain at safe limits and the pH value is neutral thus minimizing corrosion risks (GeoPentech, 2024).

2.1.4. Building Dimensions

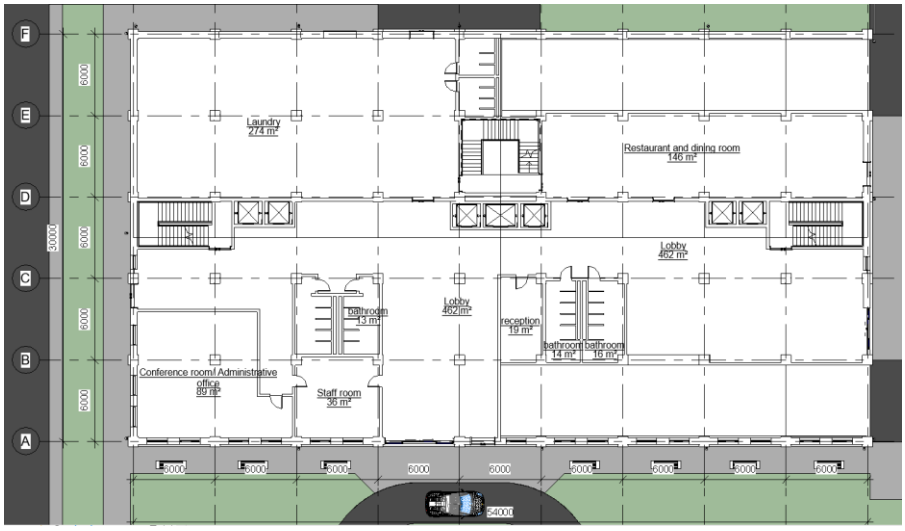

Figure 3. First floor layout

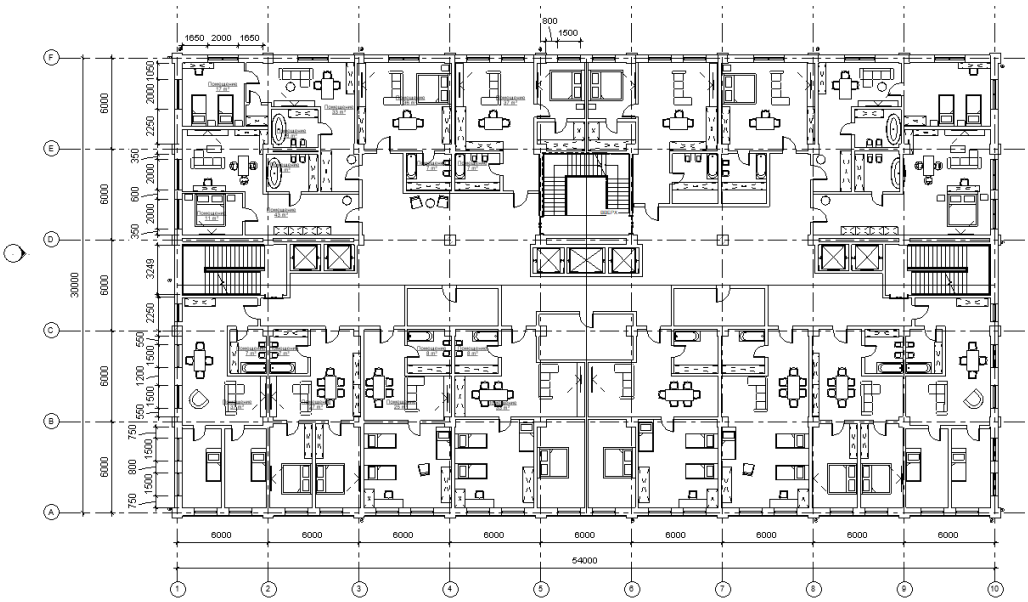

Figure 4. 2-15 floor layout

2.1.5. Non-structural members design

2.1.5.1 Ceiling

According to specifications the construction ceiling spans 135 mm with two specified layers as its foundation. Each piece of the mechanical duct allowance creates a thickness of 120 mm while distributing a pressure of 0.19 kN/m². The gypsum board layer adds a secondary weight of 0.008 kN/m² to the construction design through its 15 mm thickness. The structural and functional ceiling assembly combines multiple parts to achieve its complete design configuration.

2.1.5.2. Floor finishing

The residential building uses specifically chosen floor finishing materials across its corridors and apartment areas to achieve their purpose while taking advantage of current materials capabilities. The multi-layer flooring in corridors starts with a 19 mm thick quarry tiles as top cover layer which carries 1.1 kN/m² load capacity before descending to a 25 mm mortar bed then a 30 mm concrete fill finish layer after which is a 5 mm bituminous waterproofing layer finishes with a 13 mm fiberboard insulation layer. The residential apartment flooring has hardwood as its uppermost layer with 0.19 kN/m² load capacity followed by cinder concrete at 50 mm to create a flat surface then waterproofing by 5 mm single-ply before using polystyrene foam at 13 mm for insulation. The entire floor finishing throughout both sections measures 105 mm without counting the reinforced concrete slab.

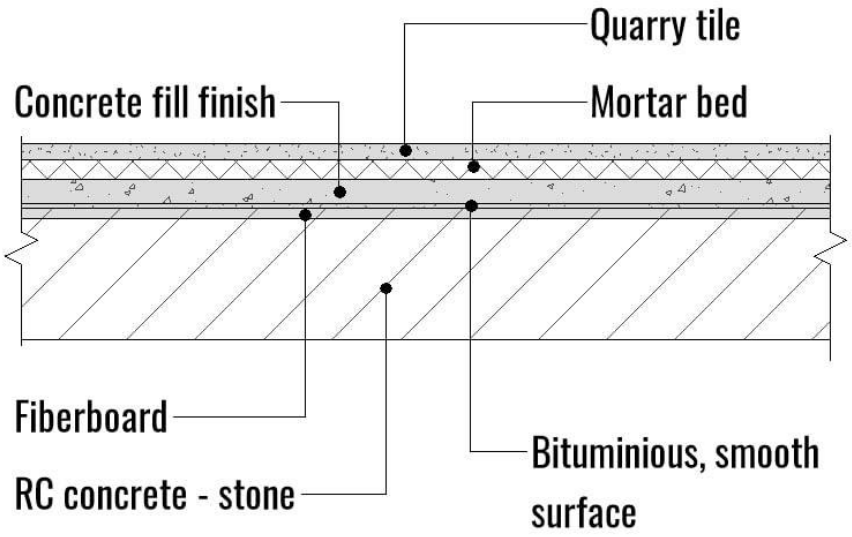

Figure 5. Floor sectional view

2.1.5.3.Partition and exterior walls

The structural layers of this building feature materials that build thermal efficiency alongside fire protection and increase wall resistance along exterior and interior walls. The building uses architectural precast panels to form its exterior walls since they deliver protection against weather elements and maintain durability. Both synthetic stucco and RBEC (EIFS) serve as exterior insulation materials that minimize thermal heat transmission. The installation of polyethylene vapor barrier membrane intercepts moisture and air while spray foam insulation ensures exceptional thermal insulation along with acoustic performance. The use of reinforced lightweight concrete stabilizes structures while fire-rated gypsum board enhances security against fires. Inside walls that divide apartments use lightweight steel frames to maintain structural integrity while fire-rated gypsum board along with spray foam act as effective insulation for heat distribution and noise reduction. The application of extra insulation layers improves acoustic capabilities. These materials work in combination to deliver walls that have excellent strength combined with energy conservation and fire resistance and sound insulation properties.

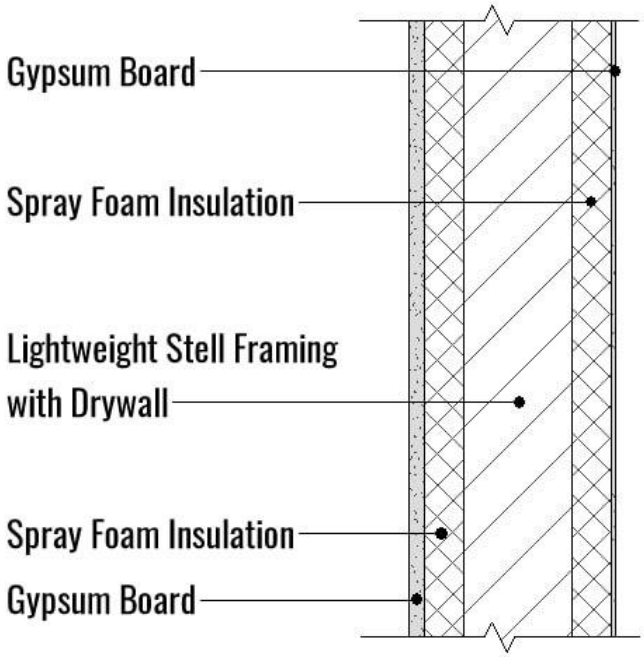

Figure 6. Interior walls section view

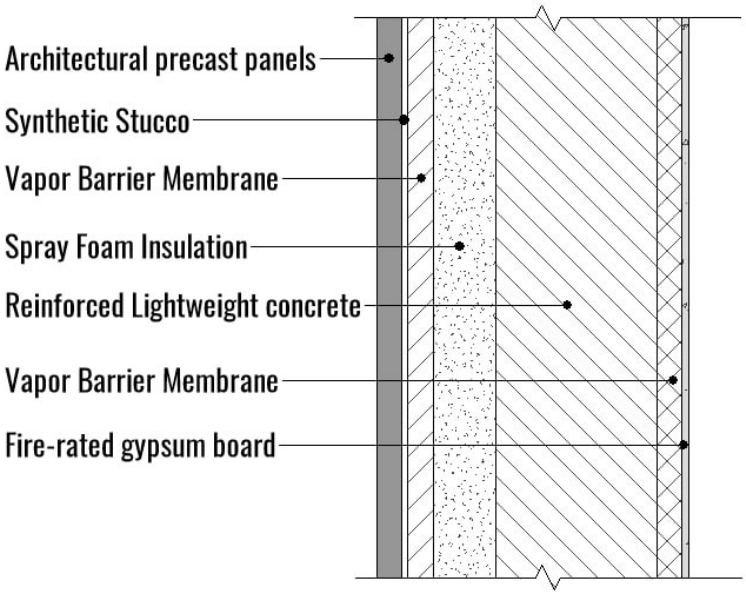

Figure 7. External walls section view

2.1.5.4. Parapets

AAC (Autoclaved Aerated Concrete) blocks form the roof level parapets because they possess excellent thermal properties and light weight density. The 250 mm thickness of AAC blocks creates effective heat insulation that contributes to building structural strength. The weight of each cubic meter AAC block amounts to 580 kg which makes the roof structure lighter and supports both adequate sturdiness and prolonged lifespan. The soundproofing characteristics together with fire resistance qualities of AAC allow it to excel in rooftop applications especially at fuse box locations for enhancing safety purposes.

2.1.5.5. Shaft for elevators

Seven elevators serve different purposes at our building with four fulfilling guest elevators and the other three serving laundry and housekeeping needs and meal delivery. The guest elevators have dimensions of 1549 x 1600 mm while the freight elevators employed for laundry and housekeeping and meal delivery are 2210 x 1600 mm wide. The elevator shafts for guest elevators measure 2032 x 1753 mm and freight elevators measure 2540 x 1753 mm to satisfy their different utility requirements.

2.1.6. Fire safety design

2.1.6.1. Evacuation routes

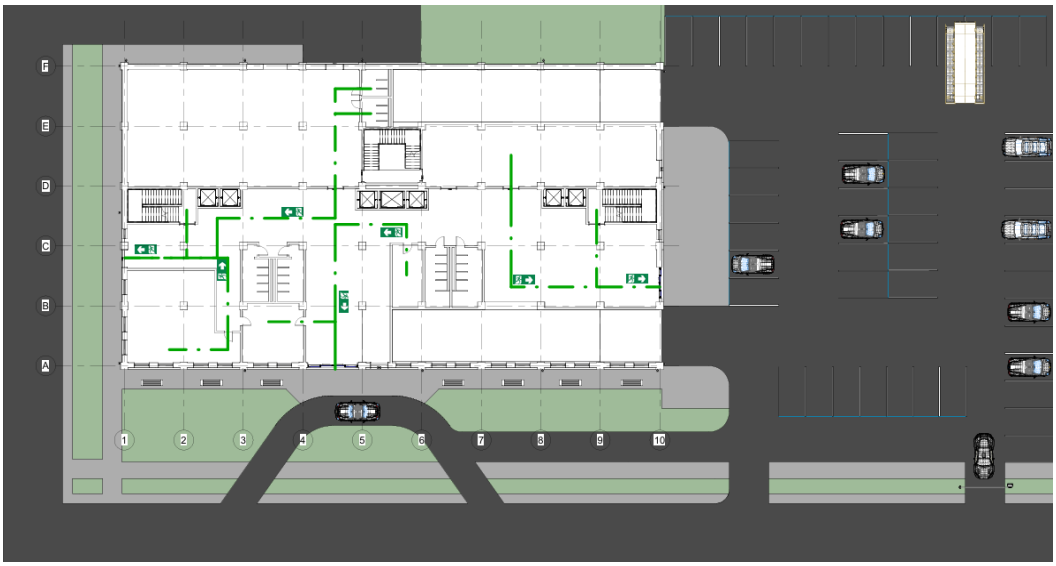

Figure 8. Emergency exit plan floor 1

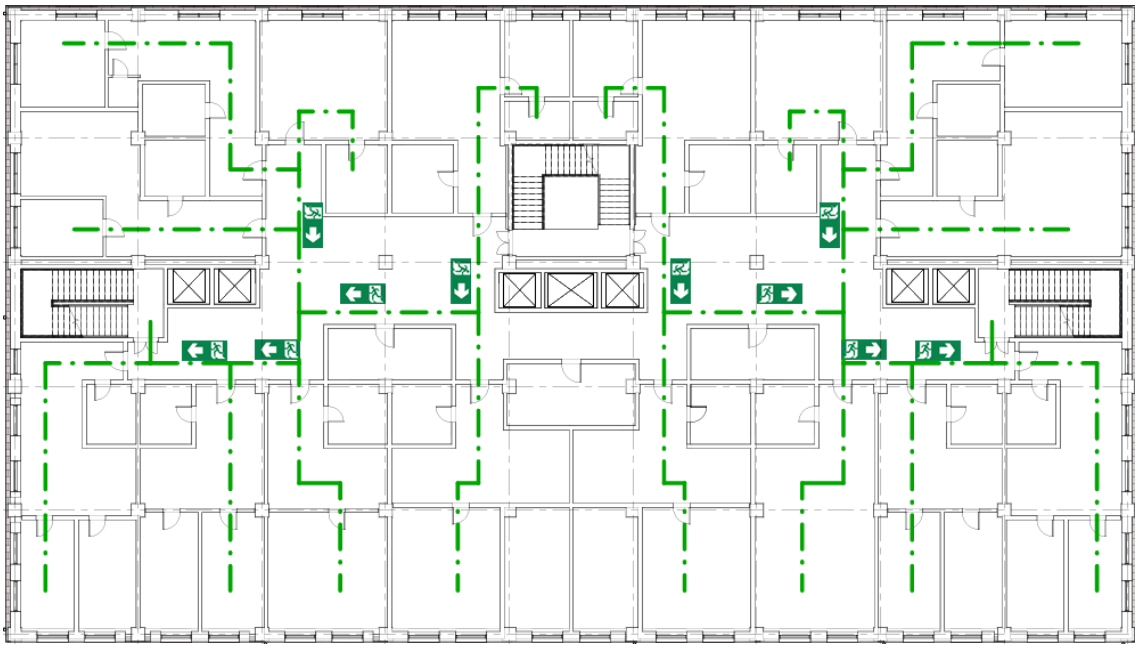

Figure 9. Emergency exit plan 2-15 floor

2.1.7. Parking and site layout

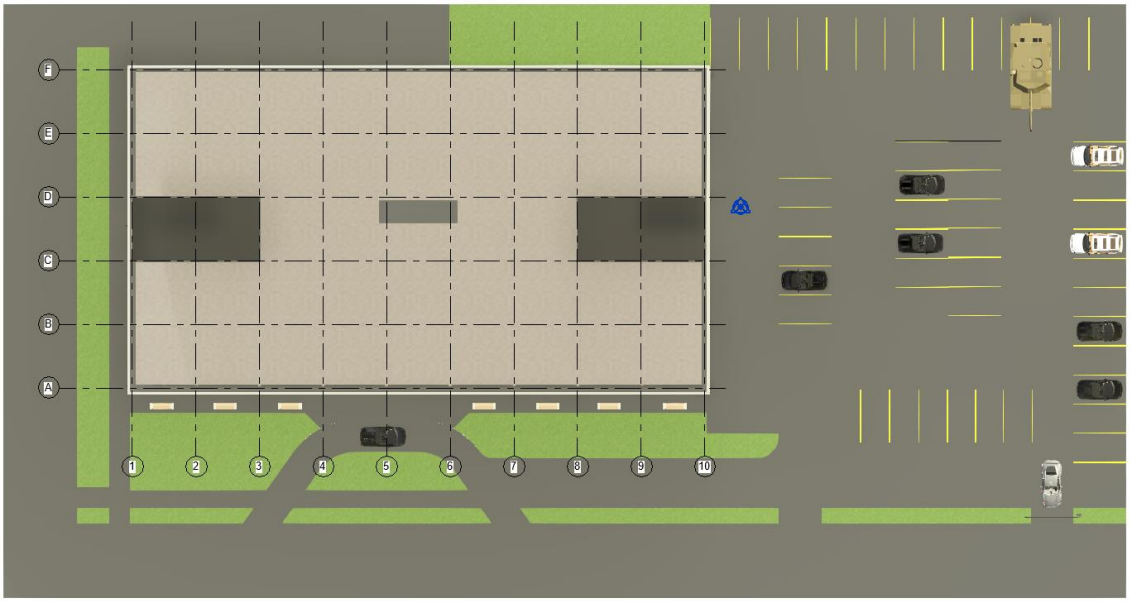

Figure 10. Parking and site layout

2.1.8 Concrete mixture

These concrete mixes were developed using the Life365 software to estimate how long each would last in real-world conditions. Each mix was designed with specific goals in mind—whether it's resisting chloride penetration, being environmentally friendly, or performing well in harsh marine environments. Here's a quick look at what each mix offers:

- **Mix A**: w/c ratio 0.36, fly ash 20%, silica fume 0%, slag 25%, corrosion inhibitor 5 L/m³
  Designed for long-term durability with high SCM content. Improves chloride resistance and lowers heat of hydration.

- **Mix B**: w/c ratio 0.35, fly ash 0%, silica fume 10%, slag 15%, corrosion inhibitor 7 L/m³
  Ideal for marine and bridge structures. Produces a dense, low-permeability matrix with high strength.
- **Mix C**: w/c ratio 0.37, fly ash 25%, silica fume 0%, slag 10%, no corrosion inhibitor, silane sealer applied
  Eco-friendly mix for inland use. Offers chloride protection via surface treatment instead of admixtures.
- **Mix D**: w/c ratio 0.36, fly ash 0%, silica fume 7%, slag 20%, corrosion inhibitor 5 L/m³
  Great for precast or vertical elements. Compact structure with strong resistance to water and chemicals.
- **Mix E**: w/c ratio 0.38, fly ash 15%, silica fume 0%, slag 15%, corrosion inhibitor 6 L/m³, membrane coating applied
  Balanced and practical mix for general infrastructure. Good workability and durability with surface protection.

Based on the software, the life cycle cost was also included. The following values of costs for materials were used:

- Concrete - $211/m3
- Black steel - $2/kg
- Membrane - $50/m2
- Sealer - $20/m2
- Inhibitor - $6.8/L
- Repair - $200/m2

The life cycle cost can be seen in the following Table 1.

Table 1. Total life cycle cost

Type of mixture	Construction cost, $	Barrier cost, $	Repair cost, $	Life-cycle cost, $
Base case	37565	7560	96004	141129
Mixture A	38944	7560	96004	142509
Mixture B	38944	4560	96004	139509
Mixture C	38944	0	96004	134949
Mixture D	38944	0	96004	92745

2.1.9. Service Life

Life Cycle Cost (LCC) report showed the service life of each mixture where the calculations were made and it can be seen in Table 2, where the Mixture C shows the most service life.

Table 2. Service Life

Type	Base case	Mixture A	Mixture B	Mixture C	Mixture D
Service life	60	80	61	151	42

2.1.10. Corrosion prevention

For corrosion protection of concrete the combination of smart materials with protective solutions succeeds in its implementation. Densifying concrete occurs through silica fume treatment at levels ranging from 5–10% while fly ash up to 30% reduces porosity and promotes chemical reactions with remaining compounds. The use of slag at dosages between 30 to 50 percent provides excellent protection against chemical sulfates while stopping alkali-silica reactions from expanding. The steel protection inside concrete structures improves through addition of Calcium Nitrite inhibitor at rates nearing 5 L/m^3. Surface sealing or coating becomes an added measure to prevent chloride ion penetration through concrete.

2.1.11. Leadership in Energy and Environmental Design (LEED)

Leadership in Energy and Environmental Design (LEED) functions as a system that evaluates building sustainability and environmental friendliness. The rating system evaluates building efficiency alongside water usage as well as environmental comfort and material sustainability decisions. Building sustainability aims at developing intelligent and eco-friendly structures which improve life for both residents and the environment.

This building received a total of 77 points out of 110 which demonstrates an excellent rating. The score's distribution makes the building potentially qualify for Platinum status with LEED Gold certification as the base category. The facility demonstrates mindful sustainable design while performing excellently regarding its energy conservation and water efficiency along with lowering its environmental footprint.

2.1.11.1. Location

The site location was specifically chosen because of its efficient access to the city's financial zone. The site has excellent walkability features because most people living there will work Downtown while maintaining quick access to public transit and bike route options. The eco-friendly transportation options boost the reduction of greenhouse gas emissions through vehicle usage reduction and support residents to walk routes under 5 to 10 minutes. The scoring information for this category appears in Figure 11.

Location and Transportation		**14**
Credit	LEED for Neighborhood Development Location	0
Credit	Sensitive Land Protection	1
Credit	High Priority Site and Equitable Development	2
Credit	Surrounding Density and Diverse Uses	4
Credit	Access to Quality Transit	4
Credit	Bicycle Facilities	1
Credit	Reduced Parking Footprint	1
Credit	Electric Vehicles	1

Figure 11. Location and Transportation score

2.1.11.2. Sustainable sites

Site examination of local natural regions together with biodiversity assessment formed a part of the team's analysis. Residents can access natural spaces throughout the property because of its designed open areas. The roof drainage system functioned as an efficient wet-weather management solution that supported urban water cycle operations in the city. Light pollution received attention because low-rise structures in the vicinity provide residents with unperturbed night sky and city views. This category rating appears in Figure 12.

Sustainable Sites		10
Prereq	Construction Activity Pollution Prevention	Required
Prereq	Environmental Site Assessment	Required
Credit	Site Assessment	1
Credit	Protect or Restore Habitat	1
Credit	Open Space	2
Credit	Rainwater Management	2
Credit	Heat Island Reduction	1
Credit	Light Pollution Reduction	1
Credit	Places of Respite	1
Credit	Direct Exterior Access	1

Figure 12. Sustainable Sites score

2.1.11.3. Water efficiency

LEED sets water efficiency as an essential requirement that applies to building water usage both indoors and out. The project must reduce its usage of drinking water for landscaping needs along with interior installations. The building officials will oversee the water management plan with residents following established water-saving policies in order to lower their water use while helping address water shortages. The project contains a water recycling system that retrieves gently used water from sinks as well as showers and washing machines. Local populations benefit from

the treated recycled water that can be employed either in plant irrigation and toilet flushing without depleting clean water resources. The points distributed for this category appear in Figure 13.

Water Efficiency		9
Prereq	Outdoor Water Use Reduction	Required
Prereq	Indoor Water Use Reduction	Required
Prereq	Building-Level Water Metering	Required
Credit	Outdoor Water Use Reduction	1
Credit	Indoor Water Use Reduction	5
Credit	Optimize Process Water Use	2
Credit	Water Metering	1

Figure 13. Water efficiency score

2.1.11.4. Energy & Atmosphere

Energy and Atmosphere		25
Prereq	Fundamental Commissioning and Verification	Required
Prereq	Minimum Energy Performance	Required
Prereq	Building-Level Energy Metering	Required
Prereq	Fundamental Refrigerant Management	Required
Credit	Enhanced Commissioning	4
Credit	Optimize Energy Performance	12
Credit	Advanced Energy Metering	1
Credit	Grid Harmonization	2
Credit	Renewable Energy	5
Credit	Enhanced Refrigerant Management	1

Figure 14. Energy and Atmosphere score

2.1.11.5. Materials & Resources

Materials and Resources		13
Prereq	Storage and Collection of Recyclables	Required
Prereq	PBT Source Reduction- Mercury	Required
Credit	Building Life-Cycle Impact Reduction	3
Credit	Environmental Product Declarations	1
Credit	Sourcing of Raw Materials	2
Credit	Material Ingredients	1
Credit	PBT Source Reduction- Mercury	1
Credit	PBT Source Reduction- Lead, Cadmium, and Copper	2
Credit	Furniture and Medical Furnishings	1
Credit	Design for Flexibility	1
Credit	Construction and Demolition Waste Management	1

Figure 15. Materials and Resources score

2.1.11.6. Indoor environmental quality

Indoor Environmental Quality		9
Prereq	Minimum Indoor Air Quality Performance	Required
Prereq	Environmental Tobacco Smoke Control	Required
Credit	Enhanced Indoor Air Quality Strategies	1
Credit	Low-Emitting Materials	1
Credit	Construction Indoor Air Quality Management Plan	1
Credit	Indoor Air Quality Assessment	1
Credit	Thermal Comfort	1
Credit	Interior Lighting	1
Credit	Daylight	1
Credit	Quality Views	1
Credit	Acoustic Performance	1

Figure 16. Indoor Environmental Quality

2.1.11.6. Innovation in Design

Innovation		5
Credit	Innovation	4
Credit	LEED Accredited Professional	1

Figure 17. Innovation score

2.1.11.7. Regional priority

Regional Priority		4
Credit	Regional Priority: Specific Credit	1
Credit	Regional Priority: Specific Credit	1
Credit	Regional Priority: Specific Credit	1
Credit	Regional Priority: Specific Credit	1

Figure 18. Regional priority score

2.2. Structural Design

2.2.1. Design Codes

The residential building design and analysis process followed U.S. standards through the utilization of the American Concrete Institute's "Building Code Requirements for Structural Concrete" (ACI 318-22) together with the American Society of Civil Engineers' "Minimum Design Loads and Associated Criteria for Buildings and Other Structures" (ASCE 7-16). These safety and performance regulations must be met by the structure according to both ACI 318-22 (ACI, 2022) and ASCE 7-16 (ASCE, 2016).

2.2.2. Loads summary

2.2.2.1. Dead loads

Total dead loads summary for structural and non-structural elements were calculated based on ASCE 7-16. Following table represents the dead loads.

Table 3. Summary of dead loads

	Column Load, kPa	Beam Load, kPa
Slab and Floor finishing	5.657	
Slab and Roof finishing	4.594	
Partition walls	2.429	
Exterior walls		38.141
Parapets	0.484	
Stairs	3.678	

2.2.2.2. Live loads

The design of live loads used the minimum requirements defined in ASCE 7-16 as the starting point. Adjustments of these loads depended on the specific type of structural component whether it was a corner, exterior or interior column.

Table 4. Summary of live loads

Floor	**Exterior L-Beam**	**Load, kN/m**
Floor 2-15	Private rooms and corridors serving them	1.92
First floor	Public rooms	4.79
	Corridors serving public rooms	4.79
	Ordinary flat roofs	0.96
	Stairs and exit ways	4.79

2.2.2.3. Snow loads

According to Figure 7.2-1 in ASCE 7-16 Los Angeles City falls outside the area where snow loads apply (ASCE, 2016). The analysis excluded snow loads because Figure 7.2-1 in ASCE 7-16 indicated Los Angeles City was not subject to such conditions (ASCE, 2016).

2.2.2.4. Wind loads

The analysis for wind loads followed the specifications of ASCE 7-16. The Section 3.3.2 of the Capstone I report contains comprehensive documentation for conducting the load computations. Torsional effects calculation procedures can be found within the Appendix of the identical report. The updated wind loads for each floor in its longitudinal and transverse orientations appear in Table 5.

Table 5. Summary of wind loads

	Longitudinal	**Transverse**
Story	**Wind load per frame, kN**	
15	55.02	8.74
14	21.89	17.36
13	21.64	17.12
12	21.38	16.87
11	21.11	16.61
10	20.82	16.33
9	20.52	16.04
8	20.19	15.73
7	19.84	15.39
6	19.46	15.02
5	19.04	14.62

4	18.58	14.18
3	18.06	13.68
2	17.46	13.10
1	16.74	12.75

2.2.2.5. Seismic loads

The analysis for wind loads followed the specifications of ASCE 7-16. The Section 3.3.2 of the Capstone I report contains comprehensive documentation for conducting the load computations. Torsional effects calculation procedures can be found within Appendix of the identical report. The updated wind loads for each floor in its longitudinal and transverse orientations appear in Table 7.

Table 6. Summary of seismic loads

Floors	**Longitudinal**	**Transverse**
Story	**Seismic load per frame, kN**	
15	736.74	147.35
14	284.53	170.72
13	256.54	153.92
12	229.59	137.75
11	205.87	123.52
10	183.05	109.83
9	161.08	96.65
8	139.95	83.97
7	119.66	71.80
6	100.26	60.15

5	80.30	48.18
4	63.13	37.88
3	45.73	27.44
2	31.96	19.17
1	18.99	11.39

2.2.3. SAP2000 calculations and development of analytical model

This section describes how SAP2000 was used to build the analytical model. It describes the setup procedure, including the materials utilized, the structures' form and arrangement, the boundary conditions used, and the unique properties of the various structural components. The next sections go into further depth about these factors.

2.2.3.1. Materials

The material that was used for the building was reinforced concrete. In the following table the properties of reinforced concrete is shown.

Table 7. Reinforced concrete properties

Material	□□□ (MPa)	ρ (□□/□^{3})	□□□ (MPa)	ν	□□□ (MPa)
Reinforced concrete	40	24.3	33185	0.2015	13810

2.2.3.2. Sections

In Table X. there are cracking moment of inertia written for each component of the building.

Table 8. Cracking moment of inertia factors of structural members

Component	**Cracking moment of inertia**

Beams	0.35
Slabs	0.7
Columns	0.25
Stairs	0.25

2.2.3.3. Elements and connections

Shell elements with mesh sizes of 1000 mm by 1000 mm or less were used to represent slabs in SAP2000 in order to precisely simulate how the building would respond to various stresses. Frame components were used to depict beams and columns. Furthermore, it was believed that the joints in the moment frame where beams and columns meet are securely attached, which means that they transfer moments without any flexibility.

2.2.3.4. Boundary conditions

To stop any rotation or movement, the base of the basement columns was designed with fixed supports. Both vertical and horizontal motions were prohibited at the locations where the building touches the ground, which is the connecting points between the basement and the first level. But because the model permitted rotation at these joints, the structure could react to lateral forces like wind or earthquakes in a realistic manner.

2.2.4. Structural analysis

2.2.4.1. Lateral drift analysis

2.2.4.1.1. Hand calculation of lateral drift under wind load

Table 9. Wind shear drift

Story	hi (mm)	hi-avg (mm)	Vi (kN)	Vi-col (kN)	Vavg (kN)	Ic,cr (mm^4)	Ib,cr (mm^4)	Ic-avg (mm^4)

16	3000	1500	15.42	1.54	0.77	7.56E+09	5.00E+09	3.78E+09
15	3000	3000	30.64	3.06	2.30	1.04E+10	5.00E+09	8.99E+09
14	3000	3000	45.64	4.56	3.81	1.04E+10	5.00E+09	1.04E+10
13	3000	3000	60.41	6.04	5.30	1.40E+10	5.00E+09	1.22E+10
12	3000	3000	74.95	7.49	6.77	1.40E+10	5.00E+09	1.40E+10
11	3000	3000	89.23	8.92	8.21	1.40E+10	5.00E+09	1.40E+10
10	3000	3000	103.25	10.32	9.62	1.40E+10	5.00E+09	1.40E+10
9	3000	3000	116.97	11.70	11.01	1.40E+10	5.00E+09	1.40E+10
8	3000	3000	130.39	13.04	12.37	1.40E+10	5.00E+09	1.40E+10
7	3000	3000	143.47	14.35	13.69	1.85E+10	5.00E+09	1.62E+10
6	3000	3000	156.18	15.62	14.98	1.85E+10	5.00E+09	1.85E+10
5	3000	3000	168.47	16.85	16.23	1.85E+10	5.00E+09	1.85E+10
4	3000	3000	180.29	18.03	17.44	2.39E+10	5.00E+09	2.12E+10
3	3000	3000	191.62	19.16	18.60	2.39E+10	5.00E+09	2.39E+10
2	3000	3000	202.71	20.27	19.72	3.05E+10	5.00E+09	2.72E+10
1	3300	3150	214.87	21.49	20.88	3.05E+10	5.00E+09	3.05E+10

Table 10. Continuation of Table 10

db(mm)	**dc (mm)**	**dt (mm)**	**Interstory (mm)**	**abs (mm)**
0.06	0.26	0.32	0.88	37.13

0.35	0.77	1.13	1.50	36.25
0.58	1.28	1.87	1.97	34.75
0.81	1.25	2.07	2.01	32.78
1.04	0.91	1.95	1.94	30.77
1.26	0.67	1.94	1.96	28.83
1.48	0.51	1.99	2.04	26.87
1.70	0.39	2.09	2.15	24.83
1.91	0.31	2.21	2.31	22.68
2.11	0.29	2.41	2.50	20.37
2.32	0.27	2.59	2.68	17.87
2.51	0.25	2.77	2.85	15.20
2.71	0.23	2.94	3.02	12.34
2.89	0.21	3.10	5.44	9.32
7.09	0.69	7.77	3.89	3.89

Table 11. Wind flexural drift

Story	**M (N-mm)**	**a=b (m)**	**A (mm^2)**	**fi**	**Dqi (rad)**	**qi (rad)**	**Interstory (mm)**	**Absolute (mm)**
16	4.63E+07	0.6	360000	2.67E-11	8.01E-08	3.74E-05	0.11	1.32
15	1.38E+08	0.65	422500	6.79E-11	2.04E-07	3.73E-05	0.11	1.21
14	2.75E+08	0.65	422500	1.35E-10	4.06E-07	3.71E-05	0.11	1.10
13	4.56E+08	0.7	490000	1.93E-10	5.80E-07	3.67E-05	0.11	0.99
12	6.81E+08	0.7	490000	2.89E-10	8.66E-07	3.61E-05	0.11	0.88
11	9.49E+08	0.7	490000	4.02E-10	1.21E-06	3.53E-05	0.11	0.77
10	1.26E+09	0.7	490000	5.33E-10	1.60E-06	3.41E-05	0.10	0.66

9	1.61E+09	0.7	490000	6.82E-10	2.05E-06	3.25E-05	0.10	0.56
8	2.00E+09	0.7	490000	8.48E-10	2.54E-06	3.04E-05	0.09	0.46
7	2.43E+09	0.75	562500	8.98E-10	2.69E-06	2.79E-05	0.08	0.37
6	2.90E+09	0.75	562500	1.07E-09	3.21E-06	2.52E-05	0.08	0.29
5	3.41E+09	0.75	562500	1.26E-09	3.77E-06	2.20E-05	0.07	0.21
4	3.95E+09	0.8	640000	1.28E-09	3.84E-06	1.82E-05	0.05	0.15
3	4.52E+09	0.8	640000	1.47E-09	4.40E-06	1.44E-05	0.04	0.09
2	5.13E+09	0.85	722500	1.47E-09	4.42E-06	9.96E-06	0.03	0.05
1	5.84E+09	0.85	722500	1.68E-09	5.54E-06	5.54E-06	0.02	0.02

Table 12. Shear drift on Frame G under wind load (transverse)

Story	**hi (mm)**	**hi-avg (mm)**	**Fi (kN)**	**Vi (kN)**	**Vi-col (kN)**	**Vavg (kN)**	**Ic,cr (mm^4)**	**Ib,cr (mm^4)**	**Ic-avg (mm^4)**
15	3300	3300	17.36	17.36	3.47	3.47	4.73E+08	1.89E+09	4.73E+08
14	3300	3300	17.12	34.48	6.90	5.18	4.73E+08	1.89E+09	4.73E+08
13	3300	3300	16.87	51.36	10.27	8.58	4.73E+08	1.89E+09	4.73E+08
12	3300	3300	16.61	67.97	13.59	11.93	8.75E+08	1.89E+09	6.74E+08
11	3300	3300	16.33	84.30	16.86	15.23	1.49E+09	1.89E+09	1.18E+09
10	3300	3300	16.04	100.34	20.07	18.46	2.39E+09	1.89E+09	1.94E+09
9	3300	3300	15.73	116.06	23.21	21.64	3.65E+09	1.89E+09	3.02E+09
8	3300	3300	15.39	131.45	26.29	24.75	5.34E+09	1.89E+09	4.49E+09
7	3300	3300	15.02	146.47	29.29	27.79	7.56E+09	1.89E+09	6.45E+09
6	3300	3300	14.62	161.10	32.22	30.76	7.56E+09	1.89E+09	7.56E+09
5	3300	3300	14.18	175.28	35.06	33.64	1.04E+10	1.89E+09	8.99E+09
4	3300	3300	13.68	188.95	37.79	36.42	1.04E+10	1.89E+09	1.04E+10
3	3300	3300	13.10	202.05	40.41	39.10	1.40E+10	1.89E+09	1.22E+10

2	3300	3300	12.75	214.80	42.96	41.69	1.40E+10	1.89E+09	1.40E+10
1	5000	4150	15.98	230.78	46.16	44.56	1.85E+10	1.89E+09	1.62E+10

Table 13. Continuation of Table 13

db(mm)	dc (mm)	dt	Interstory	abs
0.08	0.37	0.45	1.26	52.32
0.50	1.11	1.61	2.13	51.06
0.83	1.83	2.66	2.80	48.93
1.16	1.78	2.94	2.86	46.13
1.48	1.30	2.77	2.76	43.27
1.79	0.96	2.75	2.78	40.51
2.10	0.72	2.82	2.89	37.73
2.40	0.56	2.95	3.04	34.84
2.69	0.43	3.13	3.26	31.80
2.98	0.41	3.39	3.51	28.54
3.26	0.38	3.64	3.76	25.03
3.53	0.35	3.88	4.00	21.27
3.79	0.32	4.11	4.23	17.27
4.04	0.30	4.34	7.61	13.05
9.91	0.96	10.88	5.44	5.44

Table 14. Flexural drift on Frame G under wind load (transverse)

Story	M (N-mm)	a=b (m)	A (mm2)	fi	Dqi (rad)	qi (rad)	interstory (mm)	Absolute
15	5.73E+07	0.3	90000	1.47E-11	4.85E-08	8.22E-06	0.03	0.28
14	1.71E+08	0.3	90000	4.39E-11	1.45E-07	8.17E-06	0.03	0.25
13	3.41E+08	0.3	90000	8.73E-11	2.88E-07	8.03E-06	0.03	0.23
12	5.65E+08	0.35	122500	1.06E-10	3.51E-07	7.74E-06	0.03	0.20
11	8.43E+08	0.4	160000	1.22E-10	4.01E-07	7.39E-06	0.02	0.18
10	1.17E+09	0.45	202500	1.34E-10	4.41E-07	6.99E-06	0.02	0.15
9	1.56E+09	0.5	250000	1.44E-10	4.74E-07	6.55E-06	0.02	0.13
8	1.99E+09	0.55	302500	1.52E-10	5.01E-07	6.07E-06	0.02	0.11

7	2.47E+09	0.6	360000	1.59E-10	5.23E-07	5.57E-06	0.02	0.09
6	3.01E+09	0.6	360000	1.93E-10	6.36E-07	5.05E-06	0.02	0.07
5	3.58E+09	0.65	422500	1.96E-10	6.46E-07	4.41E-06	0.01	0.05
4	4.21E+09	0.65	422500	2.30E-10	7.58E-07	3.77E-06	0.01	0.04
3	4.87E+09	0.7	490000	2.30E-10	7.57E-07	3.01E-06	0.01	0.02
2	5.58E+09	0.7	490000	2.63E-10	8.68E-07	2.25E-06	0.01	0.01
1	6.74E+09	0.75	562500	2.76E-10	1.38E-06	1.38E-06	0.01	0.01

2.2.4.1.2. Hand calculation of lateral drift under seismic load

Calculation of drift analysis under seismic load was performed the same way as wind load. The results can be seen in the following Table 10.

Table 15. Shear drift on Frame G under Seismic Load (Long Side)

Story	hi (mm)	hi-avg (mm)	Fi (kN)	Vi (kN)	Vi-col (kN)	Vavg (kN)	Ic,cr (mm^4)	Ib,cr (mm^4)	Ic-avg (mm^4)
15	3300	1650	284.53	284.53	31.61	15.81	4.73E+08	1.89E+09	2.36E+08
14	3300	3300	256.54	541.07	60.12	45.87	4.73E+08	1.89E+09	4.73E+08
13	3300	3300	229.59	770.66	85.63	72.87	4.73E+08	1.89E+09	4.73E+08
12	3300	3300	205.87	976.53	108.50	97.07	8.75E+08	1.89E+09	6.74E+08
11	3300	3300	183.05	1159.57	128.84	118.67	1.49E+09	1.89E+09	1.18E+09
10	3300	3300	161.08	1320.65	146.74	137.79	2.39E+09	1.89E+09	1.94E+09
9	3300	3300	139.95	1460.59	162.29	154.51	3.65E+09	1.89E+09	3.02E+09
8	3300	3300	119.66	1580.26	175.58	168.94	5.34E+09	1.89E+09	4.49E+09
7	3300	3300	100.26	1680.52	186.72	181.15	7.56E+09	1.89E+09	6.45E+09
6	3300	3300	80.30	1760.81	195.65	191.18	7.56E+09	1.89E+09	7.56E+09
5	3300	3300	63.13	1823.94	202.66	199.15	1.04E+10	1.89E+09	8.99E+09
4	3300	3300	45.73	1869.67	207.74	205.20	1.04E+10	1.89E+09	1.04E+10
3	3300	3300	31.96	1901.62	211.29	209.52	1.40E+10	1.89E+09	1.22E+10
2	3300	3300	18.99	1920.61	213.40	212.35	1.40E+10	1.89E+09	1.40E+10
1	5000	4150	9.53	1930.15	214.46	213.93	1.85E+10	1.89E+09	1.62E+10

Table 16. Continuation of Table 16

db (mm)	dc (mm)	dt (mm)	Interstory (mm)	Absolute (mm)
0.38	3.37	3.75	10.87	328.12

4.45	9.78	14.23	18.41	317.25
7.06	15.54	22.60	23.26	298.84
9.41	14.51	23.92	22.76	275.58
11.50	10.09	21.60	21.05	252.82
13.35	7.15	20.50	20.32	231.78
14.98	5.16	20.13	20.15	211.46
16.37	3.79	20.16	20.27	191.31
17.56	2.83	20.39	20.73	171.04
18.53	2.55	21.08	21.31	150.31
19.30	2.23	21.53	21.70	129.00
19.89	1.99	21.87	21.95	107.30
20.31	1.73	22.03	22.07	85.34
20.58	1.53	22.11	37.16	63.27
47.60	4.62	52.22	26.11	26.11

Table 17. Flexural Drift on Frame G under Seismic Load (Long Side)

Story	**M (N-mm)**	**a=b (m)**	**A (mm2)**	**fi**	**Dqi (rad)**	**qi (rad)**	**Interstory (mm)**	**Absolute (mm)**
15	9.39E+08	0.3	90000	2.41E-10	7.94E-07	1.04E-04	0.34	3.39
14	2.72E+09	0.3	90000	6.98E-10	2.31E-06	1.03E-04	0.34	3.04
13	5.27E+09	0.3	90000	1.35E-09	4.46E-06	1.00E-04	0.33	2.71
12	8.49E+09	0.35	122500	1.60E-09	5.28E-06	9.60E-05	0.32	2.37
11	1.23E+10	0.4	160000	1.78E-09	5.86E-06	9.07E-05	0.30	2.06
10	1.67E+10	0.45	202500	1.90E-09	6.27E-06	8.48E-05	0.28	1.76
9	2.15E+10	0.5	250000	1.98E-09	6.55E-06	7.86E-05	0.26	1.48
8	2.67E+10	0.55	302500	2.04E-09	6.72E-06	7.20E-05	0.24	1.22
7	3.23E+10	0.6	360000	2.07E-09	6.82E-06	6.53E-05	0.22	0.98
6	3.81E+10	0.6	360000	2.44E-09	8.05E-06	5.85E-05	0.19	0.77
5	4.41E+10	0.65	422500	2.41E-09	7.94E-06	5.04E-05	0.17	0.57
4	5.03E+10	0.65	422500	2.74E-09	9.06E-06	4.25E-05	0.14	0.41
3	5.65E+10	0.7	490000	2.66E-09	8.78E-06	3.34E-05	0.11	0.27
2	6.29E+10	0.7	490000	2.96E-09	9.77E-06	2.46E-05	0.08	0.16
1	7.25E+10	0.75	562500	2.97E-09	1.49E-05	1.49E-05	0.07	0.07

Table 18. Shear Drift on Frame G under Seismic Load (Short Side)

Story	hi (mm)	hi-avg (mm)	Fi (kN)	Vi (kN)	Vi-col (kN)	Vavg (kN)	Ic,cr (mm^4)	Ib,cr (mm^4)	Ic-avg (mm^4)
15	3300	1650.00	170.72	170.72	34.14	17.07	4.73E+08	1.89E+09	2.36E+08
14	3300	3300.00	153.92	324.64	64.93	49.54	4.73E+08	1.89E+09	4.73E+08
13	3300	3300.00	137.75	462.39	92.48	78.70	4.73E+08	1.89E+09	4.73E+08
12	3300	3300.00	123.52	585.92	117.18	104.83	8.75E+08	1.89E+09	6.74E+08
11	3300	3300.00	109.83	695.74	139.15	128.17	1.49E+09	1.89E+09	1.18E+09
10	3300	3300.00	96.65	792.39	158.48	148.81	2.39E+09	1.89E+09	1.94E+09
9	3300	3300.00	83.97	876.36	175.27	166.87	3.65E+09	1.89E+09	3.02E+09
8	3300	3300.00	71.80	948.15	189.63	182.45	5.34E+09	1.89E+09	4.49E+09
7	3300	3300.00	60.15	1008.31	201.66	195.65	7.56E+09	1.89E+09	6.45E+09
6	3300	3300.00	48.18	1056.49	211.30	206.48	7.56E+09	1.89E+09	7.56E+09
5	3300	3300.00	37.88	1094.36	218.87	215.08	1.04E+10	1.89E+09	8.99E+09
4	3300	3300.00	27.44	1121.80	224.36	221.62	1.04E+10	1.89E+09	1.04E+10
3	3300	3300.00	19.17	1140.97	228.19	226.28	1.40E+10	1.89E+09	1.22E+10
2	3300	3300.00	11.39	1152.37	230.47	229.33	1.40E+10	1.89E+09	1.40E+10

1	5000	4150.00	5.72	1158.09	231.62	231.05	1.85E+10	1.89E+09	1.62E+10

Table 19. Continuation of Table 19

db (mm)	dc (mm)	dt (mm)	Interstory (mm)	Absolute (mm)
0.41	3.64	4.05	9.71	352.34
4.80	10.56	15.36	19.89	342.63
7.63	16.78	24.41	25.12	322.75
10.16	15.67	25.83	24.58	297.63
12.42	10.90	23.32	22.73	273.05
14.42	7.72	22.14	21.94	250.32
16.17	5.57	21.74	21.76	228.38
17.68	4.09	21.78	21.90	206.62
18.96	3.06	22.02	22.39	184.72
20.01	2.75	22.76	23.01	162.33
20.85	2.41	23.26	23.44	139.32
21.48	2.14	23.62	23.71	115.88
21.93	1.87	23.80	23.84	92.17
22.23	1.65	23.88	40.14	68.33
51.41	4.99	56.39	28.20	28.20

Table 20. Flexural Drift on Frame G under seismic Load (Short Side)

Story	M (N-mm)	a=b (m)	A (mm2)	fi	Dqi (rad)	qi (rad)	interstory (mm)	Absolute
15	5.63E+08	0.3	90000	1.44E-10	4.77E-07	6.21E-05	0.21	2.03
14	1.63E+09	0.3	90000	4.19E-10	1.38E-06	6.16E-05	0.20	1.83
13	3.16E+09	0.3	90000	8.10E-10	2.67E-06	6.03E-05	0.20	1.62
12	5.09E+09	0.35	122500	9.60E-10	3.17E-06	5.76E-05	0.19	1.42
11	7.39E+09	0.4	160000	1.07E-09	3.52E-06	5.44E-05	0.18	1.23
10	1.00E+10	0.45	202500	1.14E-09	3.76E-06	5.09E-05	0.17	1.05
9	1.29E+10	0.5	250000	1.19E-09	3.93E-06	4.71E-05	0.16	0.89
8	1.60E+10	0.55	302500	1.22E-09	4.03E-06	4.32E-05	0.14	0.73

7	1.94E+10	0.6	360000	1.24E-09	4.09E-06	3.92E-05	0.13	0.59
6	2.28E+10	0.6	360000	1.46E-09	4.83E-06	3.51E-05	0.12	0.46
5	2.65E+10	0.65	422500	1.44E-09	4.77E-06	3.03E-05	0.10	0.34
4	3.02E+10	0.65	422500	1.65E-09	5.43E-06	2.55E-05	0.08	0.24
3	3.39E+10	0.7	490000	1.60E-09	5.27E-06	2.01E-05	0.07	0.16
2	3.77E+10	0.7	490000	1.78E-09	5.86E-06	1.48E-05	0.05	0.09
1	4.35E+10	0.75	562500	1.78E-09	8.92E-06	8.92E-06	0.04	0.04

2.2.4.1.3. Comparison of lateral drifts between hand, 2D and 3D SAP calculations

As part of the analytical work SAP2000 was employed to generate 3D and 2D Frame G and 3 models for evaluating wind and seismic induced drift levels. According to ASCE (2016) each floor must operate independently as seismic resisting frames (ASCE, 2016). The maximum inelastic displacement ($\delta_{\square}$) was obtained by enhancing the inter-story seismic deflections through use of following equation:

$$\delta_{\square} = \frac{\square_{\square}\square_{\square\square}}{\square_{\square}} \qquad (2.1)$$

Where,

$\delta_{\square\square}$- interstory elastic deflection

$\square_{\square}$- deflection amplification factor

At the same time allowable story drift $\Delta_{\square} = 0.020h_{\square\square}$. Where $h_{\square\square}$is the height of the typical and first floors (3300 mm for 2-15 floors and 5000 mm for first floor). Allowable limit of deflection is 60 mm. In the following tables comparison between hand, 2D and 3D calculations can be seen.

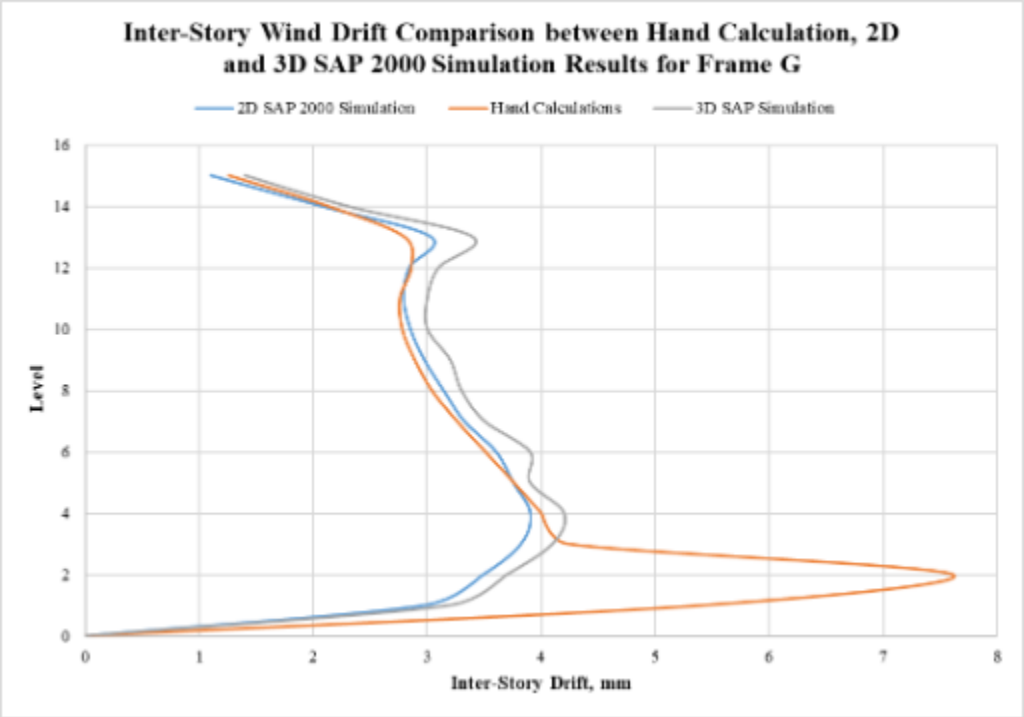

Figure 19. Comparison of hand, 2D and 3D calculations if interstory deflection under wind loads for frame G

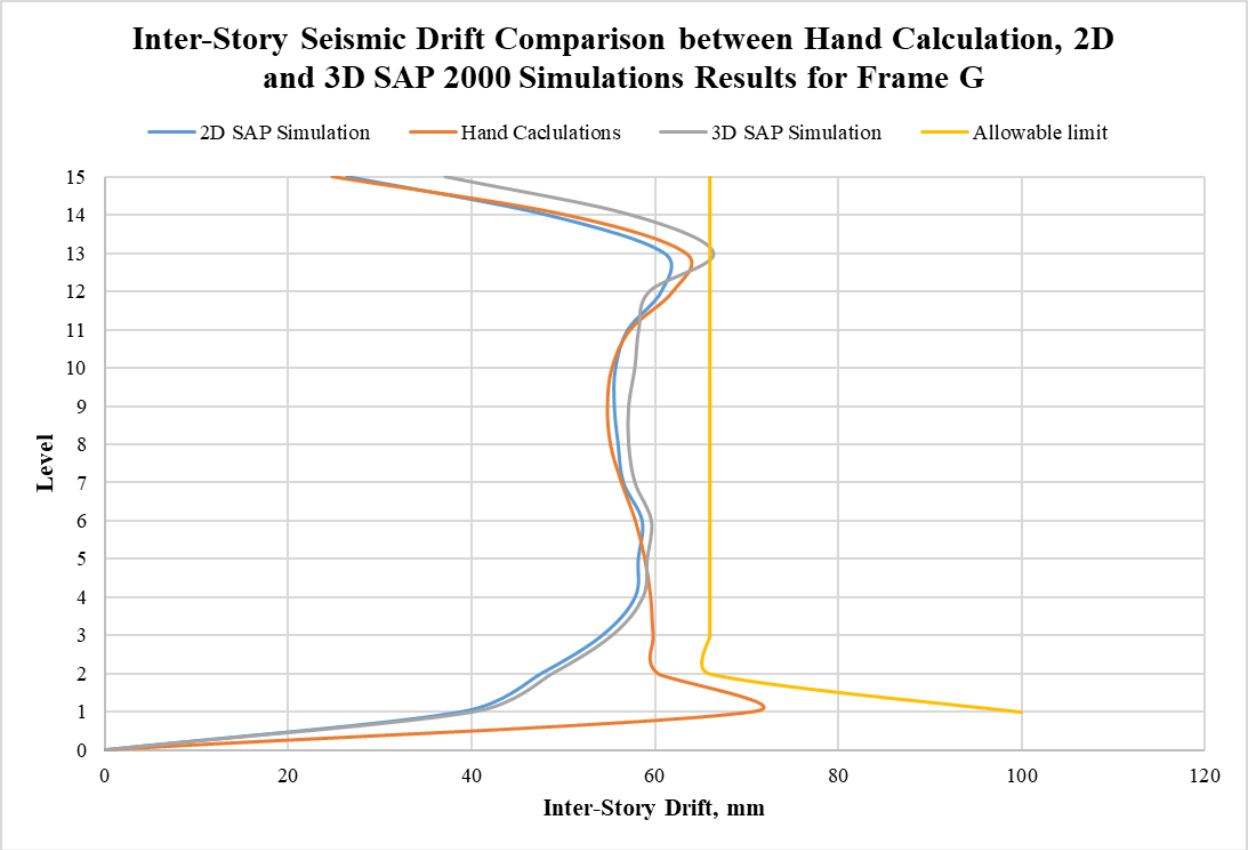

Figure 20. Comparison of hand, 2D and 3D calculations of amplified interstory deflection under seismic loads for frame G

The analysis of inter-story deflections for Frame 3 and Frame G, under both wind and seismic loads, shows that hand, 2D, and 3D methods usually give similar results, with some exceptions in the 3D models under wind loads (Figures 11 and 13). For both frames, the 3D calculations show bigger changes at the top floors. This suggests that the 3D model is picking up more complex behaviors that the simpler 2D and hand calculations don't catch. For seismic loads, all methods line up well and keep within safe limits (Figures 12 and 14), proving they are dependable. The differences observed in the 3D wind load analysis underline the impact of how loads are handled in the model and highlight the importance of carefully reviewing and interpreting these results to ensure the building's safety and functionality.

2.2.4.1.4. Stability analysis

It should be assessed whether the P-delta effects can be neglected in drift calculations by evaluating the stability coefficient (θ).

$$\theta = \frac{\square_{\square}\square\square_{\square}}{\square_{\square}h_{\square\square}\square_{\square}} \qquad (2.2)$$

where,

$\square_{\square}$ - total vertical design load (kN)

Δ - design story drift (mm)

$\square_{\square}$ - importance factor

$\square_{\square}$ - seismic shear force

2.2.4.2. Internal forces calculations

The results of calculated internal forces from SAP2000 on Frame 3 under different loading can be observed in the following Figures (?-?). Our critical loadings were chosen to be Dead and Wind loads.

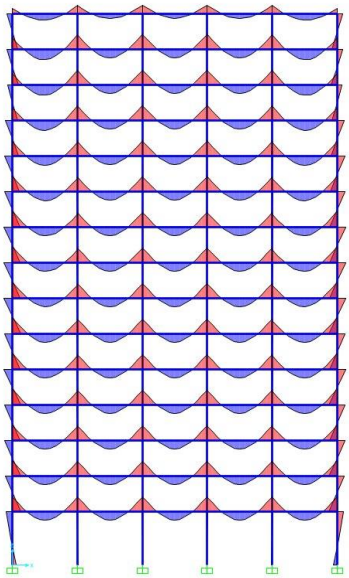

Figure 21. Moment force diagram under dead load in SAP2000

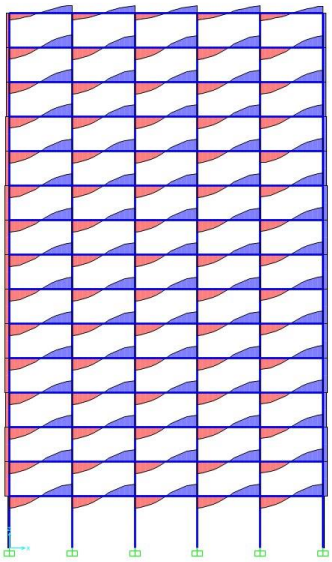

Figure 22. Shear force diagram under dead load in SAP2000

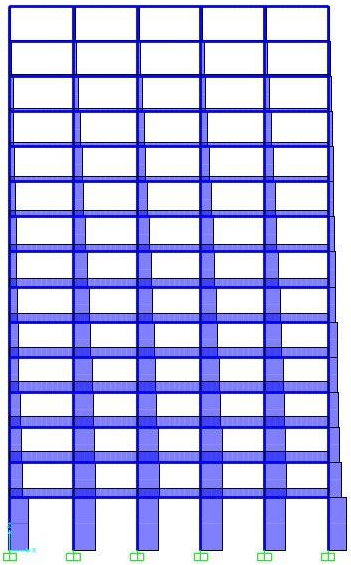

Figure 23. Shear force diagram under wind load in SAP2000

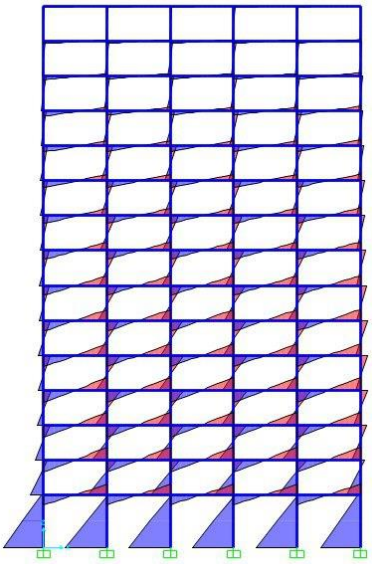

Figure 24. Moment diagram under wind load in SAP2000

Tables shear and moment for wind, live and seismic loads

2.2.4.2.1. Internal force verifications under Dead load

In order to calculate the internal forces under the dead load the approximate analysis of the structures. Inflection point was assumed to be 0.1 L.

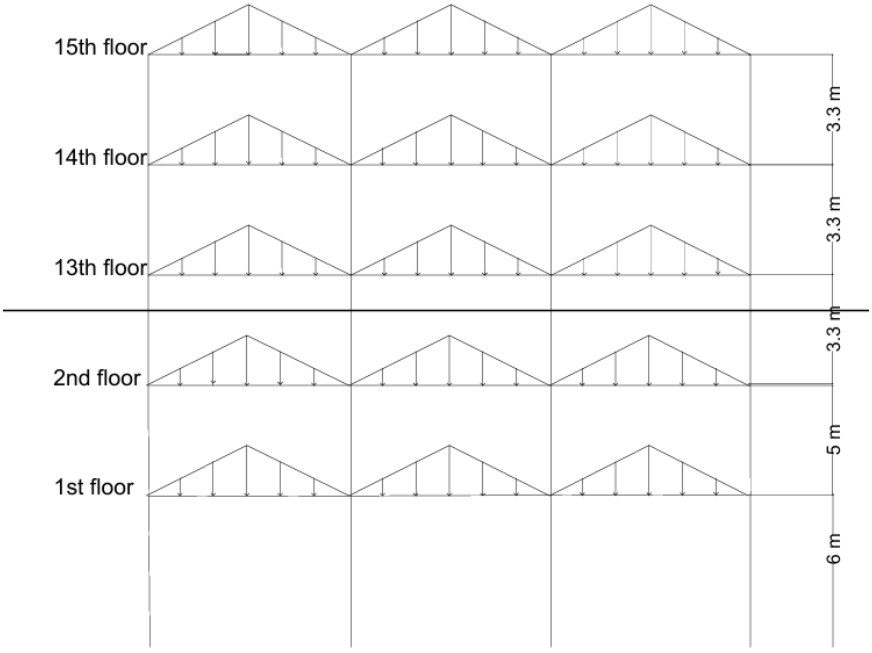

Figure 25. Loading arrangement for approximate analysis method

$$\square = 6\ \square, 0.1\square = 0.6\ \square, 0.8\square = 4.8\ \square$$

2.2.4.2.1.1. Floor dead load

$$\square = 29.28\ \square\square/\square \text{ (maximum distributed load)}$$

$$\square_2 = 29.28 * \frac{2.4}{5.4} = 13.01\ \square\square/\square$$

$$\square_2 = 13.01 * 0.8 * 0.6 + (29.28 - 13.01) * 0.4 * 0.6 = 101.51\ \square\square$$

$$\square_{\square\square\square\ (\square\square\square\square\square\square\square\square\ \square\square\square\square\square\square)} = 2.736 * \frac{101.51}{2} = 53.49\ \square\square$$

$$\square_{\square\square\square\ (\square\square\square\square\square\square\square\square\ \square\square\square\square\square\square)} = \frac{13.01 * 0.6}{2} + \frac{101.51}{2} = 54.66\ \square\square$$

$$\square_{\square\square\square} = \frac{29.28 * 6 * 6}{12} = 87.85\ \square\square - \square$$

$$□_{□□□} = \frac{29.28 * 5 * 6 * 6}{96} = 54.91\ □□ - □$$

Internal moments computed for floors 1 through 14 served as the foundation for the bending moment diagram (BMD). It's crucial to remember that all floors are 3.3 meters tall, with the first floor standing at 5 meters. This discrepancy necessitates recalculating the top and bottom moments on the first floor. The column stiffness for the first and second floors is unchanged, despite the fact that the equations already take flexural stiffness variations into account. Below are simplified formulas for this modification:

$$M_{top} = \frac{\frac{E_t I_t}{L_t}}{\frac{E_t I_t}{L_t} + \frac{E_b I_b}{L_b}} \cdot M = \frac{\frac{1}{L_t}}{\frac{1}{L_t} + \frac{1}{L_b}} \cdot M \qquad (2.3)$$

$$M_{bottom} = \frac{\frac{E_b I_b}{L_b}}{\frac{E_t I_t}{L_t} + \frac{E_b I_b}{L_b}} \cdot M = \frac{\frac{1}{L_b}}{\frac{1}{L_t} + \frac{1}{L_b}} \cdot M \qquad (2.4)$$

The calculations are done as follows:

$$□_{□□□} = \frac{\frac{1}{3.3}}{\frac{1}{3.3} + \frac{1}{5}} * 54.91 = 33.08\ □□ - □$$

$$□_{□□□} = \frac{\frac{1}{5}}{\frac{1}{3.3} + \frac{1}{5}} * 54.91 = 21.83\ □□ - □$$

2.2.4.2.1.2 Roof dead load

The calculations for roof dead load were implemented the same. However the maximum dead load is changed:

$$□ = 13.78\ □□/□$$

$$□_2 = 13.78 * \frac{2.4}{5.4} = 6.13\ □□/□$$

$$□_2 = 6.13 * 0.8 * 6 + (13.78 - 6.13) * 0.4 * 6 = 47.78\ □□$$

$$□_{□□□\ (□□□□□□□□\ □□□□□□)} = \frac{6.13 * 0.6}{2} + \frac{47.78}{2} = 25.73\ □□$$

$$□_{□□□\ (□□□□□□□□\ □□□□□□)} = 2.736 + \frac{47.78}{2} = 26.62\ □□$$

$$\square_{\square\square\square} = \frac{13.78 * 6 * 6}{12} = 41.35\ \square\square - \square$$

$$\square_{\square\square\square} = \frac{5 * 13.78 * 6 * 6}{96} = 25.84\ \square\square - \square$$

$$\square_{\square\square\square} = \frac{\frac{1}{3.3}}{\frac{1}{3.3} + \frac{1}{5}} * 25.84 = 15.57\ \square\square - \square$$

$$\square_{\square\square\square\square\square\square} = \frac{\frac{1}{5}}{\frac{1}{3.3} + \frac{1}{5}} * 25.84 = 10.27\ \square\square - \square$$

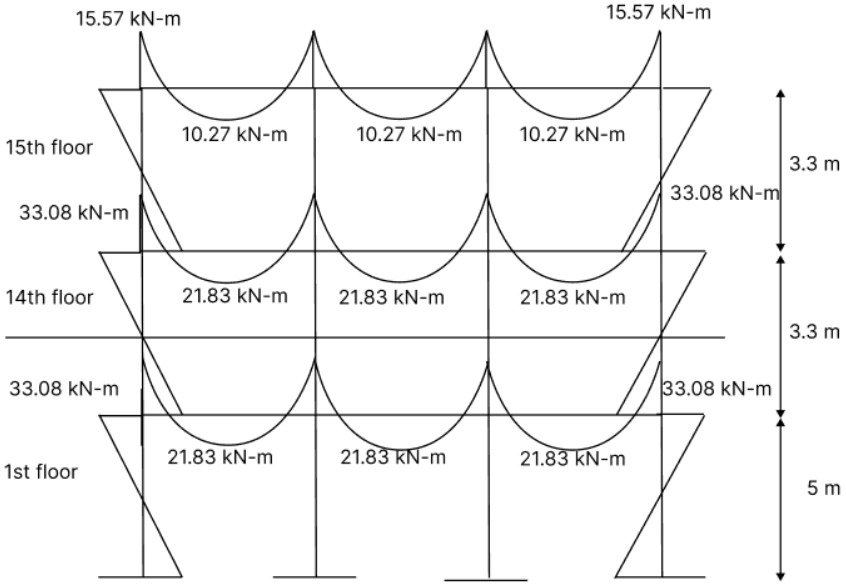

Figure 26. Moment frame diagram

In order to calculate the shear force diagram, following was used:

$$\square_{\square\square\square} = \frac{\square_{\square\square\square} + \square_{\square\square\square\square\square\square}}{h_{\square}} \qquad (2.5)$$

Figure 27. Shear force for one column

15th floor: □ $= \frac{15.57+10.27}{3.3} = 7.83$ □□

14th floor: □ $= \frac{33.08+21.83}{3.3} = 16.64$ □□

1st floor: □ $= \frac{33.08+21.83}{5} = 10.98$ □□

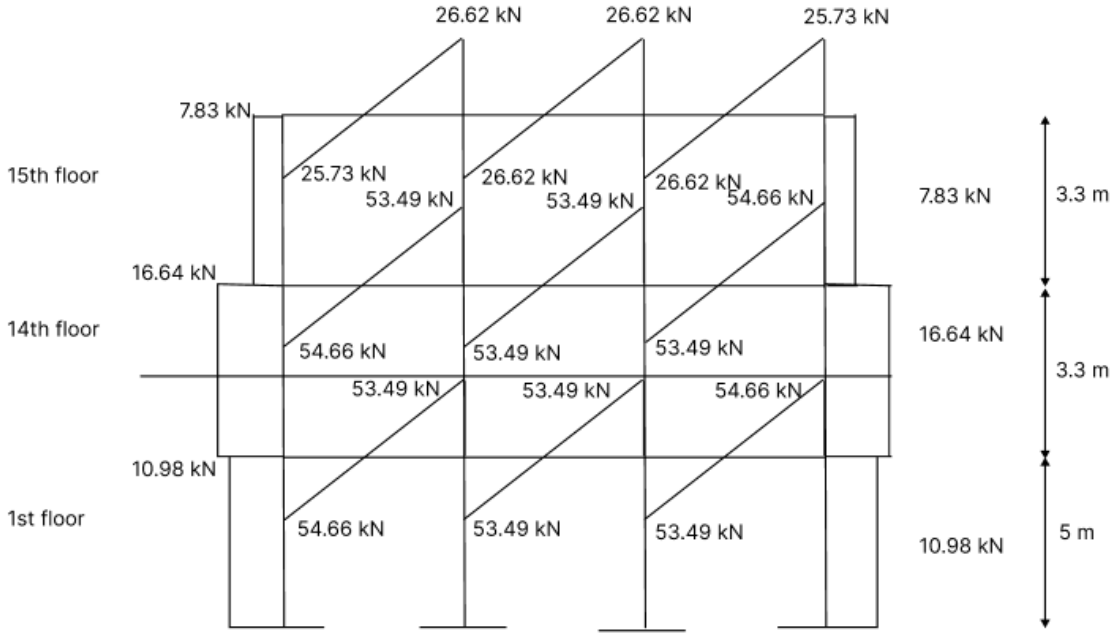

Figure 28. Shear force diagram

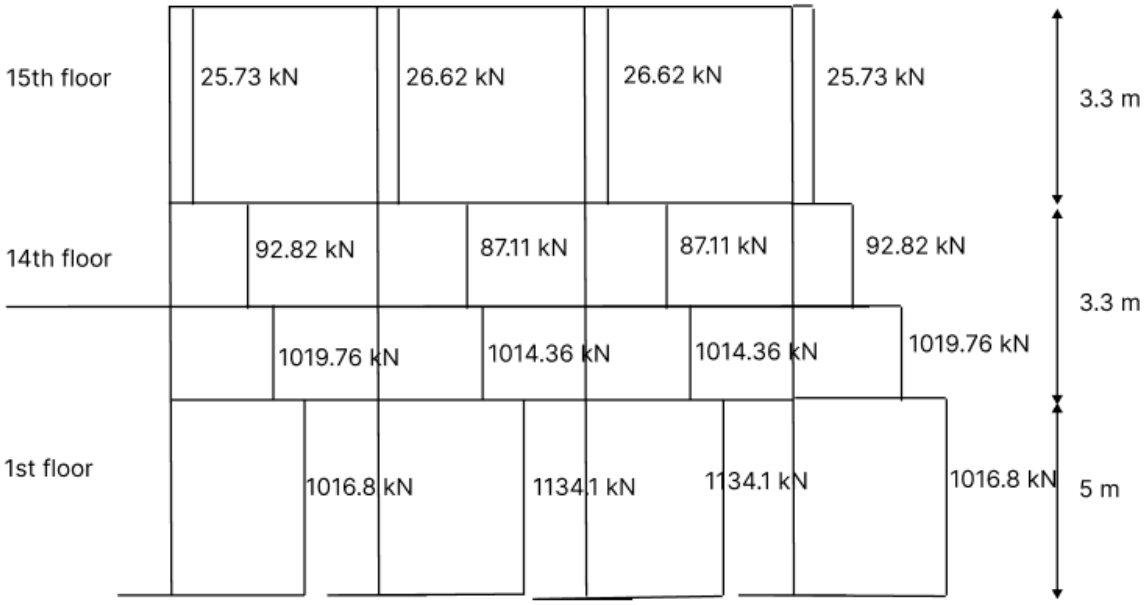

Figure 29. Axial force diagram

2.2.4.2.1.3. Internal forces verifications under Wind load

The internal forces for Frame 3 were determined using the Portal Frame Method, based on the following assumptions:

- A hinge is located at the middle of each beam (girder), as this point is assumed to have zero moment.
- A hinge is also placed at the middle of each column, assuming the moment at this point is zero.
- At any floor level, the shear force in the interior column is taken as twice the shear in each exterior column, because the frame is treated as a combination of portal structures.

The internal forces of Frame G were calculated for each of the floors. The result for all of the floors can be seen in Table 21.

Table 21. The hand calculations of the internal forces under wind load

	Internal Column			External Column		
Story	**Axial Force (kN)**	**Shear Force (kN)**	**Internal moment (kN-m)**	**Axial Force (kN)**	**Shear Force (kN)**	**Internal moment (kN-m)**
15	0.21	0.51	1.79	2.10	0.66	2.76
14	0.30	1.51	4.79	2.40	1.82	6.45
13	0.29	2.34	7.23	2.17	2.68	9.02
12	0.25	3.16	9.71	2.26	3.59	11.85
11	0.26	4.12	12.36	2.20	4.40	14.05
10	0.29	5.04	14.98	2.17	5.19	16.26
9	0.31	5.94	17.55	2.12	5.99	18.51
8	0.34	6.79	20.00	2.08	6.78	20.75
7	0.36	7.64	22.44	2.04	7.57	23.02
6	0.37	8.35	24.48	1.85	8.30	25.23
5	0.38	9.06	26.53	2.02	9.04	27.41
4	0.39	9.56	27.96	1.68	9.56	29.85
3	0.39	9.83	28.69	1.81	9.85	29.81
2	0.40	9.57	27.91	1.49	9.60	29.00
1	0.39	8.02	23.28	1.32	8.14	24.63

2.2.4.2.1.4. Comparison of internal forces between hand calculations and 2D and 3D

Figure X shows a comparison of the internal forces under dead load for Frame G using hand calculations, 2D analysis, and the 3D SAP2000 model. As seen in the figure, the axial and shear forces are nearly the same across all three methods. However, there are some slight differences in the bending moment values from the 3D SAP2000 model. This variation is likely

due to the influence of stiffness interactions between different structural elements in the 3D analysis.

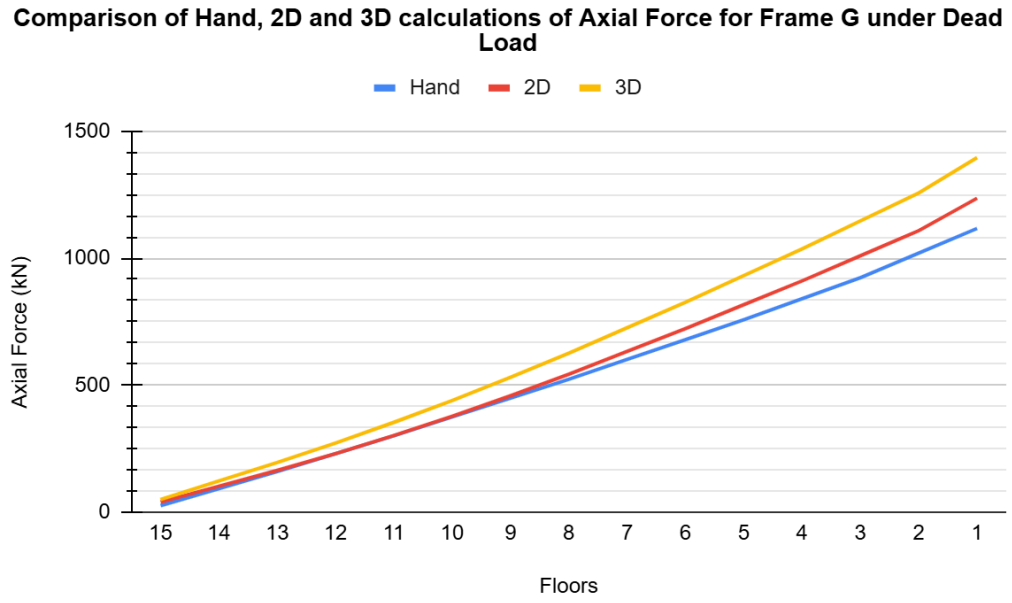

FIgure 30. Comparison of internal axial forces on Frame G under dead load

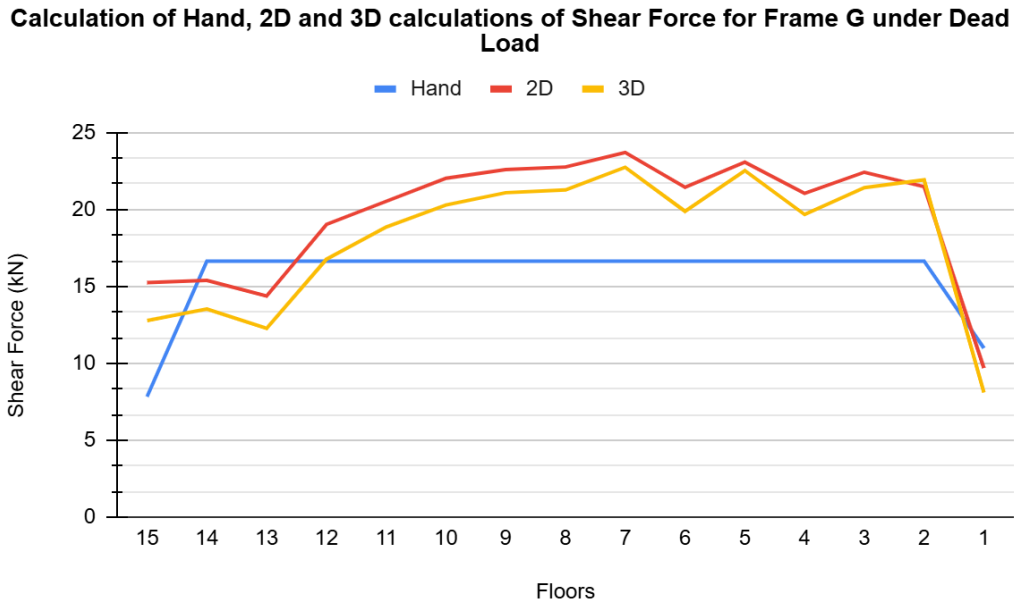

Figure 31. Comparison of internal shear forces on Frame G under dead load

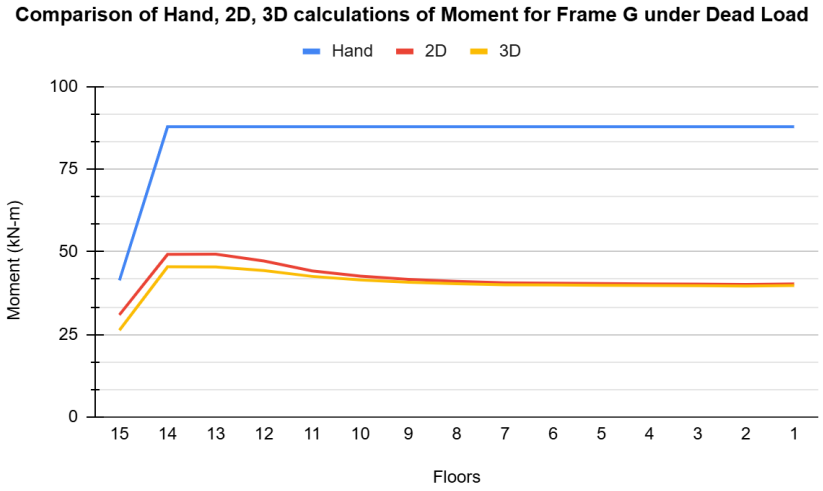

Figure 32. Comparison of internal forces of moment on Frame G under dead load

Likewise, the comparison of internal forces under wind load for Frame 3 is shown in Figure 33-35. As seen in the figure, the axial and shear force diagrams from the hand calculations, 2D, and 3D models are consistent with each other. However, there are some differences in the bending moment diagram on the lower floors for the hand calculations. This is mainly because an approximate analysis method was used to estimate the internal forces manually.

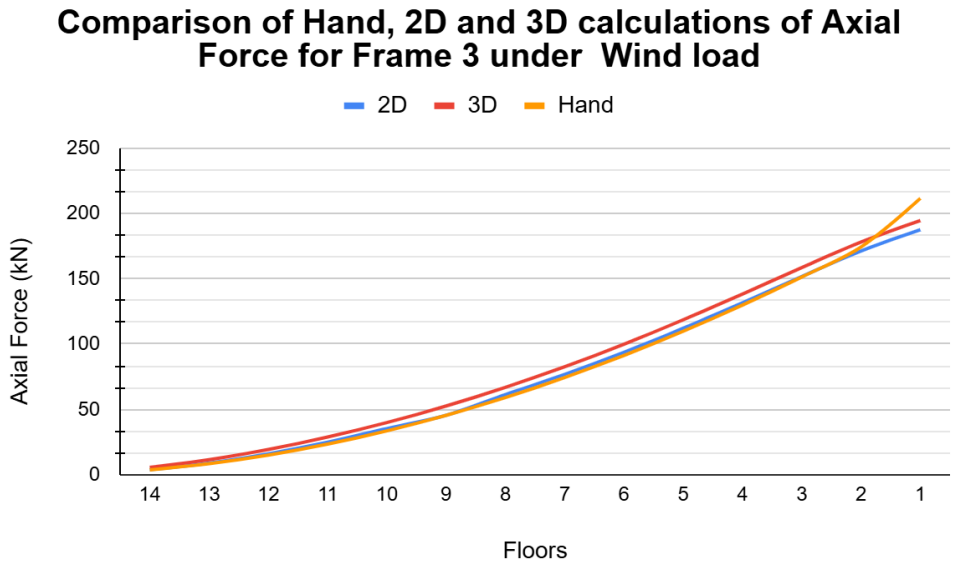

Figure 33. Comparison of internal axial forces on Frame 3 under Wind load

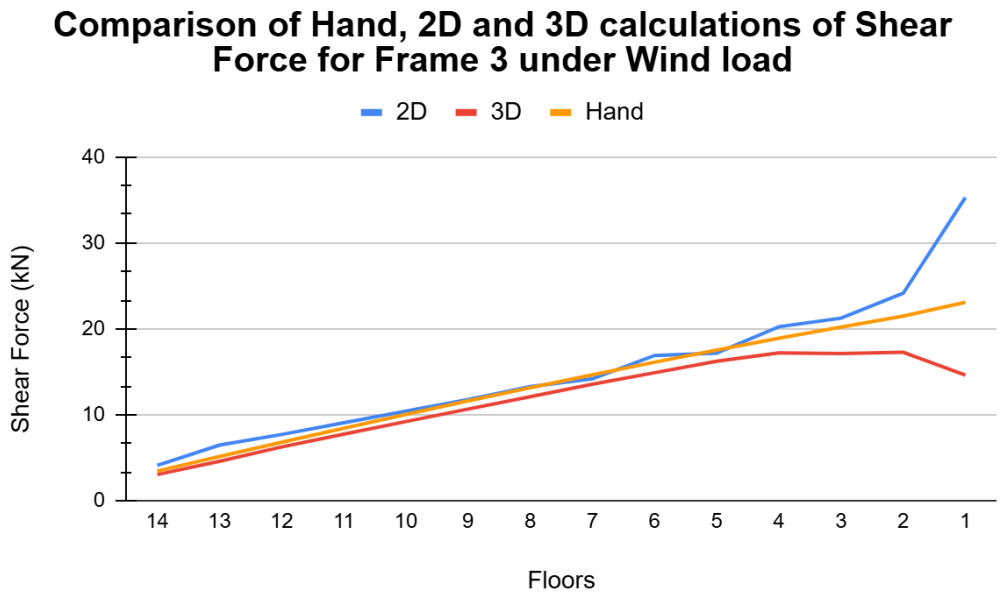

Figure 34. Comparison of internal shear forces on Frame 3 under Wind load

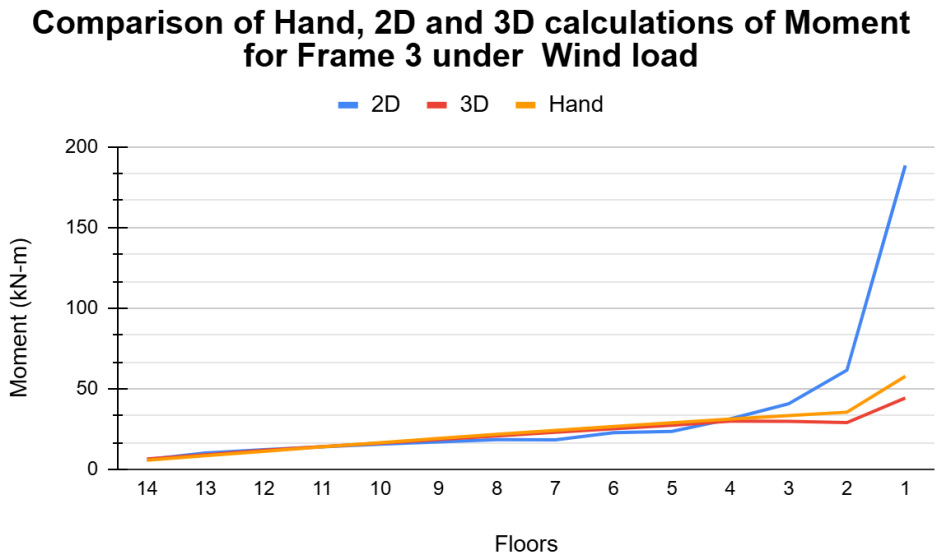

Figure 35. Comparison of internal forces on moment on Frame 3 under Wind load

2.2.4.2.2. Load combinations

The load combinations were chosen according to the Chapter 2 of ASCE 7-16. Combination includes wind, dead, live, seismic and roof live loads. All 4 cases for wind loads were considered. During the analysis it was found that 1.2D+1.6L+1□□ is the critical combination. In the following Figure X, there are load combinations that were applied.

3	1.2D+1.6L+0.5Lr	Combination
3	1.2D+1.6L+0.5Lr	Combination
3	1.2D+1.6L	Combination
3	1.2D+1.6L	Combination
3	1.2D+1L-1Ex	Combination
3	1.2D+1L+1Ex	Combination
3	1.2D+1.6L+0.5Lr	Combination
3	1.2D+1.6L+0.5Lr	Combination
3	1.2D+1.6L	Combination
3	1.2D+1.6L	Combination
3	1.2D+1L-1Ex	Combination
3	1.2D+1L+1Ex	Combination
3	1.2D+1L+1W	Combination
3	1.2D+1L+1W(8)	Combination
3	1.2D+1L+1W(12)	Combination

Figure 36. Load combinations

2.2.5. Structural design

2.2.5.1. Structural design using SAP2000 software

The structural design of the building was done using SAP2000. This software can automatically run the analysis and calculate the required reinforcement percentages for each structural element based on the ACI 318 code for reinforced concrete. In this project, SAP2000's features were used to carry out the design, and the results were later checked using hand calculations.

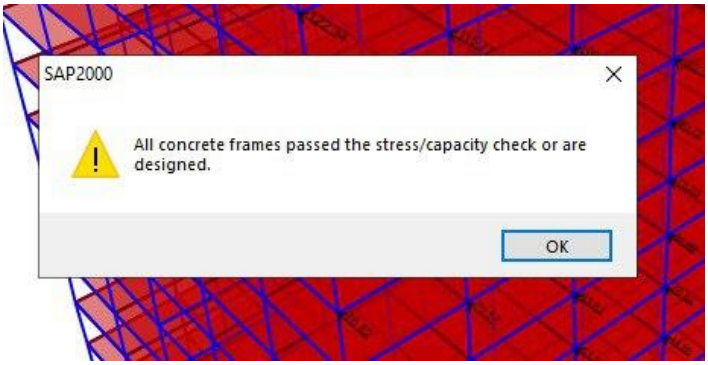

Figure 37. The structural design check in SAP2000

2.2.5.1.1. Major beams

For designing the main beams, the most critical positive and negative moments were considered. Since the building is exposed to significant earthquake forces, it is assumed that seismic loads mainly control the structural design. As a result, both positive and negative moments were taken from the critical load combinations.

Because of the horizontal earthquake forces, the most critical moments tend to occur at the ends of the beams. Therefore, the bottom reinforcement is designed to run continuously based on the critical positive moment at the beam ends, while the top reinforcement is placed at the edges to resist the negative moment.

Figure 38 shows the design details for a major beam at the edge where the critical negative moment occurs.

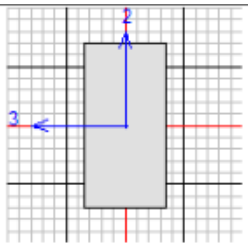

Units KN, m, C

ACI 318-14 BEAM SECTION DESIGN Type:Sway Special Units: KN, m, C (Summary)

Element	: 1775	D=0.600	B=0.300	bf=0.300
Section ID	: Major Beam	ds=0.000	dct=0.060	dcb=0.060
Combo ID	: COMB5	E=24855578.1	fc=27579.032	Lt.Wt. Fac.=1.000
Station Loc	: 6.000	L=6.000	fy=420000.000	fys=420000.000

Phi(Bending):	0.900
Phi(Shear):	0.750
Phi(Seis Shear):	0.600
Phi(Torsion):	0.750

Design Moments, M3

	Positive Moment	Negative Moment	Special +Moment	Special -Moment
	262.441	-524.882	262.441	-524.882

Flexural Reinforcement for Moment, M3

	Required Rebar	+Moment Rebar	-Moment Rebar	Minimum Rebar
Top (+2 Axis)	0.003	0.000	0.003	5.319E-04
Bottom (-2 Axis)	0.001	0.001	1.771E-04	5.319E-04

Shear Reinforcement for Shear, V2

Rebar Av/s	Shear Vu	Shear phi*Vc	Shear phi*Vs	Shear Vp
0.002	317.086	0.000	317.086	166.814

Reinforcement for Torsion, T

Rebar At/s	Rebar Al	Torsion Tu	Critical Phi*Tcr	Area Ao	Perimeter Ph
0.000	0.000	1.916	23.524	0.092	1.444

Figure 38. Design of major beam

2.2.5.1.2. Columns

The design of the of the column can be seen in the following Figure X

Units KN, mm, C

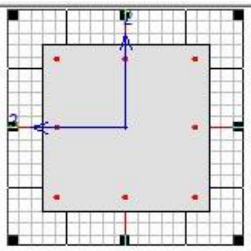

ACI 318-14 COLUMN SECTION DESIGN Type: Sway Special Units: KN, mm, C (Summary)

Element : 235	B=750.000	D=750.000	dc=64.000
Section ID : Column 1st floor	E=29.725	fc=0.040	Lt.Wt. Fac.=1.000
Combo ID : COMB5	L=5000.000	fy=0.420	fys=0.420
Station Loc : 5000.000	RLLF=1.000		

Phi(Compression-Spiral):	0.750	Overstrength Factor:	1.25
Phi(Compression-Tied):	0.650		
Phi(Tension Controlled):	0.900		
Phi(Shear):	0.750		
Phi(Seismic Shear):	0.600		
Phi(Joint Shear):	0.850		

AXIAL FORCE & BIAXIAL MOMENT DESIGN FOR PU, M2, M3

Rebar Area	Design Pu	Design M2	Design M3	Minimum M2	Minimum M3
24684.136	14484.725	16841.877	546653.511	546653.511	546653.511

AXIAL FORCE & BIAXIAL MOMENT FACTORS

	Cm Factor	Delta_ns Factor	Delta_s Factor	K Factor	L Length
Major Bending(M3)	0.601	1.000	1.000	1.000	5000.000
Minor Bending(M2)	0.606	1.000	1.000	1.000	5000.000

SHEAR DESIGN FOR V2,V3

	Rebar Av/s	Shear Vu	Shear phi*Vc	Shear phi*Vs	Shear Vp
Major Shear(V2)	0.000	167.662	1162.132	0.000	167.662
Minor Shear(V3)	0.000	262.738	1162.132	0.000	262.738

JOINT SHEAR DESIGN

	Joint Shear Ratio	Shear VuTop	Shear VuTot	Shear phi*Vc	Joint Area
Major Shear(V2)	N/A	N/A	N/A	N/A	N/A
Minor Shear(V3)	N/A	N/A	N/A	N/A	N/A

(6/5) BEAM/COLUMN CAPACITY RATIOS

Major Ratio	Minor Ratio
N/A	N/A

Notes:
- N/A: Not Applicable
- N/C: Not Calculated
- N/N: Not Needed

Figure 39. Design of the column

2.2.5.2. Hand calculation verification for structural members design

2.2.5.2.1. Major beams

2.2.5.2.1.1. *Flexural analysis*

To check the reinforcement provided by SAP2000 for the major beam shown in Figure X.X, manual calculations were carried out. In the selected frame, the negative moment was found to be critical, meaning the top reinforcement at the beam edges (tension zone) was the main focus. For the beam in Figure X.X, the critical positive moment was used to design the bottom reinforcement. It's important to mention that compression reinforcement at mid-span was not considered. The design was also assumed to be tension-controlled, so a strength reduction factor of $\phi = 0.75$ was used.

Negative moment

$$\square_{\square} = 524.88\ \square\square - \square$$

$$\square = 300\ \square\square, h = 600\ \square\square, \square = 600 - 2.5\ \square\square * 24\square\square/\square\square = 536.5\ \square\square$$

$$\square'_{\square} = 40\ \square\square\square\ (5801\ \square\square\square), \square_{\square} = 413\ \square\square\square$$

$$\square_{\square} = \frac{\square_{\square}}{\square\square\square^2} = \frac{528.88}{0.9*300*536.5} = 6078.6\ \square\square/\square^2 \qquad (2.6)$$

$$\rho = \frac{0.85\square'_{\square}}{\square_{\square}}\left[1 - \sqrt{1 - \frac{2\square_{\square}}{0.85\square'_{\square}}}\right] = 0.01634 \qquad (2.7)$$

$$\square_{\square} = \square\square\square = 0.01634 * 300 * 536.5 = 2630\ \square\square^2$$

$$\square_{\square}\square_{\square} = 0.85\square'_{\square}\square\square \Rightarrow\ \square = 106.48\ \square\square$$

$$\beta_1 = 0.85 - 0.05(\frac{5801 - 4000}{1000}) = 0.76$$

$$\square = \frac{\square}{\square} = \frac{106.48}{0.76} = 140.12\ \square\square$$

$$\varepsilon_\square = 0.003(\frac{\square - \square}{\square}) = 0.003(\frac{536.5 - 140.1}{140.1}) = 0.0084 > 0.005 \text{ (tension-controlled)}$$

$\square_\square$ calculated by SAP2000 is 3049.36 $\square^2$. As follows, error should be calculated:

$$\square\square\square\square\square = \frac{3049 - 2630}{3049} * 100\% = 13.76\%$$

The gap between SAP2000 and hand calculations can be explained as concrete cover assumptions and SAP2000 calculation approach, where he considers the compression and tension reinforcement at the same time.

Minimum steel area check as follows:

$$\square_{\square,\square\square\square} = 3\sqrt{\square'_\square}\square\square/\square_\square \geq 200\square\square/\square_\square = 612.93\ \square\square^2 \geq 536.5\ \square\square^2 \qquad (2.8)$$

$$\square_\square = 3049\ \square\square^2 \geq 612.93\ \square\square^2, \text{ sufficient reinforcement}$$

$\square_\square$ will be used as 3049 $\square\square^2$ (4.73 $\square\square^2$), where will be chosen as 5#9 bars ($\square_\square = 4.726\ \square\square^2$).

The minimum beam width should be checked. Assumption is that #3 stirrups used.

Positive moment

$$\square_\square = 262.44\ \square\square - \square$$

$$\square = 300\ \square\square, h = 600\ \square\square, \square = 600 - 2.5\ \square\square * 24\square\square/\square\square = 536.5\ \square\square$$

$$\square'_\square = 40\ \square\square\square\ (5801\ \square\square\square), \square_\square = 413\ \square\square\square$$

$$\square_\square = \frac{\square_\square}{\square\square\square^2} = \frac{262.44}{0.9*300*536.5^2} = 3039.27\ \square\square/\square^2 \qquad (2.9)$$

$$\rho = \frac{0.85\square'_{\square}}{\square_{\square}}[1 - \sqrt{1 - \frac{2\square_{\square}}{0.85\square'_{\square}}}] = 0.0077$$

$$\square_{\square} = \square\square\square = 0.0077 * 300 * 536.5 = 1242.7\ \square\square^2$$

$$\square_{\square}\square_{\square} = 0.85\square'_{\square}\square\square \Rightarrow\ \square = 50.32\ \square\square$$

$$\beta_1 = 0.85 - 0.05(\frac{5801 - 4000}{1000}) = 0.76$$

$$\square = \frac{\square}{\square} = \frac{50.32}{0.76} = 66.21\ \square\square$$

$$\varepsilon_{\square} = 0.003(\frac{\square - \square}{\square}) = 0.003(\frac{536.5 - 66.21}{66.21}) = 0.021 < 0.005$$ (compression-controlled)

$\square_{\square}$ calculated by SAP2000 is 1393.06 $\square^2$. As follows, error should be calculated:

$$\square\square\square\square\square = \frac{1393.06 - 1242.7}{1393.06} * 100\% = 10.79\%$$

The difference can be explained in the same way as negative moment. The minimum steel area also can be checked as follows:

$$\square_{\square,\square\square\square} = 3\sqrt{\square'_{\square}}\square\square/\square_{\square} \geq 200\square\square/\square_{\square} = 612.93\ \square\square^2 \geq 536.5\ \square\square^2$$

$$\square_{\square} = 1242.71\ \square\square^2 \geq 612.93\ \square\square^2$$, sufficient reinforcement

Therefore, the $\square_{\square} = 1242.71\ \square\square^2$ will be used in order to select the bar. Relying on that, the reinforcement, 5#6 ($\square_{\square} = 2.16\ \square\square^2$) will be used.

2.2.5.2.1.2.Shear strength analysis

From the SAP2000 $\square_{\square} = 317.09\ \square\square$, $\lambda = 1$for normal-weight concrete.

$$\phi\square_{\square} = 2\square\square\sqrt{\square'_{\square}}\square_{\square}\square = 0.75 * 2 * 1 * \sqrt{40 * 1000} * 300 * 536.5 = 48.29\ \square\square \quad (2.10)$$

As $\square_{\square} > \square\square_{\square}$, shear reinforcement was done

$$\square_{\square 1} = 4 * \sqrt{\square'_{\square}}\square_{\square}\square = 128.76\ \square\square, \square_{\square 2} = 8 * \sqrt{\square'_{\square}}\square_{\square}\square = 257.52\ \square\square \quad (2.11)$$

$$\square_{\square} = \frac{\square_{\square} - \square\square_{\square}}{\square} = 358.4\ \square\square > \square_{\square 2}$$, shear reinforcement was done.

2.2.5.2.1.3.Torsion check

Since the building is located in a seismic zone, torsion also should be checked ($T_u = 1.92$ kN.m – From SAP2000). Section properties are also checked:

$$A_{cp} = 300 * 600 = 1800\ cm^2 = 0.18\ m^2$$

$$P_{cp} = 2 * (300 + 600) = 1.8 m^2$$

$$T_{cr} = 0.75\sqrt{f'_c}\left(\frac{A_{cp}^2}{P_{cp}}\right) = 0.75 * 1 * \sqrt{\frac{40}{1000}}\left(\frac{0.18^2}{1.8}\right) = 2.7\ kN.m > T_u \rightarrow$$ torsional reinforcement is not needed (2.12)

Stirrups spacing also needs to be calculated as follows:

$$A_{v1} = A_v f_{yt} d/T_u = 0.159\ m \quad (2.13)$$

$$A_{v2} = A/2 = 10.56\ cm.\ \text{if}\ T_u \leq T_{u1} = \left(4\sqrt{f'_c}\right)A_{cp}$$

$$A_{v3} = A_v f_{yt} d/50 b_w \geq A_v f_{yt}/\left(0.75\sqrt{f'_c} b_w\right) = 2.36\ cm. \quad (2.14)$$

$$A_v = A_{v2} = 0.159\ m \rightarrow\ \#4\ \text{stirrups}$$

2.2.5.2.2. Columns

2.2.5.2.2.1. Slenderness ratio check

Steel reinforcement was provided for each type of column used in the structural design of the building. The first step is to check the column's slenderness ratio to determine whether it is considered short or slender. Since the columns are not supported laterally by braces or shear walls, they are classified as sway columns. The slenderness check for these sway columns is shown below.

$$\psi_A = \frac{\Sigma(EI/l)\ \text{columns}}{\Sigma(EI/l)\ \text{beams}} = 6.74$$

$$\psi_B = \frac{\Sigma(EI/l)\ \text{columns}}{\Sigma(EI/l)\ \text{beams}} = 6.74$$

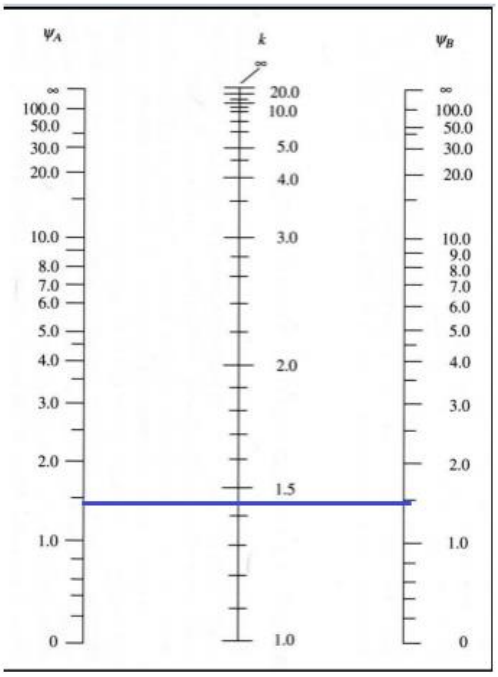

Figure 40. Slenderness check chart

$$□□□\frac{□_{□□}}{□} = 22$$

$$□□□□□□□\frac{□_{□□}}{□} = 32$$

2.2.5.2.2.1. Axial and moment analysis

According to the SAP2000 maximum moments and forces were found, using these values reinforcement ratio was found:

$$□_□ = \frac{□_□}{□} = 1027.97\ □□ - □$$

$$□_□ = \frac{□_□}{□} = 22284.19\ □□ - □$$

$$□ = \frac{□_□}{□_□} = 0.046\ □$$

$$\gamma = \frac{0.7 - 0.07 * 2}{0.7} = 0.8$$

$$\square_{\square} = \frac{\square_{\square}}{\square_{\square}\square_{\square}^{'}} = 1.14$$

$$\square_{\square} = \frac{\square_{\square}\square}{\square_{\square}\square_{\square}^{'}h} = 0.075$$

$$\rho = 3\%$$

$$\square_{\square} = 0.03 * \square_{\square} = 0.0049\ \square^{2}$$ (8#18 bar selected)

2.2.5.2.2.2.Shear analysis

$$\square_{\square} = 0.17(1 + \frac{\square_{\square}}{14\square_{\square}})\square\sqrt{\square_{\square}^{'}}\square_{\square}\square = 33408.34\ \square\square \qquad (2.15)$$

$$\varphi\square_{\square} = 0.75 * 33408.34 = 25056.26\ \square\square$$

$$\varphi\square_{\square}/2 = 12528.13\ \square\square\ >\ \square_{\square}$$

Spacing for shear reinforcement is the smallest of:

$$48 * \square_{\square} = 0.4572\ \square$$

$$16 * \square_{\square} = 0.3556\ \square$$

2.2.5.2.2.1. Biaxial bending analysis

As the corner column was selected, it is important to claim biaxial bending and use Bresler Reciprocal Load Method to determine whether the column is safe or not. SAP2000 values of bending moment values for both of the axes:

$$\square_{\square\square} = 16.48\ \square\square - \square$$

$$\square_{\square\square} = 546.65\ \square\square - \square$$

Bresler Reciprocal Load Method:

$$\square_{\square\square} = \frac{\square_{\square\square}}{\square} = 25.37\ \square\square - \square \qquad (2.16)$$

$$\square_{\square\square} = \frac{\square_{\square\square}}{\square} = 841.01\ \square\square - \square \qquad (2.17)$$

$$\square_{\square} = \frac{\square_{\square}}{\square} = 22284.19\ \square\square \qquad (2.18)$$

$$\gamma_{\square} = \square_{\square} = 0.813$$

$$\square_{\square} = \frac{\square_{\square\square}}{\square_{\square}} = 0.0011 \qquad (2.19)$$

$$\square_{\square} = \frac{\square_{\square\square}}{\square_{\square}} = 0.0377 \qquad (2.20)$$

$$\rho = \frac{\square_{\square}}{\square_{\square}} = 0.0367 \qquad (2.21)$$

$$\square_{\square}/h = 0.0015$$

$$\square_{\square}/h = 0.0503$$

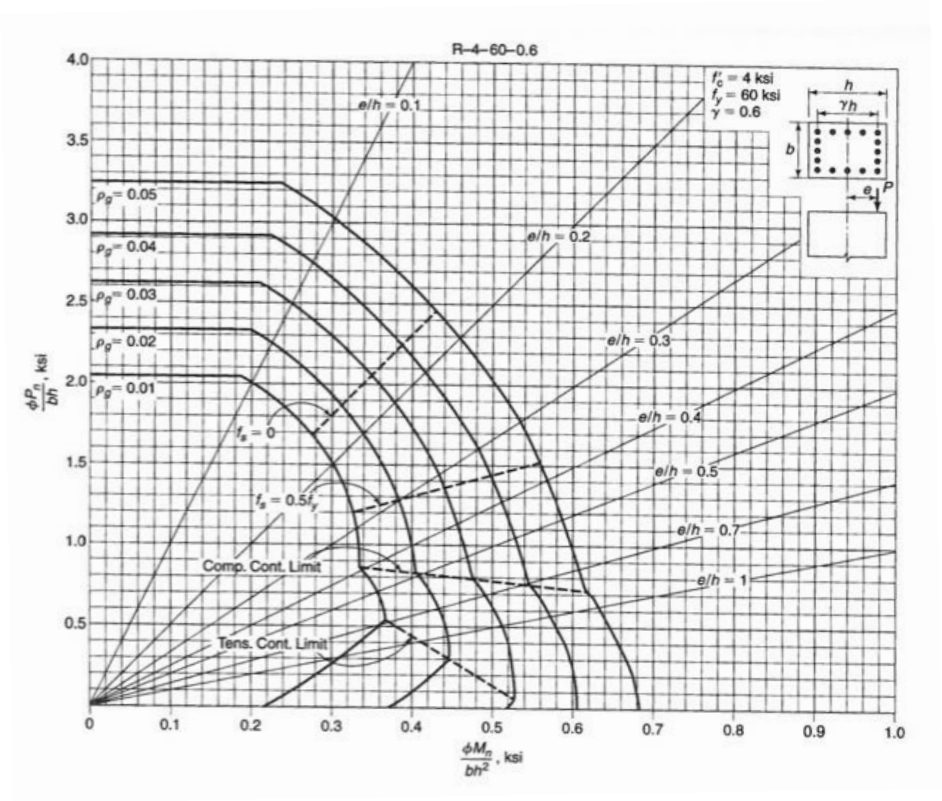

Figure 41. Interaction diagram

From the chart we can obtain Kn values to be equal to 1.3 and 0.7.

$$\square_{\square\square} = \frac{K_{nx} * f_c\prime * A_g}{\varphi} = 128076.92\ kN \qquad (2.22)$$

$$P_{ny} = \frac{K_{ny} * f_c\prime * A_g}{\varphi} = 128076.92\ kN \qquad (2.23)$$

$$P_0 = 0.85 * f_c' * A_g + A_{st}(f_y - 0.85f_c') = 19132.82\ kN$$

Calculations of Pn:

$$\frac{1}{P_n} = \frac{1}{P_{nx}} + \frac{1}{P_{ny}} - \frac{1}{P_0} \qquad (2.24)$$

$$P_n = -27284.69\ kN$$

Check proceeding:

$$P_n = |-27284.69| > 0.1P_0 -> the\ method\ is\ valid$$
$$\varphi P_n = |-17735.05| > P_u -> the\ column\ is\ safe\ against\ biaxial\ bending$$

2.2.5.2.3. Two-way slab

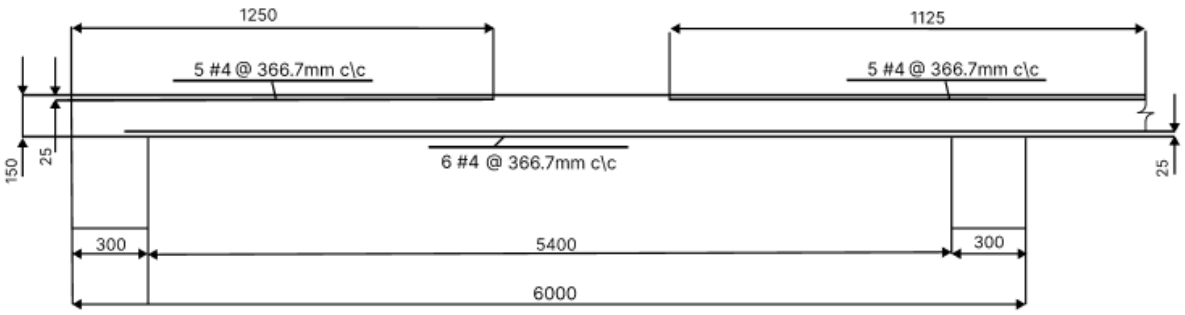

Figure 42. Two way-slab reinforcement

2.2.5.2.3.1. Flexural analysis

$$\underline{\square} = \frac{13500 * 75 + 150 * 375}{13500 + 150} = 165\ \square\square$$

$$\square_{\square} = \frac{1050 * 150^3}{12} + 13500(165 - 75)^2 + (150 * 450^3)/12 + 150 * (375 - 75)^2$$
$$= 5.7 * 10^9\ \square\square^4$$
$$\square_{\square} = 6000/2 * 150^3/12 = 8.4 * 10^8\ \square\square^4$$
$$\alpha_{\square\square} = \square_{\square} = \frac{\square\square_{\square}}{\square\square_{\square}} = 4.48$$

As $\alpha_{\square\square}$ is greater than 2.0, minimum height can be calculated as follows:

$$h_{\square\square\square} = \frac{\square_{\square}(0.8+\frac{\square_{\square}}{1400})}{36+9\square} = 2625 * (0.8 + 420/1400)/(36 + 9 * 1) = 64.17\ \square\square \qquad (2.25)$$

As the thickness is satisfied, factored loads can be calculated:

$$\square_{\square} = 1.2\square_{\square} + 1.6\square_{\square} = 1.2 * 5.6568 + 1.6 * 4.79 = 14.45\ \square\square/\square^2$$

Total static moment:

$$\square_0 = \frac{\square_{\square}\square_2\square_0^2}{8} = \frac{14.45*6.75*6^2}{8} = 438.98\ \square\square - \square \quad (2.26)$$

$$\square(-) = 0.65 * \square_0 = 0.65 * 438.98 = 285.34\ \square\square - \square$$

$$\square(+) = 438.98 - 285.34 = 153.64\ \square\square - \square$$

$$\alpha_{\square 1} = \square_{\square} = 4.48 \geq 1.0$$

$$\frac{\square_2}{\square_1} = 1.0$$

Table 22**.** Summary of exterior beam-supported panel

Exterior						
M	Column Strip				Middle Strip	
	negative	positive	negative	negative	positive	negative
%	97.29	75.00	75.00	2.71	25.00	25.00
new Mu (kN-m)	277.61	115.23	214.00	7.73	38.41	71.33
Mu slab (kN-m)	41.64	17.29	32.10	1.16	5.76	10.70
b	1.25	1.25	1.25	1.25	1.25	1.25
Rn (kPa)	2795.21	1160.26	2154.77	77.82	386.75	718.26
Ro	0.0070	0.0028	0.0053	0.0002	0.0009	0.0017
As (m^2)	0.00100	0.00040	0.00076	0.00003	0.00013	0.00025
As (in^2)	1.55043	0.62681	1.18261	0.04136	0.20649	0.38540
Asmin (in^2)	0.52313	0.52313	0.52313	0.52313	0.52313	0.52313
As final (in^2)	1.55043	0.62681	1.18261	0.52313	0.52313	0.52313
Bar Selected	4#6 (OR 8#4)	4#6	4#5	5#3	5#4	5#5
Spacing (m)	0.35473	0.87745	0.32766	0.262843	0.46594	0.74074
Minimum spacing (in)	1	1	1	1	1	1
Minimum spacing (m)	0.01968	0.01968	0.01968	0.01968	0.01968	0.01968

$$\bar{\square} = \frac{67500 * 75 + 0 * 375}{67500 + 0} = 75 \square\square$$

$$\square_{\square} = 1.27 * 10^{8} \square\square^{4}$$

$$\square_{\square} = 7.38 * 10^{8} \square\square^{4}$$

$$\alpha_{\square\square} = \square_{\square} = \frac{\square\square_{\square}}{\square\square_{\square}} = 4.48$$

As $\alpha_{\square\square}$ is greater than 2.0, minimum height can be calculated as follows:

$$h_{\square\square\square} = \frac{\square_{\square}(0.8 + \frac{\square_{\square}}{1400})}{36 + 9\square} = 2625 * (0.8 + 420/1400)/(36 + 9 * 1) = 64.17 \square\square$$

As the thickness is satisfied, factored loads can be calculated:

$$\square_{\square} = 1.2\square_{\square} + 1.6\square_{\square} = 1.2 * 5.6568 + 1.6 * 4.79 = 14.45 \square\square/\square^{2}$$

Table 23**.** Summary of interior beam-supported panel

Interior						
M	Column Strip				Middle Strip	
	(-ve)	(+ve)	(-ve)	(-ve)	(+ve)	(-ve)
%	75.00	75.00	75.00	25.00	25.00	25.00
new Mu (kN-m)	214.00	115.23	214.00	71.33	38.41	71.33
Mu slab (kN-m)	32.10	17.29	32.10	10.70	5.76	10.70
b	2.25	2.25	2.25	2.25	2.25	2.25
Rn (kPa)	1197.09	644.59	1197.09	399.03	214.86	399.03
Ro	0.0029	0.0015	0.0029	0.0010	0.00051	0.00096
As (m^2)	0.00075	0.00040	0.00075	0.00025	0.00013	0.00025
As (in^2)	1.16474	0.62188	1.16474	0.38355	0.20596	0.38355
Asmin (in^2)	0.94163	0.94163	0.94163	0.94163	0.94163	0.94163
As final (in^2)	1.16474	0.94163	1.16474	0.94163	0.94163	0.94163
Bar Selected	6#4	5#4	6#4	5#4	5#4	5#4
Spacing (m)	0.37669	0.37669	0.37669	0.37669	0.37669	0.37669
Minimum spacing (in)	1	1	1	1	1	1

Minimum spacing (m)	0.01968	0.01968	0.01968	0.01968	0.01968	0.019685

2.2.5.2.3.1. Shear analysis

$$\square_{\square\square\square\square\square\square\square} = 4.92 - 3/4 - 5/8 = 3.545\ \square\square$$

$$\square_{\square\square\square\square\square\square\square} = 3.545 * 25.4 = 90.043\ \square\square$$

$$V_u = [l_1 l_2 - (b + d_{avg})(h + d_{avg})] * q_u \quad (2.27)$$

$$\square_{\square} = (36 * (0.75 + 90.043/1000)) * 14.45 = 510.08\ \square\square$$

$$\lambda = 1.0$$

$$\varphi\square_{\square 1} = \square(0.17\square\sqrt{\square'_{\square}} + \frac{\square_{\square}}{6\square_{\square}})\square_{\square}\square = 348.05\ \square\square \quad (2.28)$$

$$\varphi\square_{\square 2} = \square(0.66\square\square^{(1/3)}\sqrt{\square'_{\square}} + \frac{\square_{\square}}{6\square_{\square}})\square_{\square}\square = 37.36\ \square\square \quad (2.29)$$

2.2.5.2.4. Joint design

Joint design is shown below in Figure 43.

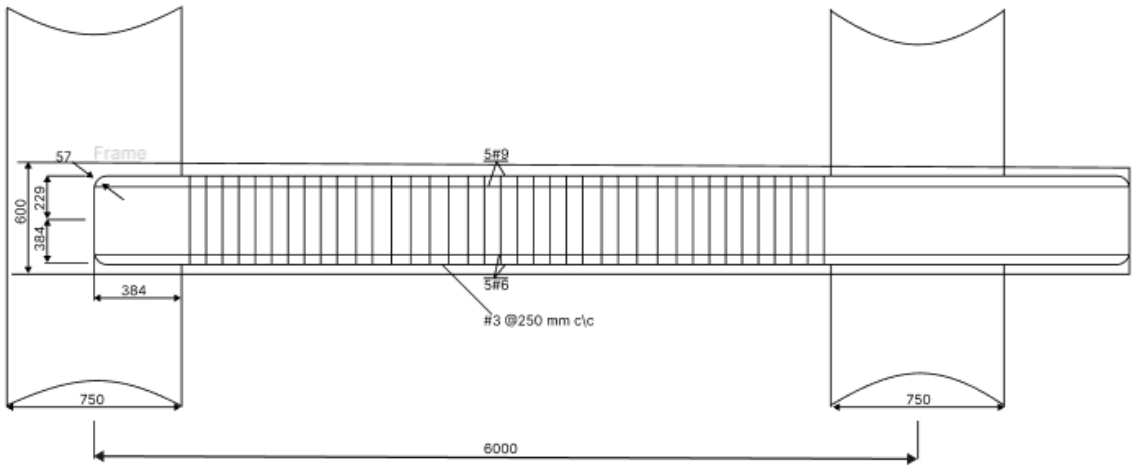

Figure 43. Beam-column joint design

The calculation for interior beam-column joint shear was calculated using formulas below:

$$V_{u,joint} = T_{pr1} + C_{pr2} - V_{col} \quad (2.30)$$

$$T_{pr1} = \alpha A_s f_y = 1.25 \cdot 3225 \cdot 420 = 1693.55\ kN \quad (2.31)$$

$$C_{pr1} = \alpha A_s f_y = 1.25 \cdot 1419.35 \cdot 420 = 745.16\ kN \quad (2.32)$$

The column joint taken from SAP2000:

$$V_{col} = 16.64\ kN$$

Result of shear as follows:

$$V_{u,joint} = 1693.55 + 745.16 - 16.64 = 2422.06\ kN$$

To calculate the shear strength of joint, it is initially important to calculate the effective width of the joint:

$$b_j = \frac{b_b + b_{col}}{2} = \frac{300 + 750}{2} = 525\ mm < b_b + h_{col} = 300 + 750 = 1050\ mm$$

$$b_j = 525\ mm\ <\ b_b + 2x = 350 + 750 = 1050\ mm$$

Shear capacity can be found as follows:

$$V_n = \gamma\sqrt{f'_c}A_j = 1.7 * \sqrt{40} * 525 * 750 = 4233.5\ kN \quad (2.33)$$

Initially it is important to know that nominal shear strength requirements are $\phi V_n \geq V_u$. ϕ is taken to 0.85.

$$0{,}85 * 4233 \geq 2422.06\ kN$$

Building is safe from shear forces. The same steps were implemented to calculate the joint's shear capacity in order to find if building is safe against shear.

According to ACI 15.4.2 spacing requirements are calculated as follows:

$$A_v = max\left(\frac{0.062\sqrt{f'_c}b_c s}{f_{yt}}, \frac{0.35 b_c s}{f_{yt}}\right) \quad (2.34)$$

$$s = min\left(\frac{A_v f_{yt}}{0.062\sqrt{f'_c}b_c}, \frac{A_v f_{yt}}{0.35 b_c}\right) \quad (2.35)$$

$$s = min\left(\frac{2 \cdot 129 \cdot 420}{0.062\sqrt{40} \cdot 750}, \frac{2 \cdot 129 \cdot 420}{0.35 \cdot 750}\right) = min(365.46, 415.04) = 365.46\ mm$$

Finally, the 2#4 ties were chosen with spacing of 360 mm to be safe and meet code requirements.

2.2.5.2.5. Reinforcement detailing

2.2.5.2.5.1. Bar selection and spacing

After reinforcement selected bars are shown in Table 24.

Table 24**.** Selected bars

Component	**Top reinforcement**	**Bottom reinforcement**	**Stirrups**
Major beam	5#9	5#6	#3 at 250 mm
Two-way slab	5#4	6#4	#4 at 366.7 mm
		Reinforcement	Ties
Column floors 0-1 (750 x 750 mm)		8#18	#4 at 200 mm
Column floors 2-3 (700 x 700 mm)		6#18	#4 at 200 mm
Column floors 4-5 (650 x 650 mm)		6#18	#4 at 200 mm
Column floors 6-7 (600 x 600 mm)		4#18	#4 at 200 mm
Column floor 8 (550 x 550 mm)		4#18	#4 at 200 mm
Column floor 9 (500 x 500 mm)		8#11	#4 at 200 mm
Column floor 10 (450 x 450 mm)		8#10	#3 at 200 mm
Column floor 11 (400 x 400 mm)		8#9	#3 at 200 mm
Column floor 12 (350 x 350 mm)		8#9	#3 at 200 mm
Column floors 13-15 (300 x 300 mm)		8#7	#3 at 200 mm

2.2.5.2.5.1. Development length

Development of length of selected 5#6 and 5#9 bars. The following equation in order to calculate the development length of bars tension:

$$l_d = \frac{f_y \psi_t \psi_e \psi_g}{25\lambda\sqrt{f'_c}} d_b \text{ for bars \#6 and smaller} \quad (2.36)$$

$\square_{\square} = 761.86\ \square\square > 750$ mm (column width)

As it meets criteria, it needs to be hooked bars. For hooked bars following can be used:

$$l_{dh} = \frac{f_y \psi_e \psi_r \psi_o \psi_c}{55\lambda\sqrt{f'_c}} {d_b}^{1.5} \quad (2.37)$$

$\square_{\square h} = 207.93\ \square\square > 8\square_{\square}$

Further magnification is needed. In order to find development length of bars in compression:

$$l_{dc} = \left(\frac{f_y \psi_r}{50\lambda\sqrt{f'_c}}\right) d_b \geq 0.0003 f_y \psi_r d_b \quad (2.38)$$

$\square_{\square\square} = 458.34\ \square\square < 523.57\ \square\square$

No further magnification needed. In the following are the results from length development for bars in compression and tension:

$\square_{\square\square} = 873\ \square\square$ (□□□□□□□□□□□□) & $\square_{\square\square} = 208\ \square\square$ (□□□□□□□□)

$\square_{\square\square} = 677\ \square\square$

2.2.5.2.5.1. Lap splices

Lap splices were calculated for beams and columns. For beams in tension:

$$l_{sc} = 8.19\ in$$

For beams in compression:

$$l_{sc} = 0.0005 f_y d_b = 34.36\ in \quad (2.39)$$

For columns $\square_{\square} = 0.875\ \square\square$:

$$l_{sc} = 0.0005 f_y d_b = 26.65\ in \quad (2.40)$$

Lap splices for all other columns are illustrated in Table X below:

Table 25. Lap splices for columns

Component	Lap splice, mm
Column floors 0-1 (750 x 750 mm)	1746.061469

Column floors 2-3 (700 x 700 mm)	1746.061469
Column floors 4-5 (650 x 650 mm)	1746.061469
Column floors 6-7 (600 x 600 mm)	1309.739507
Column floor 8 (550 x 550 mm)	1746.061469
Column floor 9 (500 x 500 mm)	1090.804905
Column floor 10 (450 x 450 mm)	982.498035
Column floor 11 (400 x 400 mm)	872.643924
Column floor 12 (350 x 350 mm)	773.6205
Column floors 13-15 (300 x 300 mm)	676.9179375

2.2.5.2.6. Serviceability design

2.2.5.2.6.1. Deflection

To ensure the building remains functional and safe during regular use, structural elements should be evaluated for deflection. Most building codes provide recommended minimum thicknesses for different members. When these minimum thickness requirements are met or exceeded, it's generally acceptable to disregard deflection checks (Nilson et al., 2010). For beam elements with a yield strength of 60,000 psi (413.7 MPa), the minimum thickness can be calculated using the formula below:

$$h_{\square} = \frac{\square}{21} = 2.5 \square\square = 63.5 \square\square$$

2.2.5.2.6.2. Crack width

Controlling cracks is crucial in reinforced concrete design to guarantee the structure's safety and good performance under load. For this reason, it's critical to verify that any cracks' widths adhere to the restrictions set forth by building rules. The maximum width of flexural cracks can be estimated using the formula below (Nilson et al., 2010).

$$w = 0.076\beta_h f_s \sqrt[3]{d_c A} \quad (2.41)$$

Where $\beta_h = 1.2$ and $d_c = 63.5\ mm$

$$\square = 300 * 63.5 * 2/5 = 7620\ \square\square^2$$

$$\square = 0.2682\ \square\square = 0.0081\ \square\square < 0.016\ \square\square$$

As it is smaller than max allowable crack, crack width is satisfactory.

3. Geotechnical Part

3.1. Site characterization

The project site is located at 1000-1034 Hill Street and 220 & 226 West Olympic Boulevard in Los Angeles, California. Geocon West, Inc. performed the geotechnical investigation of the area. As part of this investigation, two hollow-stem auger boreholes were drilled to depths of approximately 38.1 m (B-2) and 36.6 m (B-1). Table 26 provides details of the soil profile from the deepest borehole, B-2.

3.2. Soil profile

Table 26. Soil profile from Geocon West, Inc.

Depth, foot	Depth, m	Layer thickness, m	Blows/foot	γ □□y, pcf	γ □□y, kN/m3	MC, %	USCS	Description
0-10’	0-3.05	1.38	23	92.2	14.5	14.3	-	ARTIFICIAL FILL: sandy silt, stiff
10’-15’	3.05-4.57	1.52	50	135.0	21.2	5.5	SM	Silty Sand with Gravel, very dense
15’-20’	4.57-6.10	1.53	50	118.1	18.6	5.0	SM	Silty Sand

20’-30’	6.10-9.14	3.04	50	115.2	18.1	0.9	SM	Silty Sand
30’-40’	9.14-12.19	3.05	50	102.5	16.1	15.1	SM	Silty Sand
40’-50’	12.19-15.24	3.05	50	110.3	17.3	1.3	SW	Sand with Gravel, well-graded, dense
50’-60’	15.24-18.29	3.05	76	112.4	17.7	7.9	SW	Sand with Gravel
60’-70’	18.29-21.34	3.05	50	133.0	20.9	3.4	SW	Sand with Gravel
70’-75’	21.34-22.86	1.52	50	128.4	20.2	3.0	SW	Sand with Gravel
75-77.5	22.86-23.62	0.76	50	-	-	2.3	SW	Sand with Gravel
77.5-80	23.62-24.38	0.76	50	-	-	-	SW	Sand with Gravel
80-85	24.38-25.91	1.53	50	-	-	1.9	SW-SP	Sand with Gravel
85-87.5	25.91-26.67	0.76	50	-	-	3.7	SP	Sand, poorly graded, very dense
87.5-90	26.67-27.43	0.76	50	103.1	16.2	5.7	SP	Sand, poorly graded, very dense
90-95	27.43-28.96	1.53	53	-	-	6.0	SP-SM	Sand, poorly graded, very dense
95-100	28.96-30.48	1.52	50	109.4	17.2	16.7	SM	Silty Sand, very dense
100-105	30.48-32.00	1.52	50	-		4.1	SW	Sand, well-graded, very dense
105-110	32.00-33.53	1.53	50	105.8	16.6	7.0	SW-ML	Sand, well-graded, very dense
110-115	33.53-35.05	1.52	32	-		21.6	ML	Sandy Silt, hard
115-120	35.05-36.58	1.53	50	110.3	17.3	16.0	ML	Sandy Silt
120-125	36.58-38.1	1.52	50	-		2.6	SW	Sand with Gravel, well-graded, dense

3.3. Groundwater table and slope stability

A seismic hazard analysis for Hollywood found that the groundwater level is about 33 meters below the surface (Geocon West, 2017). However, our geotechnical investigation showed that none of the boreholes had groundwater, even the one that reached 38 meters deep. This means that groundwater does not affect our site, so we will not include it in our calculations. The site is flat and outside the City of Los Angeles Hillside Grading Area, as noted in the County of Los Angeles Safety Element (Geocon West, 2017).

3.4. Soil engineering properties

The standard penetration number N needs to be adjusted based on criteria such as the efficiency of the SPT hammer, the diameter of the borehole, the method of sampling, and the length of the rods (Seed et al., 1985; Skempton, 1986; as cited in Das, 2019).

The corrected value of N (to an average energy ratio of 60%) is equal to

$$\square_{60} = \frac{\square * \square_{\square} * \square_{\square} * \square_{\square} * \square_{\square}}{60} \tag{3.1}$$

In granular soil, the value $\square_{60}$ is affected by the effective overburden pressure. Therefore, the value $\square_{60}$ should be modified to $\square_{(1)60}$. That is,

$$\square_{(1)60} = \square_{60} * \square_{\square} \tag{3.2}$$

The correction factor $\square_{\square}$ can be estimated using several equations and we used Liao and Whitman's (1986), Seed et al.'s (1975), and Peck et al.'s (1974) equations. The formulas are given in the following table.

Table 27. Correction factor formulas.

Liao and Whitman (1986)	Seed et al. (1975)	Peck et al. (1974)
$\square_{\square(1)} = \left[\frac{1}{(\frac{\square_0'}{\square_{\square}})}\right]^{0.5}$	$\square_{\square(2)} = 1 - 1.25\square\square\square(\frac{\square_0'}{\square_{\square}})$	$\square_{\square(3)} = 0.77\square\square\square\left[\frac{20}{(\frac{\square_0'}{\square_{\square}})}\right]$

In our analysis, we calculated the average of the values obtained from three different methods. Since groundwater does not influence our soil profile, the effective overburden pressure is equivalent to the overburden pressure itself. The values for effective overburden pressure, correction factor, and corrected penetration number for the soil layers are provided in Table 28.

The modulus of elasticity is calculated using the following formula:

$$\square_{\square} = \square\square_{60}\square_{\square} \quad (3.3)$$

Poisson's ratio equation:

$$\mu_{\square} = 0.1 + 0.3(\frac{\square'-25}{20}) \quad (3.4)$$

So, Table 28 summarizes the physical properties of the soil.

Table 28. Physical properties of soil layers.

Depth, m	Soil type	Layer thickness, m	N	N60	γ dry, *k*N/m3	$\square_0'$,kN/m2	$\square_{\square(1)}$	$\square_{\square(2)}$	$\square_{\square(3)}$	$\square_{\square}$ ave.	$\square_{(1)60}$	φ	Es, Mpa	μ	c', kN/m2
0-3.05	sandy silt	3.05	23	31	14.5	44.23	1.50	1.44	1.27	1.41	44	43	15.53	0.37	28.2
3.05-4.57	Silty Sand with Gravel	1.52	50	68	21.2	76.45	1.14	1.15	1.09	1.13	76	43	33.75	0.37	0
4.57-6.10	Silty Sand	1.53	50	68	18.6	104.91	0.98	0.97	0.99	0.98	66	36	33.75	0.27	0
6.10-9.14	Silty Sand	3.04	50	68	18.1	159.93	0.79	0.75	0.84	0.79	54	36	33.75	0.27	0

9.14-12.19	Silty Sand	3.05	50	68	16.1	209.04	0.69	0.60	0.76	0.68	46	39	33.75	0.31	0
12.19-15.24	Sand with Gravel	3.05	50	68	17.3	261.80	0.62	0.48	0.68	0.59	40	39	33.75	0.31	0
15.24-18.29	Sand with Gravel	3.05	76	103	17.7	315.79	0.56	0.38	0.62	0.52	53	40	51.30	0.33	0
18.29-21.34	Sand with Gravel	3.05	50	68	20.9	379.53	0.51	0.28	0.56	0.45	30	40	33.75	0.33	0
21.34-22.86	Sand with Gravel	1.52	50	68	20.2	410.24	0.49	0.23	0.53	0.42	28	37	33.75	0.28	0
22.86-23.62	Sand with Gravel	0.76	50	68	20.2	425.59	0.48	0.21	0.52	0.41	27	37	33.75	0.28	0
23.62-24.38	Sand with Gravel	0.76	50	68	20.2	440.94	0.48	0.19	0.51	0.39	26	37	33.75	0.28	0
24.38-25.91	Sand with Gravel	1.53	50	68	20.2	471.85	0.46	0.16	0.48	0.37	25	37	33.75	0.28	0
25.91-26.67	Sand	0.76	50	68	20.2	487.20	0.45	0.14	0.47	0.36	24	37	33.75	0.28	0
26.67-27.43	Sand	0.76	50	68	16.2	499.51	0.45	0.13	0.46	0.35	23	37	33.75	0.28	0
27.43-28.96	Sand	1.53	53	72	16.2	524.30	0.44	0.10	0.45	0.33	23	37	35.78	0.28	0
28.96-30.48	Silty Sand	1.52	50	68	17.2	550.44	0.43	0.07	0.43	0.31	21	37	33.75	0.28	6.2
30.48-32.00	Sand	1.52	50	68	17.2	576.58	0.42	0.05	0.42	0.29	20	37	33.75	0.28	0
32.00-33.53	Sand	1.53	50	68	16.6	601.98	0.41	0.03	0.40	0.28	19	37	33.75	0.28	0

33.53-35.05	Sandy Silt	1.52	32	43	16.6	627.21	0.40	0.00	0.39	0.26	11	37	21.60	0.28	4.7
35.05-36.58	Sandy Silt	1.53	50	68	17.3	653.68	0.39	-0.02	0.37	0.25	17	37	33.75	0.28	4.7
36.58-38.1	Sand with Gravel	1.52	50	68	17.3	679.98	0.38	-0.04	0.36	0.23	16	37	33.75	0.28	0

The following figure shows soil profile made in Plaxis 3D.

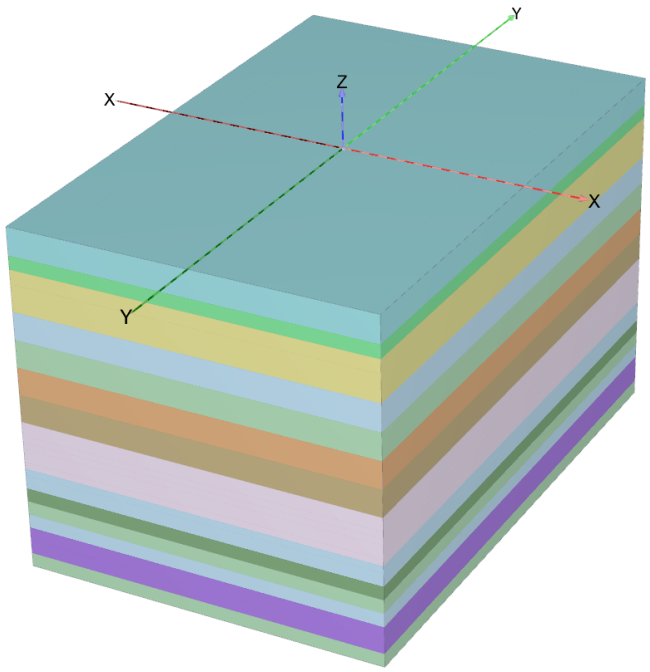

	Layers	Borehole_2	
#	Material	Top	Bottom
1	sandy silt	0.000	-3.050
2	silty sand with Gravel	-3.050	-4.570
3	silty sand	-4.570	-9.140
4	silty sand	-9.140	-12.19
5	sand with Gravel	-12.19	-15.24
6	sand with Gravel	-15.24	-18.29
7	sand with Gravel	-18.29	-21.34
8	sand with Gravel	-21.34	-26.67
9	sandy silt	-26.67	-28.96
10	silty sand	-28.96	-30.48
11	sand with Gravel	-30.48	-32.00
12	silty sand	-32.00	-33.53
13	sandy silt	-33.53	-36.58
14	sand with Gravel	-36.58	-38.10

Figure 44. Soil Profile in Plaxis 3D.

3.5. Seismicity and liquefaction potential

The top 30 meters of soil exhibit a site-specific shear wave velocity (Vs30) of 416 m/s (Geocon West, 2017). This measurement is classified within Site Class "C" (ASCE, 2013). The seismic design category of the site was also evaluated, and under the 2016 California Building Code and ASCE 7-16 standards, it is categorized in Seismic Design Category D and risk category I (Geocon West, 2017). Current regulations for assessing and addressing seismic hazards in California mandate that liquefaction analysis be performed to a depth of 50 feet below the ground surface (Martin et al., 1999). Nevertheless, the site does not appear on the California Seismic Hazards map as an area at risk for liquefaction.

3.6. Site response analysis

As the site is located in a high seismic area, there is a need to perform site response analysis to accurately estimate how soil behaves under ground motion. In 2014, a significant earthquake measuring 5.1 on the Richter scale struck the La Habra area, located near Los Angeles. To better understand the geological implications of this event, a comprehensive site analysis was conducted using PLAXIS 2D software. This analysis utilized comprehensive geological data gathered from the U.S. Geological Survey (USGS).

We accomplished site response to an earthquake by modelling the soil with an advanced HS small model. To replicate an earthquake, we applied a prescribed line displacement at the model's base. Next, we assigned a multiplier to this displacement. We utilized the table option to

import an accelerogram from an actual earthquake event. This input data corresponds with the accelerogram recorded during the La Habra earthquake in 2014. The subsequent figure illustrates the input data.

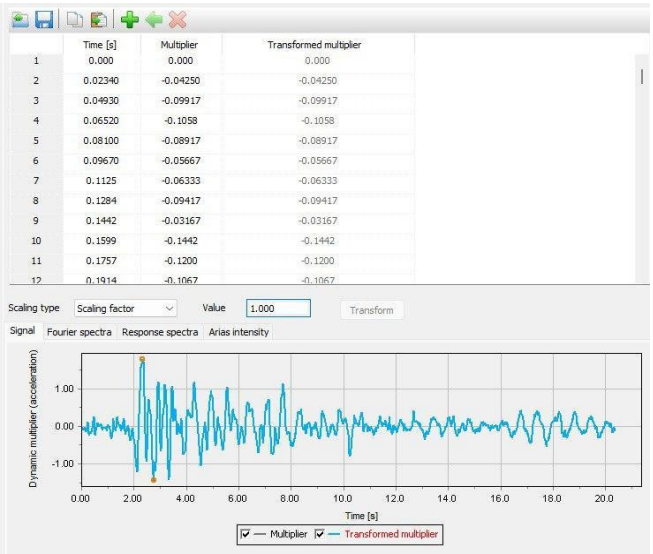

Figure 45. Accelerogram data.

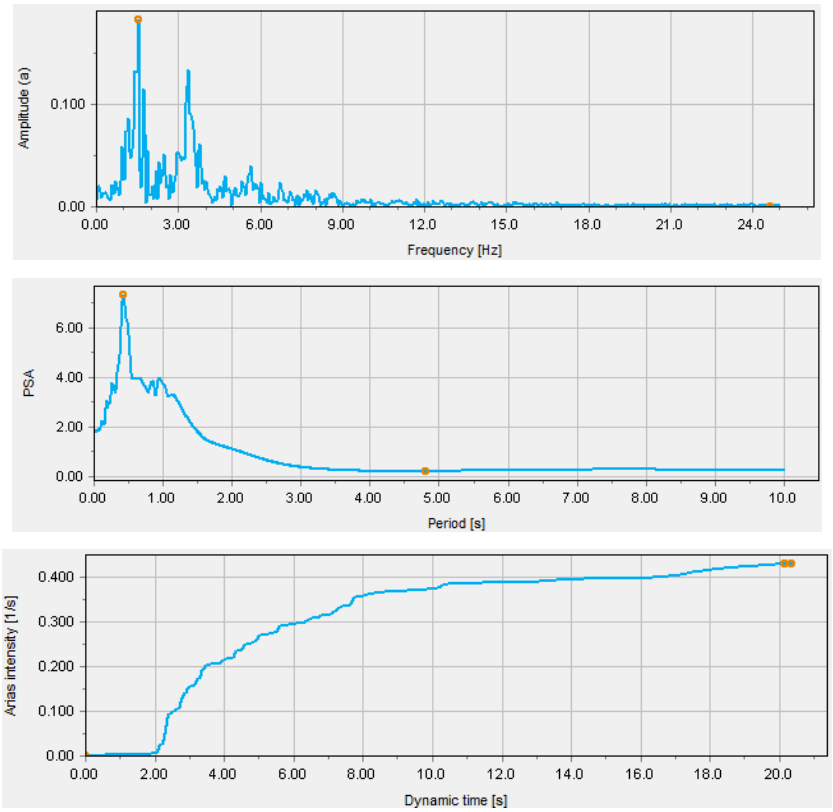

Figure 46. (a) Amplitude vs. Frequency; (b) PSA vs. Period; (c)Arias Intensity vs. Dynamic time.

During staged construction, we selected stress points and nodes in the model so we can analyse the calculation results of certain areas. We select the following stress points:

Name	X	Y
Node 87	6.00	0.00
Node 2906	6.00	-34.29
Stress point 4264	6.00	-34.29

Figure 47. Selected nodes.

In phase 1, we activated the Line displacements and the DynaLineDisplacement. Then, we deactivated the deformations checkbox and modified the dynamic boundary conditions. We created a soil column that connects the nodes on either side of the model by configuring "BoundaryXMIN" to Tied degrees of freedom. The fully reflective rigid base was modeled by

setting “BoundaryYMin” to none. We then selected the calculator type as Dynamic and set the Dynamic time interval to 20 seconds, which corresponds to the length of the earthquake signal. The maximum steps and the sub step count were automatically adjusted by Plaxis. Then, we performed a calculation. The deformed mesh is illustrated in the figure below, with a maximum deformation of 0.022 m.

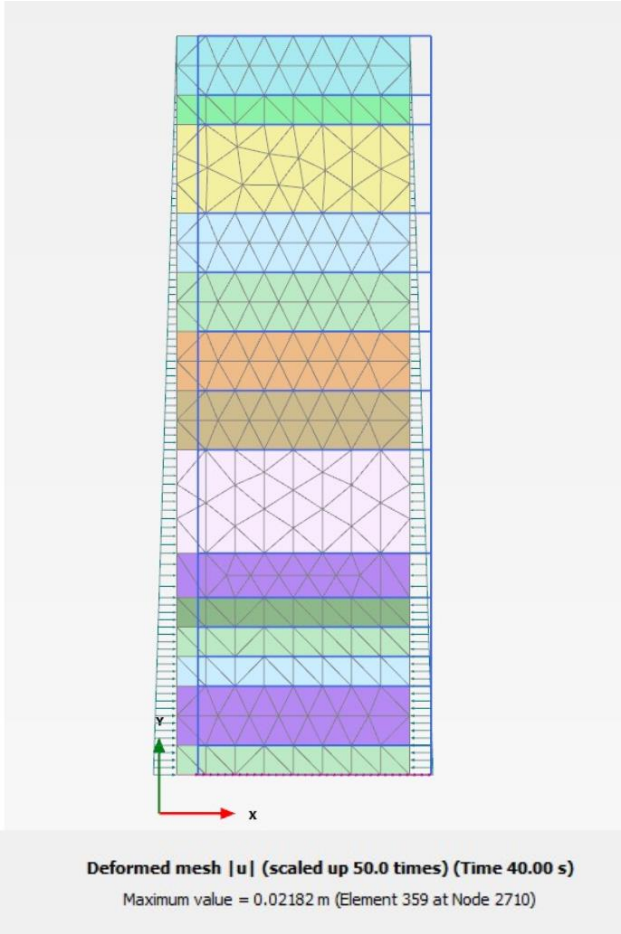

Figure 48. Deformed mesh |u|.

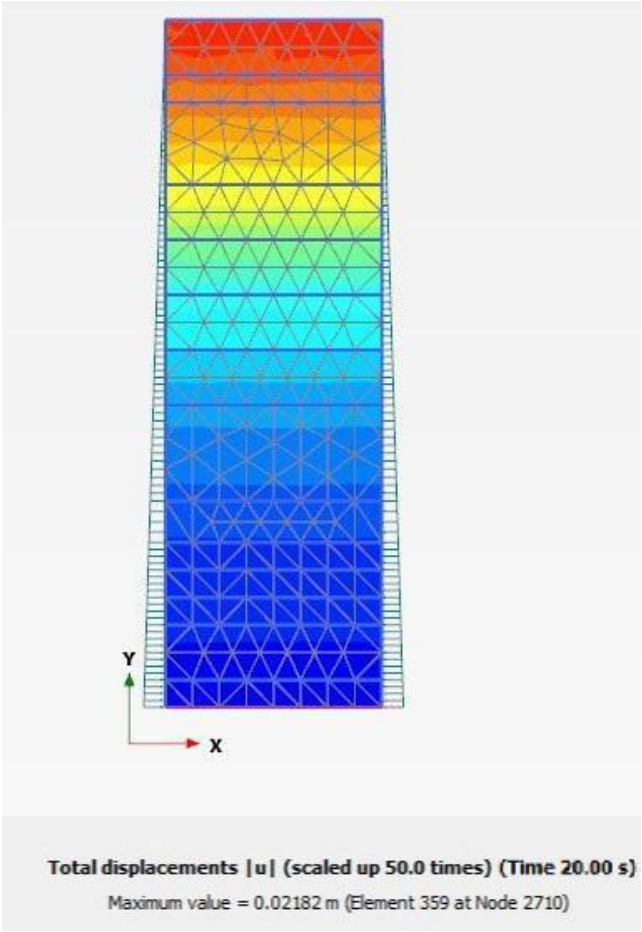

Figure 49.Total displacement.

Figure 50 illustrates the accelerogram, a detailed graphical representation that captures the variations in ground acceleration over time during a seismic event. The x-axis of this plot outlines the chronological progression of the earthquake, showcasing how acceleration fluctuates dynamically as the tremors unfold. This accelerogram is crucial for providing insights into the intensity and duration of the earthquake, which is vital for assessing its potential impact on structures and the surrounding environment.

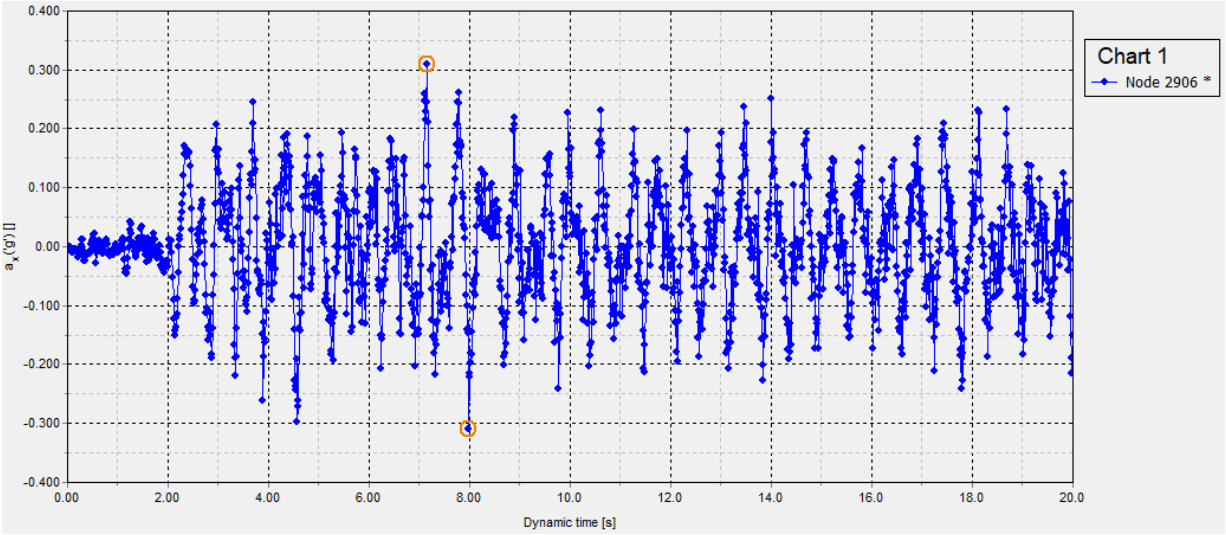

Figure 50. Acceleration vs. time

Moving on to Figure 51, we explore the characteristics of ground motion more thoroughly by applying Fast Fourier Transformation (FFT) to the accelerogram data. This method enables us to convert the time-domain signal into the frequency domain, allowing us to analyze the amplitude of ground motion across different frequencies. The resulting plot reveals the frequency spectrum, helping us understand how various frequencies contribute to the overall seismic response.

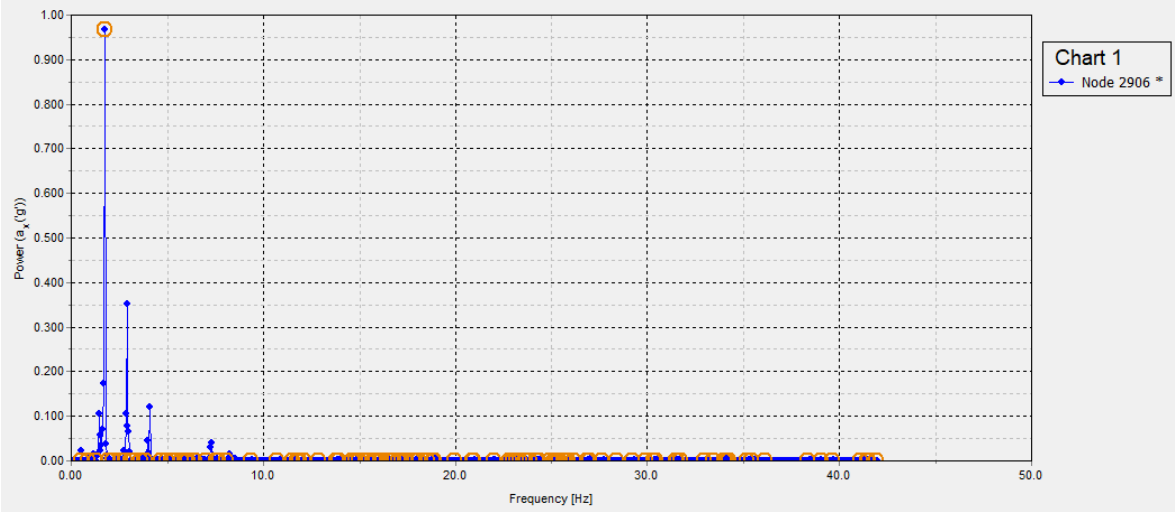

Figure 51. Amplitude of the ground motion

Finally, we present a peak spectral acceleration plot created from data gathered at a node strategically positioned at the bottom of the soil layer (Figure 52). This plot highlights the maximum spectral acceleration experienced at that depth during the earthquake, offering valuable insights into how the soil reacts to seismic forces.

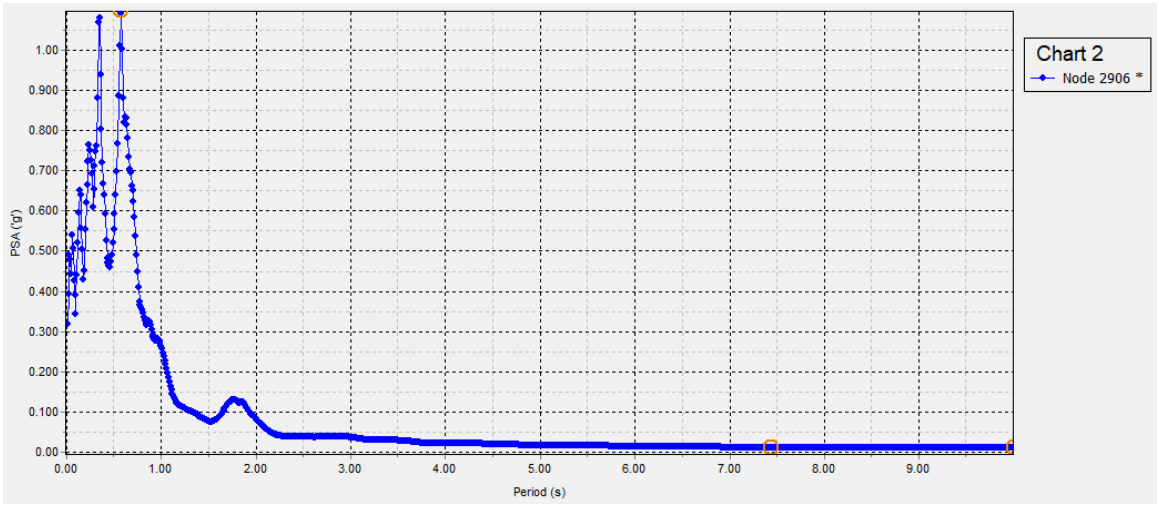

Figure 52. PSA plot

3.7. Foundation design: Shallow.

The foundation design is crucial to ensure safety of a building. We calculated bearing capacity values for both shallow and deep foundations.

3.7.1. Pad foundation

The general bearing capacity was calculated using Meyerhof's (1963) equation:

$$□_□ = □′□_□□_□□□_□□□_□□ + □□_□□_□□□_□□□_□□ + \frac{1}{2}□□□□_□□_□□□_□□□_□□ \quad (3.5)$$

The foundation was designed as a square footing and the depth of a foundation is 2 m, and the basement height of 6.255 m was taken into account.

Table 29. Factors.

Factor	$□_□$	$□_□$	$□_□$	$□_{□□}$	$□_{□□}$	$□_{□□}$	$□_□$
Formula	-	-	-	$1 + (\frac{□}{□})□□□□′$	$1 − 0.4(\frac{□}{□})$	$1 + 2□□□□′(1 − □□□□′)^2□□□^{−1}(\frac{□_□}{□})$	
Value	50.59	37.75	56.31	1.436	0.76	2.428	1

The shallow foundation design results are shown in Table 3.5 and compared to the loads of the building.

Table 30. Bearing capacity of the Shallow foundation.

Column type	Corner	Exterior	Interior
B, m	2.42	2.60	2.77
Load, kN	6526	8854	10051

□□□□, □□/□²	5463	7787	8934
□□□□, □□/□²	5200	5246.72	5390
Acceptance	No	No	No

The results show that the bearing capacity of the shallow foundation is not sufficient.

3.7.2. Mat foundation

The mat foundation supports multiple columns and walls beneath a structure (Das, 2019). The bearing capacity factors were found similarly as for pad foundations:

Table 31. Factors.

□□	□□	□□	□□□	□□□	□□□	□□□	□□□	□□□
50.59	37.75	56.31	1.436	0.76	2.428	1	1	1

The net ultimate capacity for cohesionless soil is equal to:

$$□_{□(□□□)} = □_□ − □ \quad (3.7)$$

$$□_□ = □□_□□_{□□}□_{□□}□_{□□} + \frac{1}{2}□□□_□□_{□□}□_{□□}□_{□□}$$

$$□_□ = 27.15 * 37.75 * 1.436 * 2.428 * 1 + 0.5 * 18.1 * 30 * 56.31 * 0.76 * 1 * 1$$

$$□_{□(□□□)} = □_□ − □ = 9382.97 − 27.15 = 9355.82\ □□/□^2$$

$$□_{□□□(□□□)} = \frac{□_{□(□□□)}}{□□} = \frac{9355.82}{3} = 3118.61\ □□/□^2$$

The factor of safety is equal to 3. The calculation of bearing capacity of sand should take settlement into account (Terzaghi and Peck (1948):

$$□_{□□□} = \frac{□_{60}}{0.08}□_□\frac{□_□}{25} \quad (3.8)$$

$$\square_{\square} = (1 + 0.33(\frac{\square_{\square}}{\square}) \quad (3.9)$$

$$\square_{\square\square\square} = \frac{\square_{60}}{0.08}\square_{\square}\frac{\square_{\square}}{25} = \frac{68}{0.08} * (1 + 0.33(\frac{1.5}{30}))(\frac{50}{25}) = 792.05\ \square\square/\square^2$$

$$\square_{\square\square\square(\square\square\square)} = \frac{\square_{\square\square\square}}{\square\square} = \frac{792.05}{3} = 264.02\ \square\square/\square^2$$

Therefore,

$$\square_{\square\square\square\square} > \square_{\square\square\square(\square\square\square)}$$

Since the distributed load exceeds the allowable bearing capacity of a mat foundation, it is not suitable for this building.

3.8 Pile foundation

Pile foundations are used when shallow foundation is not sufficient, as the depth of the pile foundation is much larger than the width. The ultimate load is calculated as a sum of point bearing capacity and friction resistance:

$$\square_{\square} = \square_{\square} + \square_{\square} \quad (3.10)$$

3.8.1. The point-bearing capacity

The diameter of the pile is chosen to be 0.4 m. Some research suggests that it is the most economical pile diameter for foundation design in most cases (Bassioni et al., 2024). It can be seen from the soil profile that there are no clay layers, therefore, the ultimate bearing capacity of the pile was determined by considering only sand.

Meyerhof's Method for Estimating Qp:

$$Q_p = A_P q_p = A_P q' N_q * \leq A_P p_l \quad (3.11)$$

$$q_l = 0.5 p_a N_q * tan\phi' \quad (3.12)$$

Vesic's Method for Estimating Qp:

$$Q_P = A_p q_p = A_p \underline{\sigma_0}' N_\sigma * \quad (3.13)$$

$$\underline{\sigma_0}' = (\frac{1+2K_0}{3}) q' \quad (3.14)$$

The $N_\sigma{}^*$ values were determined by finding the reduced rigidity index.

$$I_{rr} = \frac{I_r}{1+I_r \Delta} \quad (3.15)$$

$$I_r = \frac{E_s}{2(1+\mu_s) q\prime tan\phi\prime} \quad (3.16)$$

$$E_s = m * p_a \quad (3.17)$$

$$\mu_s = 0.1 + 0.3(\frac{\phi\prime - 25}{20}) \quad (3.18)$$

$$\Delta = 0.005(1 - \frac{\phi\prime - 25}{20}) \frac{q\prime}{p_a} \quad (3.19)$$

Coyle and Castello's Method:

$$Q_P = A_p q' N_q * \quad (3.20)$$

Meyerhof's method based on SPT results:

$$Q_p = A_p q_p = A_p 0.4 p_a N_{60} \frac{L}{D} \leq A_p 4 p_a N_{60} \quad (3.21)$$

Briaud's method based on SPT results:

$$\square_{\square} = \square_{\square}\square_{\square} = \square_{\square}19.7\square_{\square}\square_{60}^{0.36} \quad (3.22)$$

Table 32. Point bearing capacity in Sand with D=0.4 m.

Length, m	Meyerhof	Vesic	Coyle & Costello	Meyerhof SPT	Briaud SPT	**Average**
9	2808.59	1306.56	3128.56	2123.72	952.74	**2156.92**
10	3648.38	1333.91	3199.24	2123.72	952.74	**2352.92**
11	3648.38	1374.61	3214.74	2086.02	946.62	**2355.51**
12	3648.38	1415.76	3208.00	1859.82	908.30	**2307.41**
13	3648.38	1464.53	3208.51	1734.16	885.71	**2286.73**
14	3648.38	1513.97	3273.59	1648.71	869.74	**2289.47**

3.7.2 Friction Resistance (Qs) in Sand

The soil at the construction site consists mainly of sand, including silty sand and gravelly sand. We calculate the pile's frictional resistance using three methods for sandy soil.

General Formula

The frictional resistance of the pile in sand can be calculated using the following equation:

$$\square_{\square} = \square\square\square\square\square \quad (3.23)$$

In our calculations, we assumed $\square' \simeq 15\square$.

For z = 0 to $\square'$,

$$\square = \square\square_{0}\,'\square\square\square(\square') \quad (3.24)$$

For z = $\square'$ to $\square$,

$$\square = \square_{\square=\square'}$$

The skin friction is equal to:

$$□_□ =$$

$$□1.5□_0\,'□□□(□')□□□ \quad (3.25)$$

Coyle and Castello's (1981) equation.

Coyle and Castello (1981) suggested that average standard penetration resistance values can be obtained using the following equation:

$$f_{ave} =$$

$$K\underline{\sigma_0\,'}\,tan(0.8\varphi') \quad (3.26)$$

The effective earth pressure coefficient is taken from the K variation graph with L/D redrawn by Coyle and Castello (1981). Then, Q_s can be estimated as follows:

$$Q_s = K\underline{\sigma_0\,'}\,tan(0.8\varphi')pL \quad (3.27)$$

Correlation with standard penetration test results.

Briaud et al. (1985) suggested that the average unit frictional resistance can be obtained from the average standard penetration resistance:

$$f_{ave} =$$

$$0.224p_a\underline{(N_{60})}^{0.29} \quad (3.28)$$

The, frictional resistance equals to:

$$Q_s = pLf_{ave}$$

The summary of all methods is shown in Table .

Table 33. Frictional resistance in Sand with D=0.4 m.

		Pile length, m					
		9	10	11	12	13	14
Qs kN/m3	**General Formula**	**1847.92**	**2561.87**	**2221.83**	**2464.57**	**3265.08**	**2894.50**
	Coyle and Castello's	4546.22	5608.49	6232.01	8224.91	8932.44	9691.44

	Correlation with SPT	1367.50	1456.00	1545.58	1635.15	1696.63	1784.74

The total ultimate bearing capacity of a pile is calculated as a sum of the point bearing capacity and the frictional resistance, and divided by a factor of safety equal to 3.

Table 34. Final values of the Qu and Qall for the pile with D = 0.4 m.

Length,m	□□, kN	□□, kN	□□, kN	□□□□, kN
9	2156.92	1847.92	4000.84	1334.95
10	2352.92	2561.87	4914.79	1638.26
11	2355.51	2221.83	45777.34	1525.78
12	2307.41	2464.57	4771.98	1590.66
13	2286.73	3265.08	5551.81	1850.60
14	2289.47	2894.50	5183.97	1727.29

The comparison of the allowable load with the loads of the building showed that single pile foundation is not sufficient.

Table 35. Loads of the building.

Column	At, m2	Wu, kN/m3	Pu, kN	Pu whole area, kN
Exterior	18	324.44	8854.13	140157
Interior	36	279.2	10051.11	321363
Corner	9	390.24	6526.41	14049
Shear walls	18	1012.84	18231.12	
Critical load			10051.11	321363

3.8. Group of piles

The efficiency of a group of piles determines its behavior. When $\eta < 1$, a group of piles acts as a block, and when $\eta \geq 1$, a group of piles acts as a single pile. It can be calculated using following formula:

$$\eta = \left[\frac{2(\square_1+\square_2-2)\square+4\square}{\square\square_1\square_2}\right] \quad (3.29)$$

Dimensions of pile cap are calculated as:

$$\square_\square = (\square_1 - 1)\square + \square \quad (3.30)$$

$$\square_\square = (\square_2 - 1)\square + \square \quad (3.31)$$

The pile length was chosen to be 10 m, and the dimensions of pile cap and calculation of allowable bearing capacity are shown on Table 3.11 below.

Table 36. Calculation of allowable bearing capacity

	Exterior	Interior	Corner
L, m	10	10	10
D, m	0.4	0.4	0.4
d, m	1	1	1
$\square_1$	3	3	2
$\square_2$	2	3	2
$\square_\square$, m	1.4	2.4	1.4
$\square_\square$, m	2.4	2.4	1.4
Efficiency, η	1.008	0.849	1.114
$\square_\square$, kN	2352.92	2352.92	2352.92

□□, kN	2561.87	2561.87	2561.87
□□□□, kN	9829.57	12515.40	6553.05
□□□□□□□, kN	8854.13	10051.11	6526.41

Figure 53. The position of the group of piles under exterior, interior and corner columns.

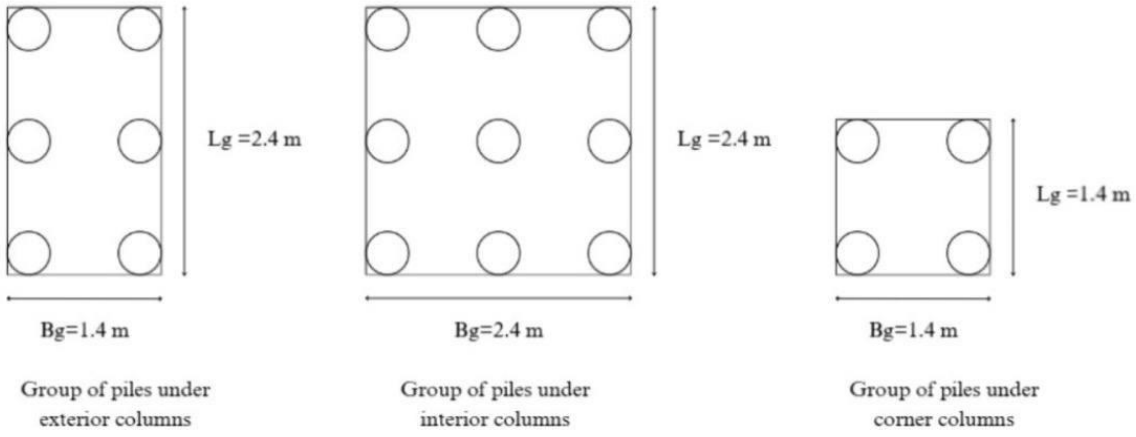

Figure 54. Configuration of group piles under each column type

3.9. Settlement

3.9.1. Settlement of a single pile

The elastic shortening of the pile was calculated as follows:

$$□_{□(1)} = \frac{(□_{□□} + □□_{□□})□}{□_{□}□_{□}} \quad (3.32)$$

The settlement of the pile due to the working load at the pile point is calculated using the equation:

$$□_{□(2)} = \frac{□_{□□}□}{□_{□}}(1 - □_{□}^{2})□_{□□} \quad (3.33)$$

The settlement of the pile due to the working load along the pile shaft is calculated as:

$$□_{□(3)} = \frac{□_{□□□}}{□□□□_{□}}(1 - □_{□}^{2})□_{□□} \quad (3.34)$$

According to ASTM D1143, settlement should not exceed 25 mm, the values shown on the following table exceed this value.

Table 37. Settlement of single piles.

Pile length, m	$□_{□(1)}$, □□	$□_{□(2)}$, □□	$□_{□(3)}$, □□	$□_{□}$, □□
9	2.652	32.800	1.597	37.049
10	3.541	35.403	2.005	40.949
11	3.674	35.442	1.606	40.722
12	4.133	34.718	1.658	40.509
13	5.076	52.299	3.127	60.502
14	5.160	52.361	2.611	60.131

3.9.2. Settlement of a group of piles

The elastic settlement was calculated using Meyerhof (1976) relation:

$$□_{□(□)} = \frac{0.96□\sqrt{□_{□}□}}{□_{60}} \quad (3.35)$$

$$□ = \frac{□_{□}}{□_{□}□_{□}} \quad (3.36)$$

Where,

$□ = 1 - \frac{□}{8□_{□}}$, influence factor

The results are shown in Table 38.

Table 38. Settlement of a group of piles.

	Ext.	Int.	Corner
□□, kN	9829.67	12515.40	6553.05
□□, m	2.4	2.4	1.4
□□, m	1.4	2.4	1.4
□, kN/m3	2925.47	2172.81	3343.39
N60	68	68	68
L, m	10	10	10
I	0.107	0.479	0.107
Sg, mm	**5.236**	**22.771**	**5.984**

3.9.3. Deflection analysis in Plaxis 3D

To check the accuracy of our hand calculations for the settlement, we analyzed the deflection behavior of each type of pile group using the advanced features of PLAXIS 3D software. In Plaxis 3D, we modelled the piles as embedded beams and pile caps as plates. Then, we applied loads to the structure and the table below shows load combinations we used for the analysis.

Table 39. Loads acting on a structure

Type of column	Load combination	F_x, kN	F_y, kN	F_z, kN	M_x, kN*m	M_y,kN*m	M_z, kN*m
Corner	1.2D+1L+1Ey	-47.45	-225.28	2860.29	1345.68	-170.73	-15.31
Exterior		-24.69	-271.76	8809.41	1426.26	14.27	-15.91
Interior		-16.93	-267.59	14506.14	1342.39	-9.705	-15.91

So, the graphical representation of results we obtained are shown in figures below.

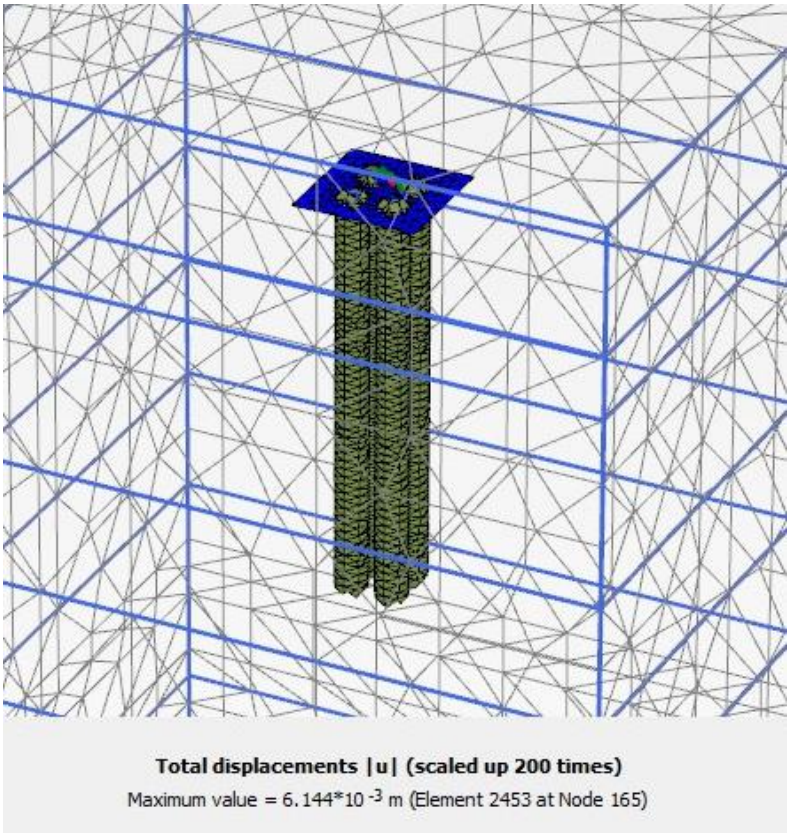

Figure 55. Corner pile group's displacement.

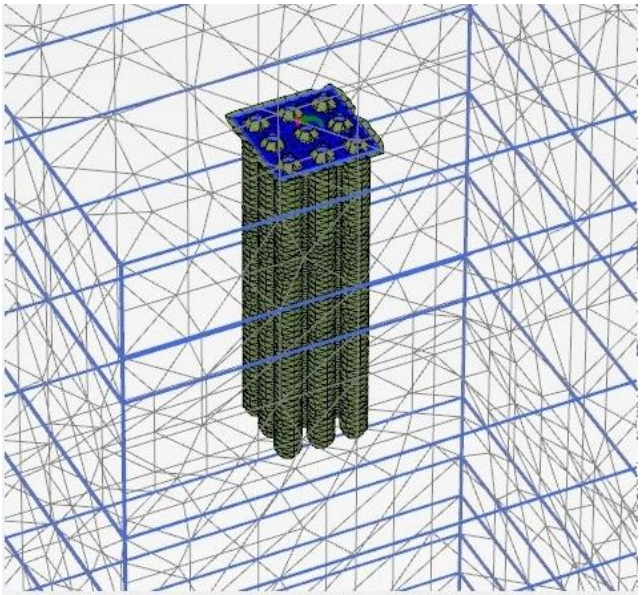

Figure 56. Interior pile group's displacement.

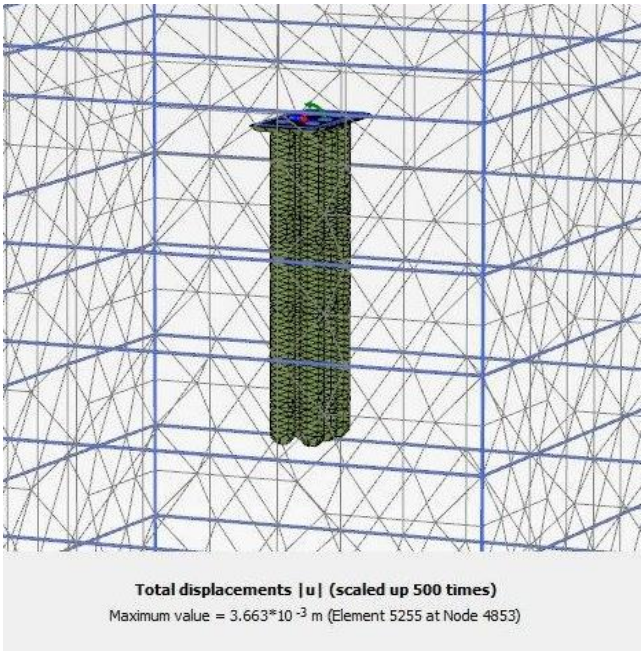

Figure 57. Exterior pile group's displacement.

We also did the settlement of a group of piles in GEO5. The example of the exterior group of piles is shown in figure below.

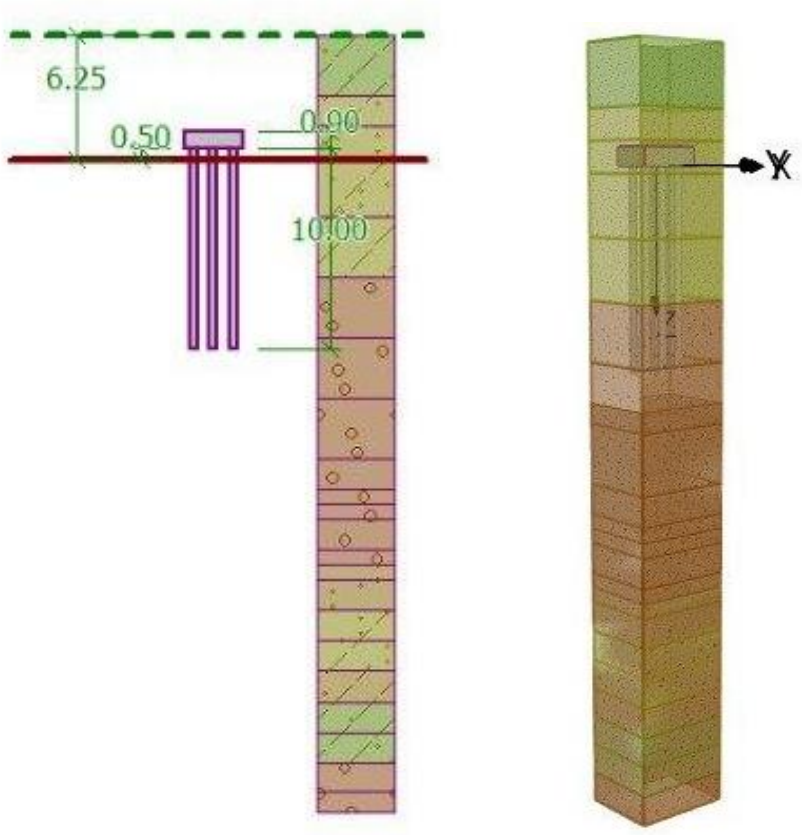

Figure 58. Group pile layout from Geo5 software.

Then, we compared the results of hand calculations, Plaxis 3D and GEO5. The results are shown in Table 40.

Table 40. Deflection analysis results.

	Interior group of piles			Exterior group of piles			Corner group of piles		
	Hand calc.	GEO5	Plaxis 3D	Hand calc.	GEO5	Plaxis 3D	Hand calc.	GEO5	Plaxis 3D
S_e, mm	22.7	24.2	27.6	5.23	4.86	3.66	5.98	5.66	6.14

3.9.4. Bearing capacity analysis in GEO5

The analysis of the bearing capacity of the pile group was done in Geo5 software and compared to hand calculations.

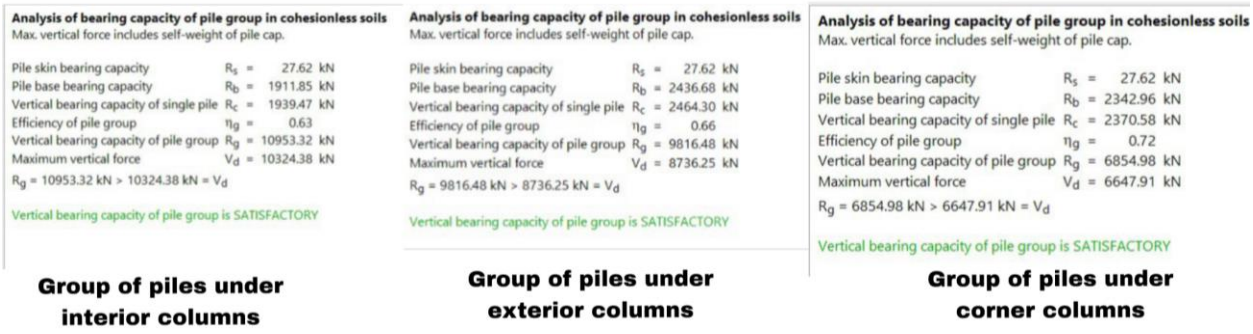

Figure 59. Analysis of bearing capacity in Geo5.

Table 41. Results of bearing capacity analysis.

	Interior group of piles		Exterior group of piles		Corner group of piles	
	Hand calc.	GEO5	Hand calc.	GEO5	Hand calc.	GEO5
Q_u, kN	37545.3	34831.56	29488.74	29449.44	19659.16	21181.89
Q_d, kN	10051.11	10324.38	8854.13	8736.25	6526.41	6647.91
FS	3	3.18	3	3.37	3	3.09
Q_{all}, kN	12515.40	10953.32	9829.57	9816.48	6553.05	6854.98

3.10. Reinforcement

3.10.1. Pile cap reinforcement

The pile cap dimensions were calculated previously and the summary for all column types is provided below:

Table 42. Pile cap dimensions

	Exterior	Interior	Corner
□□, mm	2400	2400	2400
□□, mm	1400	2400	1400
h, mm	800	800	800

The reinforcement is needed to provide structural support and distribute loads properly.

The calculations shown below are for a 3x3 pile group located under interior columns.

$$□_{□□} = □_{□□} = □^2 = 6 * 1.4^2 = 11.76 \, □^2 \quad (3.37)$$

The loads estimated in the structural part are the following:

Table 43. Loads and moments acting on piles

N, kN	□□, kN	□□, kN	□□, kNm	□□, kNm
10051	110.1	123	-144.1	129

$$□_{□□} = □_□ + □_□h = -144.1 + 123 * 0.8 = -45.7 \, □□ \quad (3.38)$$

$$□_{□□} = □_□ + □_□h = 129 + 110.1 * 0.8 = 217.08 \, □□ \quad (3.39)$$

$$□ = □ * □ * h * □_{□□□□□□□□□□} = 2.4 * 2.4 * 0.8 * 24 = 110.59 \, □□ \quad (3.40)$$

$$□_{□□□} = \frac{□}{□} + \frac{□_{□□□}}{□□□} + \frac{□_{□□□}}{□□□} \quad (3.41)$$

$$□_{□□□} = \frac{10051+110.59}{9} + \frac{-45.7*1.4}{11.76} + \frac{217.08*1.4}{11.76} = 1149.47 \, □□$$

$$\square_{\square\square\square} = \frac{\square}{\square} - \frac{\square_{\square\square}\square}{\square\square\square} - \frac{\square_{\square\square}\square}{\square\square\square} \quad (3.42)$$

$$\square_{\square\square\square} = \frac{10051+110.59}{9} - \frac{-45.7*1.4}{11.76} - \frac{217.08*1.4}{11.76} = 1108.66\ \square\square$$

Since there is no backfill, the dead load of only the pile cap is calculated.

$$1.4\square\square = 1.4 * 24 = 33.6\ \square\square/\square^2$$

The bending moment, therefore, is calculated using this equation:

$$\square'_{11} = \square'_{22} = \frac{2.4*33.6*(3.6/2-0.65/2)^2}{2} = 30.87\ \square\square\square$$

After calculating all the necessary elements, it is possible to determine the pile reactions as follows:

$$\square_1 = \square_{\square\square\square} \quad (3.43)$$

$$\square_2 = \frac{\square_1+\square_3}{2} \quad (3.44)$$

$$\square_3 = \square_{\square\square\square} = \square_4 \quad (3.45)$$

The bending moments of a pile cap are calculated as follows:

$$\square''_{11} = 1.4(\square_3 + \square_4) \quad (3.46)$$

$$\square''_{22} = 0.5(\square_1 + \square_2 + \square_3) \quad (3.47)$$

The values are:

$\square_1$= 1108.66 kN

$\square_2$ = 1129.07 kN

$\square_3 = \square_4$ = 1149.47 kN

$\square'_{11} = \square'_{22} = 30.87\ \square\square\square$

$\square''_{11} = 3218.51$ kN

$$□''_{22} = 1693.60 \text{ kN}$$

The combined moment is the sum of bending moment due to dead load and moment due to pile reactions:

$$□_{11} = □'_{11} + □''_{11} = 3187.64 □□□$$

$$□_{22} = □'_{22} + □''_{22} = 1662.73 □□□$$

Cover is chosen to be 75 mm according to ACI-318-19 building code and the rebar with a diameter of 25 mm is proposed:

$$□_□ = h - □□□□□ - 0.5□_{□□□} = 800 - 75 - 0.5 * 25 = 712.5 □□ \quad (3.48)$$

$$□ = \frac{□11}{□_{□□}□□^2} = \frac{3187.64*10^6}{35*2.4*10^3*712.5} = 0.0747 \quad (3.49)$$

$$□ = □(0.5 + \sqrt{0.25 - □/0.9}) \leq 0.95□ \quad (3.50)$$

$$□ = 712.5 * (0.5 + \sqrt{0.25 - 0.0747/0.9}) = 647.37$$

$$□_{□□} = \frac{□_{11}}{0.87□_□□} \quad (3.51)$$

$$□_{□□} = \frac{3187.64*10^6}{0.87*460*647.37} = 12303.86 □□^2$$

$$□ = (\frac{25}{2})^2 * □ = 490.87 □□^2$$

$$□ = \frac{□_{□□}}{□} = \frac{12303.86}{490.87} = 25.07 \approx 26$$

$$□ = \frac{2400}{26} = 95.75 □□$$

As a result, 26 #25 rebars should be used with a spacing of 95 mm in x-direction. For y-y direction, #25 rebar was proposed and calculated:

$$□_□ = 800 - 75 - 25 - 20/2 = 690 □□$$

$$□ = \frac{□_{22}}{□□□□□^2}$$

$$□ = \frac{1662.73*10^6}{30*2400*690^2} = 0.049$$

$$\square_{\square\square} = \frac{\square_{11}}{0.87\square_{\square}0.95\square_{\square}} = \frac{1662.73*10^6}{0.87*460*0.95*690} = 5535.97\ \square\square^2$$

$$\square_{12} = (20/2)^2 * \square = 314.16\ \square\square^2$$

$$\square = \frac{\square_{\square\square}}{\square} = 20.18 \approx 21$$

$$\square = \frac{2400}{18} \approx 114\ \square\square$$

Therefore, 21 #20 rebars with a spacing of 114 mm should be used.

The reinforcement design is summarized below:

Table 44. Reinforcement design for pile caps

Group piles	$\square_{\square}$, mm	$\square_{\square}$, mm	x-direction	y-direction
Interior	712.5	690	26T25 95 mm	21T20 114 mm
Exterior	712.5	690	35T25 70 mm	27T20 52 mm
Corner	712.5	690	31T25 46 mm	30T20 47 mm

3.10.2. Single pile reinforcement

The moment value M is taken as the combined moment from the pile group in the critical direction. To determine the load and moment acting on a single pile, the values of M and N are divided by the total number of piles in the group.

$$\frac{\square}{\square*\square^3} = \frac{3188*10^3}{9*403} = 1.99 \quad (3.52)$$

$$\frac{\square}{\square*\square^2} = \frac{10051*10^3}{9*403} = 6.28 \quad (3.53)$$

After determining these values, a graph shown below can be used to determine the percent of steel to concrete:

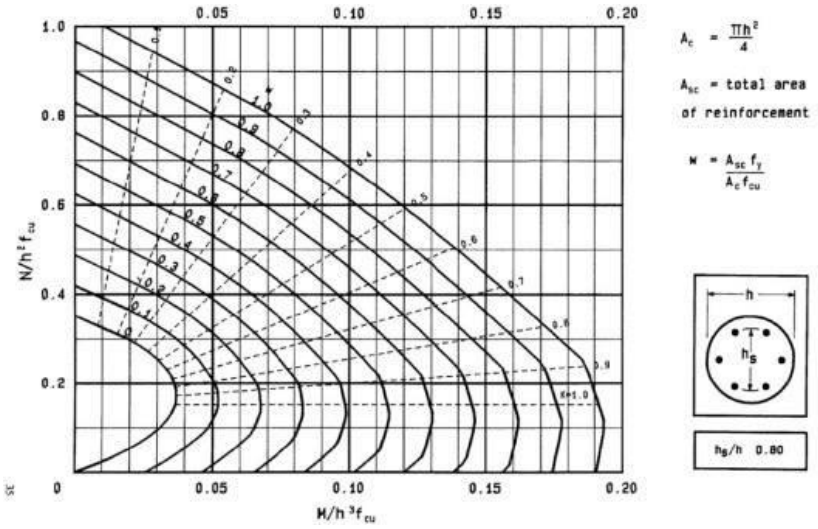

Figure 60. The graph reinforcement area determination.

The graph suggests that the percentage of steel is 1.2%, therefore:

$$\square_{\square} = (\frac{400}{2})^2 * \square = 125664 \ \square\square^2$$

$$\square_{\square\square} = 125664 * 0.012 = 1507.96 \ \square\square^2$$

$$\square_{\square 18} = (\frac{18}{2})^2 * \square = 254.5 \ \square\square^2$$

$$\square = \frac{\square_{\square\square}}{\square_{\square 18}} = 6$$

Therefore, 6 #18 bars should be used for interior column type. The reinforcement design for all the column types are shown below:

Table 45. Single pile reinforcement design

Column type	$\frac{\square}{\square * \square^3}$	$\frac{\square}{\square * \square^2}$	$\frac{\square_{\square\square}}{\square_{\square}}$, %	Design
Exterior	2.61	5.53	2	6T18
Interior	1.99	6.28	1.2	9T18
Corner	2.90	4.08	2.4	12T18

The reinforcement was also analyzed in Geo5 software:

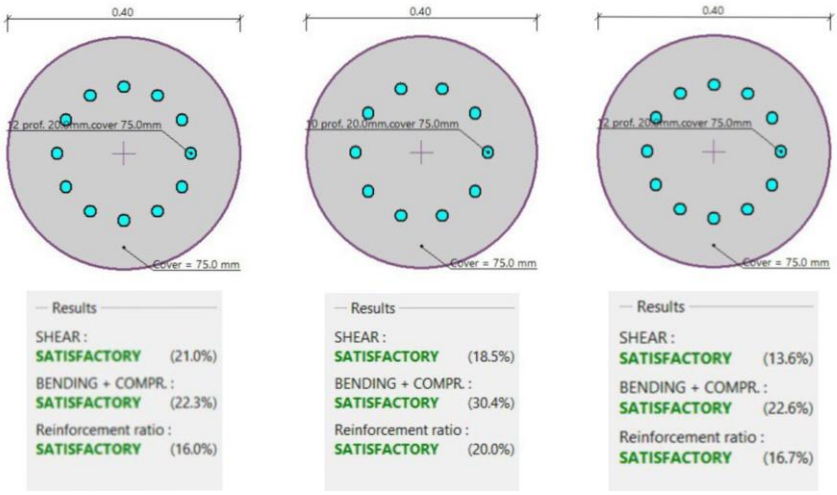

Figure 61. Pile reinforcement in Geo5

3.10.3. Software analysis of all pile groups in Plaxis 3D

After designing the reinforcement, we made a software analysis of all pile groups in Plaxis to evaluate the deformation. During the design stage, vertical reinforcements were created using beam elements. The following figure shows how reinforcement was installed.

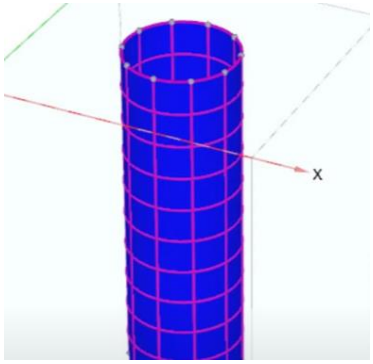

Figure 62. Reinforcement in the pile.

Then, we created exterior, interior and corner groups of piles and arranged them in the following position.

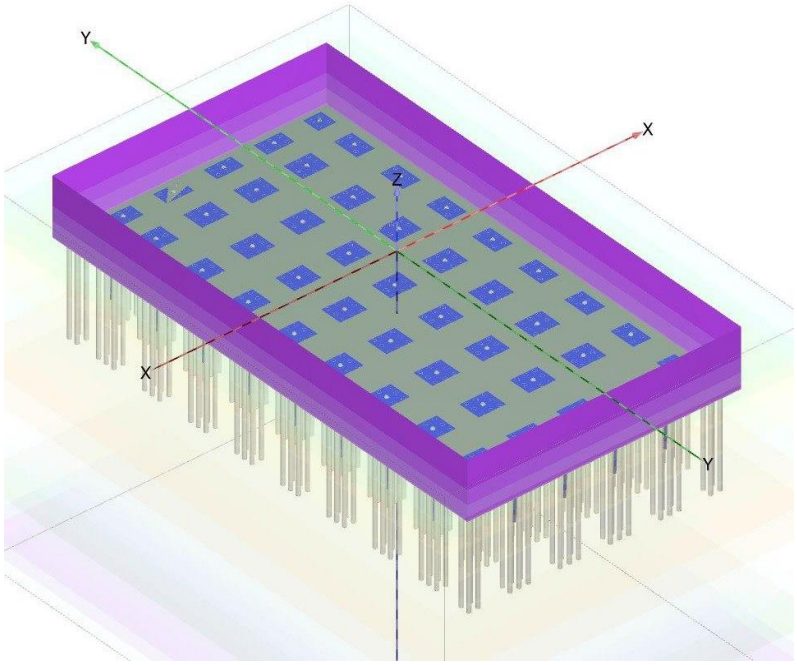

Figure 63. Layout of group piles.

The piles were represented as embedded beams. The embedded beam method is especially advantageous when dealing with a large number of piles in a PLAXIS 3D model. Pile caps were modeled by assigning plates to the basement floor slab. Sheet piles were also designed as plates. Specific material properties were assigned to beams and plates. The staged construction for the simulation of the main building encompassed several stages: 1) Initial phase; 2) Excavation; 3) Construction (walls/beams/piles/pile caps); 4) Loads; 5) Dynamic analysis. So, after calculation, we got the results shown in the Figure.

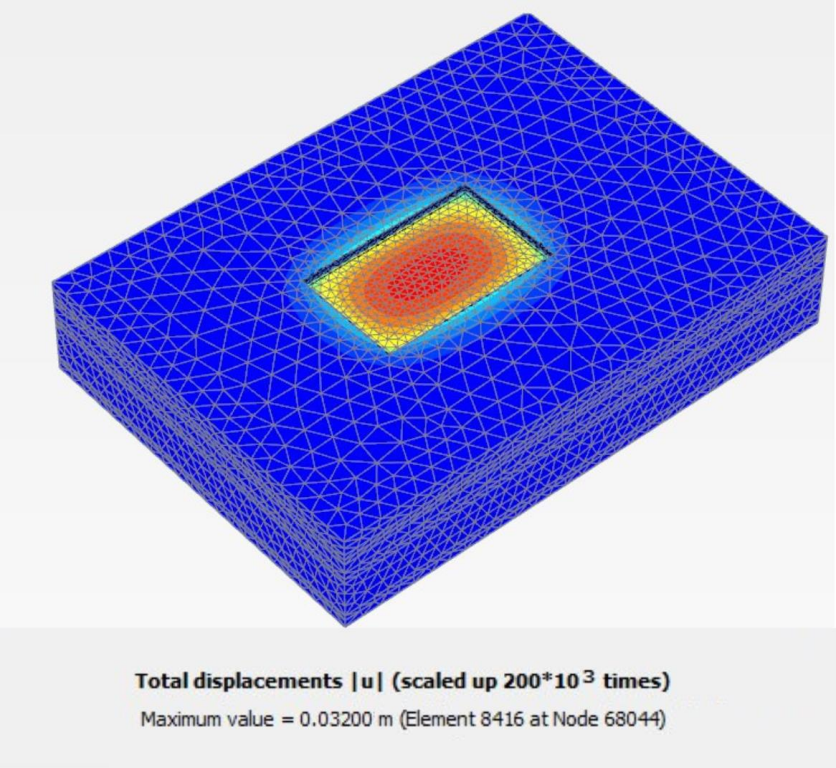

Figure 64. Deformation analysis.

Total displacement is equal to 0.032 m, which is 1.26 in. The existing California Building Code does not specify limits for total and differential settlement of foundations that support tall commercial or residential buildings (Applied Technology Council, 2018). Nevertheless, many professionals and officials in the building departments of different cities find a total settlement of less than 4 inches acceptable (Applied Technology Council, 2018). Our building does not exceed this number, therefore, it can be considered safe.

3.11 Lateral bearing

The lateral bearing capacity of a pile was determined using Brom's method. First, it was needed to determine if the pile is short rigid or long flexible. If $L/T \geq 4$, then the pile is classified as a long flexible pile:

$$\square = \sqrt[5]{\frac{\square_{\square}\square_{\square}}{\square_h}} \quad (3.54)$$

Where

$\square_{\square}$ – Modulus of elasticity,

$\square_{\square}$ –Moment of inertia

$$\square_{\square} = 4700\sqrt{\square'_{\square}} \quad (3.55)$$

$$\square_{\square} = 4700\sqrt{3.5 * 10^9} = 278.06 \square\square\square$$

$$\square_{\square} = \frac{\square\square^4}{64}$$

$$\square_{\square} = \frac{\square * 0.4^4}{64} = 125.66 * 10^{-6}\ \square^4$$

$$\square = 1.184$$

$10/1.184 \geq 4$, therefore, we consider piles as long and flexible.

Next, Rankine passive earth pressure coefficient was calculated:

$$\square_{\square} = \square\square\square^2(45 + \frac{\square}{2}) \quad (3.56)$$

$$\square_{\square} = \square\square\square^2(45 + \frac{37}{2}) = 4.023$$

The formula for section modulus of pile section:

$$\square = \frac{\square\square^3}{32} \quad (3.57)$$

$$\square = \frac{\square * 0.4^3}{32} = 0.0063$$

Lastly, the yield moment can be obtained using the following equation ($□_□$ is assumed to be 35 MPa)

$$□_□ = □□_□ \quad (3.58)$$

$$□_□ = 188.49 \, □□ \cdot □$$

After we obtain all the necessary values, we can use the graph from Figure 3.18.

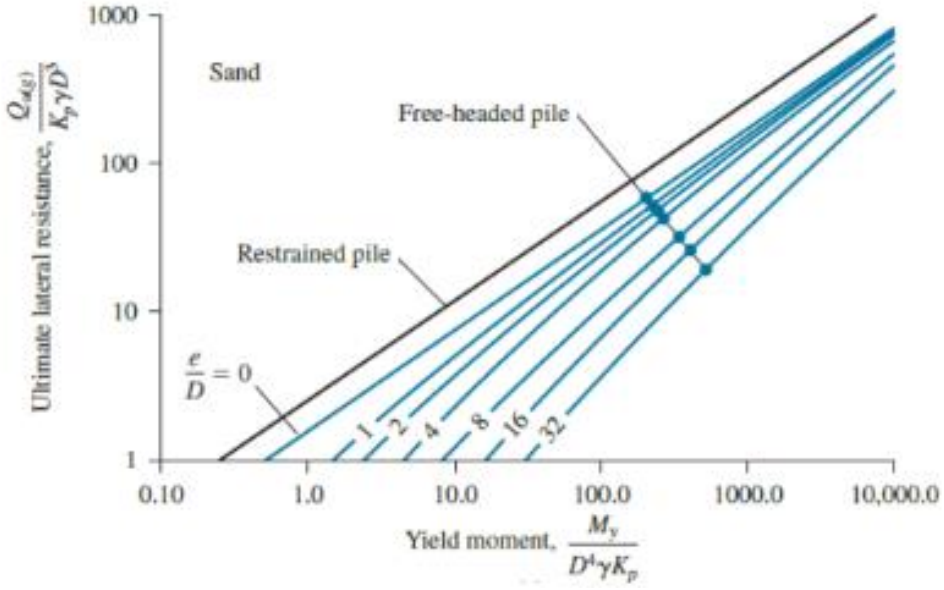

Figure 65.The solution of Broms for ultimate lateral resistance of long piles (Das & Sivakugan, 2019).

$□_□$ was determined from this graph and $□_{□□□}$ was calculated

$$□_{□□□} = \frac{□_□}{□□} = \frac{354.49}{3} = 118.16 \, □□$$

3.12. Lateral deflection

The lateral deflection of a pile needs to be calculated to see how much a pile bends under horizontal forces. The elastic method was used to calculate lateral deflection.

The deflection at the pile head was calculated using this equation:

$$\eta = \sqrt[5]{\frac{\square_h}{\square_\square \square_\square}}$$

(3.59)

Deflection at any point of the pile is calculated as follows:

$$\square_\square = \square_\square \frac{\square_\square \square^3}{\square_\square \square_\square} + \square_\square =$$

$$\frac{\square_\square \square^2}{\square_\square \square_\square}$$

(3.60)

The A_x and B_x coefficient values are taken from the table by Das & Sivakugan (2019). The results are shown in Table 46.

Table 46. Lateral deflection values

Z	Thickness, m	Ax	Bx	xz interior	xz exterior	xz corner
0	1.52	2.435	1.623	21.372	22.514	20.543
1	1.53	0.962	0.364	4.710	4.927	4.373
2	3.04	0.142	-0.07	-0.971	-1.043	-1.025
3	3.05	-0.075	-0.089	-1.184	-1.252	-1.160
4	3.05	-0.05	-0.028	-0.367	-0.386	-0.350
5	3.05	-0.009	0	0.002	0.003	0.005
6	1.52	0	0	0.000	0.000	0.000
7	1.53	0	0	0.000	0.000	0.000

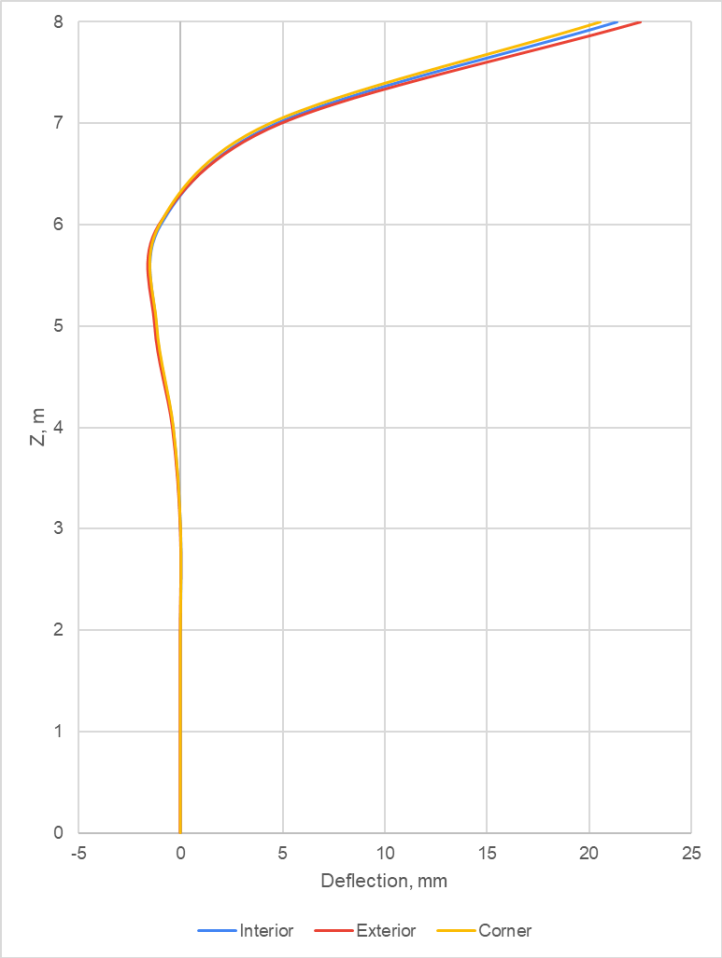

Figure 66. Pile deflection

3.13 Sheet pile design

3.13.1 Hand calculations

To prevent soil movement in a lateral direction, structures like retaining walls, sheet piles, or braced cuts are used in the construction. Retaining walls may require proper drainage behind the wall to prevent water interference (Das, 2010). Braced cuts are primarily suitable for temporary work in a relatively small area (Das, 2017). While sheet piles are used when the excavations are over a large area (Das, 2017). Also, compared with retaining walls, they do not require water removal from the site (Das, 2017). In addition, sheet piles are light, cost-effective,

and comfortable to use as they resist the stress of being driven into the hard soil (Das, 2017). Therefore, the sheet pile is chosen as a lateral load-bearing structure for the hotel's construction.

There are two types of sheet piles: cantilever and anchored. Cantilever sheet piles are usually used for walls less than 6 m in height; therefore, this type of sheet pile is chosen for this project (Das, 2017).

The length of the sheet pile is designed to be 6.255 meters, which is equal to the height of the basement. The unit weight of soil at this length is equal to 18.1 kN/m3 and the friction angle is equal to 36 degrees.

As the construction site has no water table, the equations for cantilever walls in a dry sandy soil will be used.

To start hand calculations, Rankine earth pressure coefficients should be calculated:

$$\square_{\square} = \square\square\square^{2}(45 - \frac{\square'}{2}) \quad (3.61)$$

$$\square_{\square} = \square\square\square^{2}(45 - \frac{39.34}{2}) = 0.224$$

$$\square_{\square} = \square\square\square^{2}(45 - \frac{\square'}{2}) \quad (3.62)$$

$$\square_{\square} = \square\square\square^{2}(45 - \frac{39.34}{2}) = 4.463$$

In order to minimize the risks, the factor of safety of 2 is used for calculating passive earth pressure coefficient.

$$\square_{\square(\square\square\square)} = \frac{\square_{\square}}{\square\square} = 2.23$$

Then, the active pressure can be found using the following equation:

$$\sigma_2' = \square\square\square_{\square} \quad (3.63)$$

$$\sigma_2' = 17.21 * 6.255 * 0.224 = 24.12\ \square\square/\square^2$$

The net pressure at equals to zero at a depth $\square_3$ and this length is calculated as follows:

$$\square_3 = \frac{\square\square_{\square}}{\square_{\square(\square\square\square)} - \square_{\square}} \quad (3.64)$$

$$\square_3 = \frac{6.255 * 0.224}{2.23 - 0.224} = 0.70\ \square$$

To calculate σ_5', the following formula is used:

$$\sigma_5' = \square\square\square_{\square(\square\square\square)} + \square\square_3(\square_{\square(\square\square\square)} - \square_{\square}) \quad (3.65)$$

$$\sigma_5' = 17.21 * 6.255 * 2.23 + 17.21 * 2.23(2.23 - 0.224) = 264.35\ \square\square/\square^2$$

Area of the pressure diagram is found as follows:

$$\square = 0.5\square_2'(\square + \square_3) \quad (3.66)$$

$$\square = 0.5 * 24.12(6.255 + 0.70) = 83.85\ \square\square/\square$$

$$P = 83.85\ kN/m$$

Then, the center of pressure for the area is found using the following equation:

$$\underline{\square} = \frac{\square(2\square_{\square} + \square_{\square(\square\square\square)})}{3(\square_{\square(\square\square\square)} - \square_{\square})} \tag{3.67}$$

$$\underline{\square} = \frac{6.255(2 * 0.225 + 2.23)}{3(2.23 - 0.224)} = 2.78\ \square$$

The areas $\square_1'$, $\square_2'$, $\square_3'$ and $\square_4'$ are found by following equations:

$$\square_1' = \frac{\square_5'}{\square(\square_{\square(\square\square\square)} - \square_{\square})} \tag{3.68}$$

$$\square_1' = \frac{264.35}{17.21(2.23 - 0.224)} = 7.65\ \square^2$$

$$\square_2' = \frac{8\square}{\square(\square_{9(\square\square\square)} - \square_{\square})} \tag{3.69}$$

$$\square_2' = \frac{8 * 83.85}{17.29(2.23 - 0.224)} = 19.41\ \square^2$$

$$\square_3' = \frac{6\square(2\underline{\square}\square(\square_{\square(\square\square\square)} - \square_{\square}) + \square_5')}{(\square(\square_{\square(\square\square\square)} - \square_{\square}))^2} \tag{3.70}$$

$$\square_3' = \frac{6 * 83.85 * (2 * 2.78 * 17.21(2.23 - 0.224) + 264.35)}{(17.21(2.23 - 0.224))^2} = 192.46\ \square^2$$

$$\square_4' = \frac{\square(6\underline{\square}\square_5' + 4\square)}{(\square(\square_{\square(\square\square\square)} - \square_{\square}))^2} \tag{3.71}$$

$$\square_4' = \frac{83.85(6 * 2.78 * 264.35' + 4 * 83.85)}{(17.21(2.23 - 0.224))^2} = 333.61\ \square^2$$

Then, $\square_4$ can be obtained from the following equilibrium equation:

$$\square_4{}^4 + \square_1'\square_4{}^4 - \square_2'\square_4{}^2 - \square_3'\square_4 - \square_4' = 0 \quad (3.72)$$

$$\square_4 = 3.45\ \square$$

Thus,

$$\square_{\square h\square\square\square} = \square_3 + \square_4 = 4.15\ \square$$

Total length,

$$\square_{\square\square\square\square\square} = \square + 1.3(\square_{\square h\square\square\square}) = 6.255 + 1.3(4.15) = 11.65\ \square$$

Equation for σ'_3 is:

$$\sigma'_3 = \square_4(\square_{\square(\square\square\square)} - \square_{\square})\square \quad (3.73)$$

$$\sigma'_3 = 3.45(2.23 - 0.224) * 17.21 = 119.20\ \square\square/\square^2$$

σ'_4 is calculated:

$$\sigma'_4 = \square'_5 + \square\square_4(\square_{\square(\square\square\square)} - \square_{\square}) \quad (3.74)$$

$$\sigma'_4 = 264.35 + 17.21 * 3.45 * (2.23 - 0.224) = 383.55\ \square\square/\square^2$$

Then, $\square_5$ is obtained:

$$\square_5 = \frac{\square'_3\square_4 - 2\square}{\square'_3 + \square'_4} \quad (3.75)$$

$$□_5 = \frac{119.20 * 3.45 - 2 * 83.85}{119.20 + 383.55} = 0.48 □$$

Finally, to find the maximum moment per unit length of the wall, the point of the zero shear is found:

$$□' = \sqrt{\frac{2□}{□(□_{□(□□□)} - □_□)}} \quad (3.76)$$

$$□' = \sqrt{\frac{2 * 83.85}{17.21(2.23 - 0.224)}} = 2.20□$$

Then, the magnitude of the maximum moment can be obtained as:

$$□_{□□□} = □(□ + □') - (\frac{1}{2}□□'^2(□_{□(□□□)} - □_□)\frac{1}{3}□') \quad (3.77)$$

$$□_{□□□} = 83.85(2.78 + 2.20) - (\frac{1}{2}17.21 * 2.20^2(2.23 - 0.224)\frac{1}{3} * 2.20) = 356.51 □□ \cdot □/□$$

The necessary profile of the sheet piling is then obtained using the following equation, where $\sigma_{□□□}$ is taken as 170 MN/m2 according to ASTM A328:

$$□ = \frac{□_{□□□}}{□_{□□□}} \quad (3.78)$$

$$□ = \frac{356.51}{170 * 10^3} = 2.10 * 10^{-3} □^3/□$$

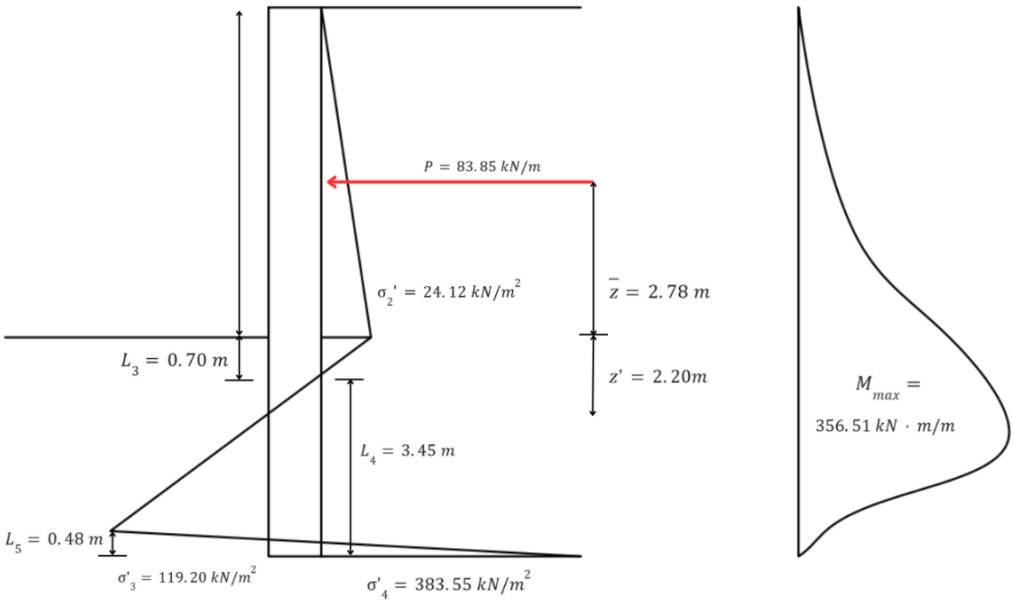

Figure 67. Sheet pile design

3.13.2 Software analysis in Geo5

The Geo5 software was used to verify hand calculations. The maximum bending moment and maximum shear force was determined and shown on Figure .

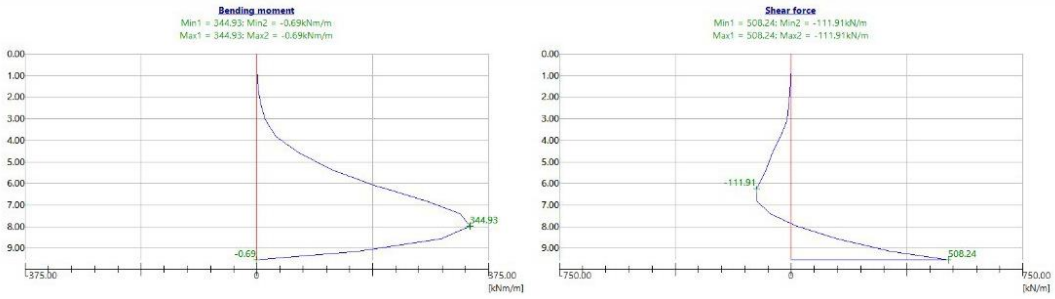

Figure 68. Maximum bending moment and shear force in Geo5

Maximum bending moment was calculated as 344.93 kN· m and maximum shear force is 508.24 kN. These results were satisfactory according to the software.

Figure 69. Maximum bending moment and shear force results

The slope stability was checked with five different methods and the results are shown in Figure .

Figure 70. Slope stability of the sheet pile

3.13. Lateral Earth Pressure

3.13.1. Lateral earth pressure at rest

The coefficient of earth pressure was estimated using Jaky's equation (1944):

$$□_0 = 1 - □□□□'$$ (3.79)

The lateral pressure is equal to:

$$\sigma_h = □_0□_0'$$ (3.80)

The values of lateral earth pressure at rest are shown in the Table

Table 47. Lateral earth pressure at rest.

Depth, m	γ , kN/m3	φ'	σ_0' , kN/m2	Ko	σ_h, kN/m2
0-3.05	14.50	43	44.23	0.32	14.06

3.05-4.57	21.20	43	76.45	0.32	24.31
4.57-6.10	18.60	36	104.91	0.41	43.24
6.10-6.225	18.10	36	107.17	0.41	44.18

The total force obtained is equal to the sum of the separate areas in the pressure diagram shown on Figure 71.

$$□_0 = □□□□□_{□□□□□□□□□□} + □□□□□_{□□□□□□□□□} = □_1 + □_2 + \ldots + □_7 \quad (3.81)$$

$$□_0 = \frac{3.05 * 14.06}{2} + 1.52 * 14.06 + \frac{1.52 * (24.31 - 14.06)}{2} + \ldots + \frac{0.125 * (44.18 - 43.24)}{2}$$

$$= 107.75 \; □□/□3$$

The location of the resultant force is calculated as follows:

$$\underline{□} = □(□□□□_{□□□□□□□□□□} \times \frac{□}{2}) + □(□□□□_{□□□□□□□□□} \times \frac{□}{3}) \quad (3.82)$$

$$\underline{□} = \frac{\frac{3.05 * 14.06}{2} \times (\frac{3.05}{3} + 3.175) + (1.52 * 14.06) \times (\frac{4.57 - 3.05}{2} + 1.655) + \ldots + \frac{0.125 * (44.18 - 43.24)}{2} \times \frac{0.12}{3}}{□_0}$$

$$= 1.87 \; □$$

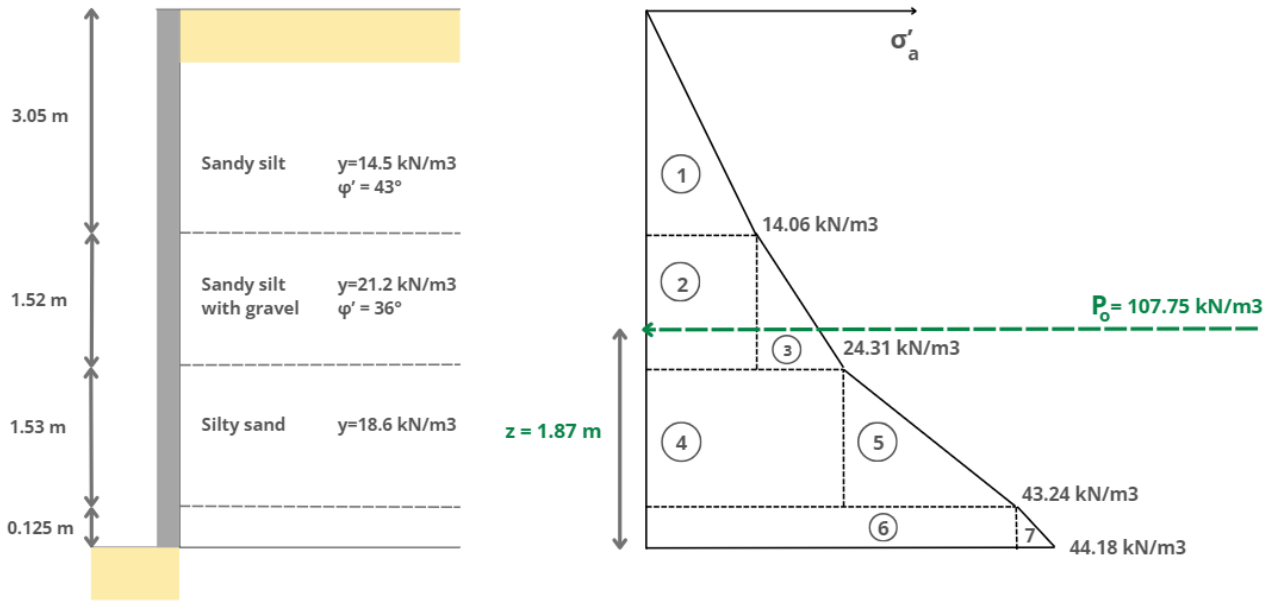

Figure 71. Pressure distribution diagram for lateral earth pressure at rest.

3.13.2. Rankine active earth pressure

The Rankine active-pressure coefficient should be calculated as it is the minimum pressure the soil exerts on the wall.

$$\square_{\square} = \square\square\square^{2}(45 - \frac{\square'}{2}) \quad (3.83)$$

The lateral pressure is equal to:

$$\sigma_{\square}' = \square_{\square}\square_{0}' - 2\square'\sqrt{\square_{\square}} \quad (3.84)$$

Values of Rankine active earth pressure are given in the table below.

Table 48. Rankine active earth pressure.

Depth, m	γ , kN/m3	φ'	σ_0', kN/m2	Ka	$\sigma_{\square}'$, kN/m2
0	0.00	43	0.00	0.19	0.00

3.05-	14.50	43	44.23	0.19	8.36
3.05+	21.20	43	44.23	0.19	8.36
4.57-	21.20	43	76.45	0.19	14.45
4.57+	18.60	36	76.45	0.26	19.85
6.1-	18.60	36	104.91	0.26	27.24
6.1+	18.10	36	104.91	0.26	27.24
6.225	18.10	36	107.17	0.26	27.82

The pressure distribution diagram is plotted in Figure 72. The force per unit length is:

$$□_0 = □□□□□_{□□□□□□□□□□} + □□□□□_{□□□□□□□□□□} = □_1 + □_2 + \ldots + □_7$$

$$= \frac{1}{2}(8.36)(3.05) + (8.36)(1.52) +$$

$$+ \ldots + \frac{1}{2}(27.82 - 27.24)(0.125) = 69.55 \; □□/□3$$

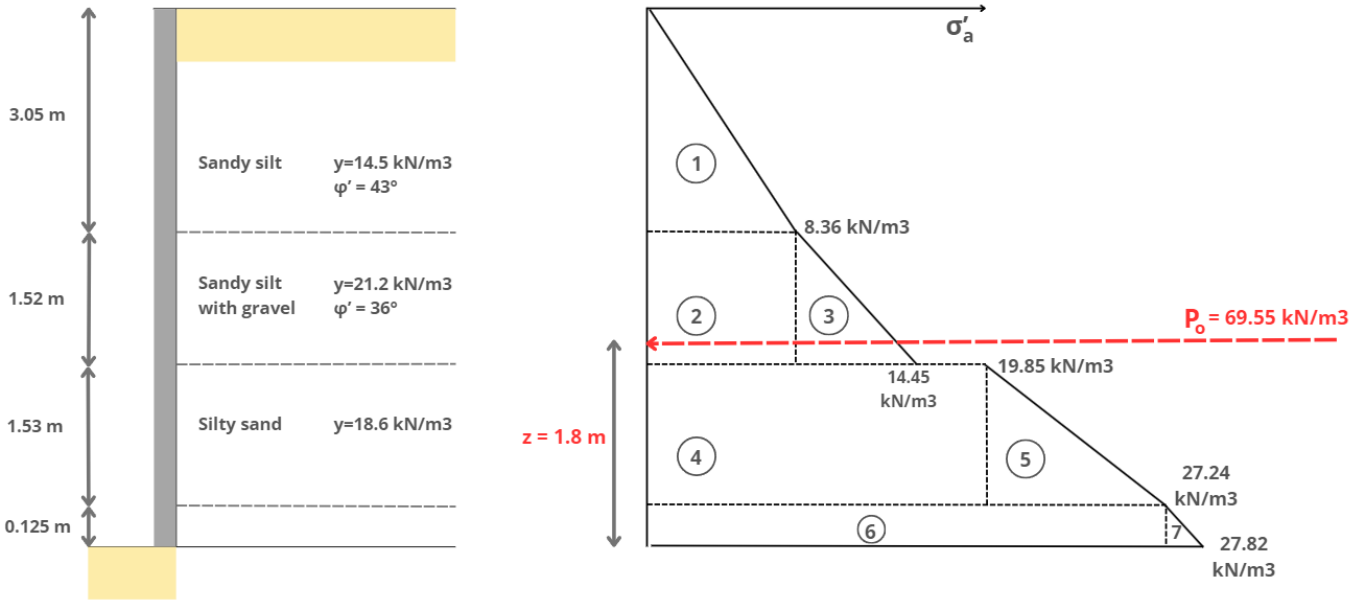

Figure 72. Pressure distribution diagram for rankine active earth pressure

The distance of the line of action of the resultant force from the bottom of the wall can be determined by taking the moments about the bottom of the wall:

$$\underline{\square} = \square(\square\square\square\square_{\square\square\square\square\square\square\square\square\square\square} \times \frac{\square}{2}) + \square(\square\square\square\square_{\square\square\square\square\square\square\square\square\square} \times \frac{\square}{3})$$

$$\underline{\square}$$

$$= \frac{\frac{3.05 * 8.36}{2} \times (\frac{3.05}{3} + 3.175) + (1.52 * 8.36) \times (\frac{4.57 - 3.05}{2} + 1.655) + \ldots + \frac{0.125 * (27.82 - 27.24)}{2} \times \frac{0.125}{3}}{\square_0}$$

$$= 1.8 \square$$

3.14. Construction procedure

Thorough site preparation is completed in order to make sure that all construction activities are performed efficiently and within a schedule. As part of high-rise construction like the South Park project, this phase commonly takes 1–2 months on average, relative to the location and site characteristics.

Clearing and Surveying the Site

The first step is clearing the parking area which includes demolishing existing structures like the asphalt covering the area. Also, it included surveying the site in detail so that all boundaries and construction zones are marked with precision. It's also worth noting that during this phase, all known underground utilities including power and telecommunication lines are marked out to avoid construction related disruptions or safety hazards.

Subsoil Testing and Investigation

A site survey is usually followed with soil testing to determine the capacity of the site to withstand loads. Results assist in classifying the soil and recommending the best type of foundation to be constructed. In instances when soils are found undesirable to work with, different engineering approaches or even abandoning the site might be decided. A site investigation consists of analyzing the soil profile, groundwater table, and soil conditions, which is important for precise foundation design.

Site Planning

Upon conducting the investigations, a site plan capturing the major layouts of the drainage, access roads, temporary site office and material storage area is prepared. This plan prepares the site and is updated periodically to reflect ongoing changes on-site.

Sheet Pile Installation and Excavation

The site is marked and cleared before sheet piles are put in place around the border, and these are installed using the shock vibration technique. This is done to protect the soil while excavation is going on, and it also fills hydraulic press requirements which ensures cost savings. Sheet piles can also be removed later by vibratory drivers with low ground vibration emission, improving the carbon footprint. Sustainably, the free excess soil can also be used for backfill, roads, and soft landscaping.

Pile Installation

Driven piles were chosen for this project as they have a high load bearing capacity, don't involve excavation, and suitable for our depth of 15.225 m. The installation process includes positioning the pile at a marked location, driving the pile using a pile driving rig and a hammer, and checking the hammer energy and perpendicularity of the pile to a ground surface to ensure proper installation.

Pile Cap Construction

Once the piles are set and trimmed to be the same level, pile caps are constructed. The construction involves placing a designed reinforcement in place before pouring concrete. This allows to create strong connections between piles and a pile cap. After the pile caps are constructed, the soil is leveled for further construction procedures.

This approach to site preparation and foundation installation ensures safety, stability, and efficiency, ensuring good groundwork for the construction project.

4. Environmental Part

4.1 Description of selected site and the climatic conditions.

The construction site is located on the southeast side of the intersection between West Olympic Boulevard and Hill Street in Los Angeles, California. The site's proximity to the airport makes it a strategic choice for a hotel, providing a convenient stay option for travellers.

Los Angeles has a Mediterranean climate characterised by dry summers and rainy winters, with relatively mild temperature fluctuations throughout the year. This climate predictability is advantageous for planning the stormwater sewer systems, as weather-related challenges are more manageable.

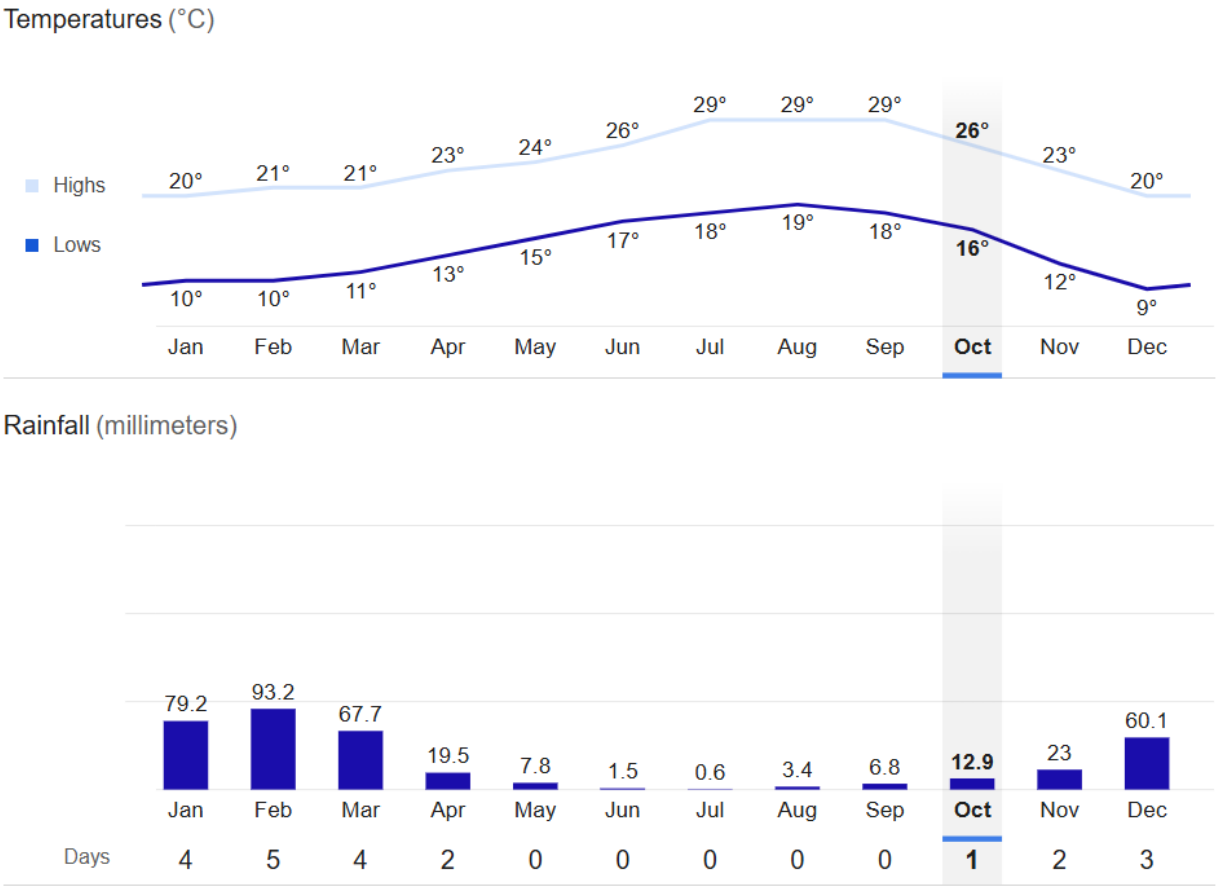

Figure 73. Weather conditions of LA city

In Los Angeles, summer is typically dry, with almost no rainy days, while rainfall increases through fall and peaks in winter. A reliable stormwater sewage design is critical to prevent flooding, which can impact city infrastructure.

4.2 Stormwater sewage system in the city.

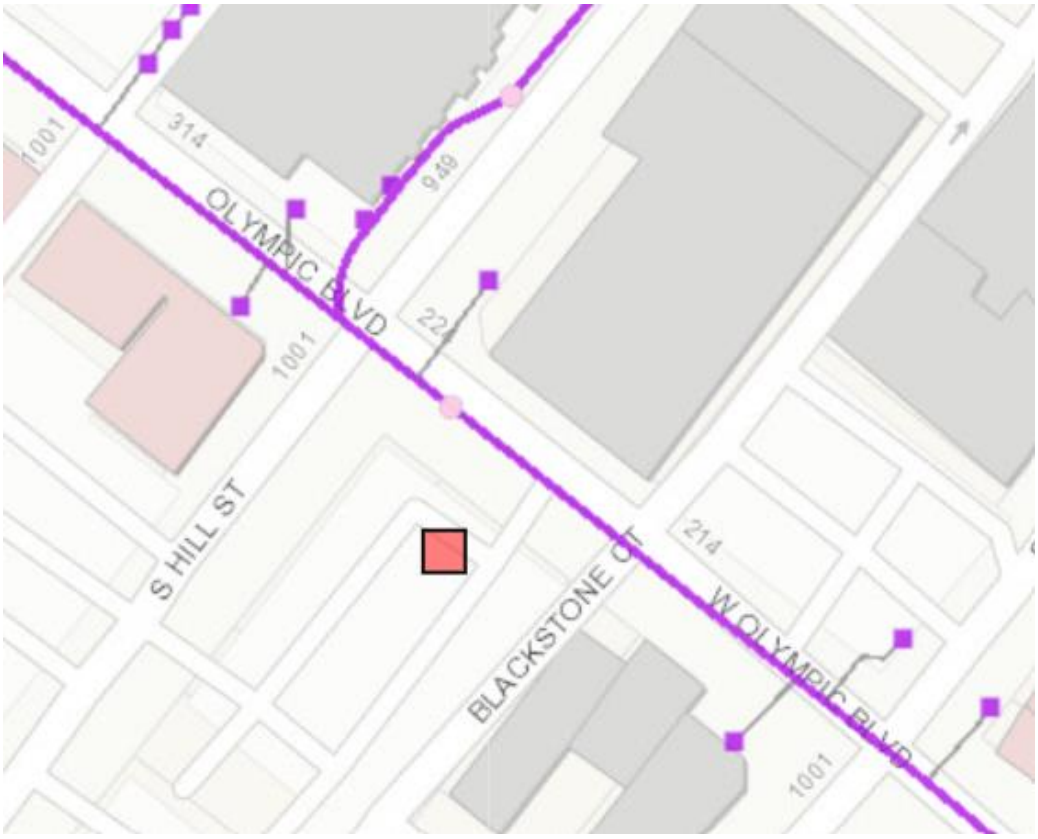

Figure 74. Site layout with flow directions and preliminary pipeline ways

The closest stormwater sewage pipelines are situated along West Olympic Boulevard. These Municipal Separate Storm Sewer System (MS4) lines are owned and operated by the City of Los Angeles.

4.3 Topographic map and cross-sectional profile

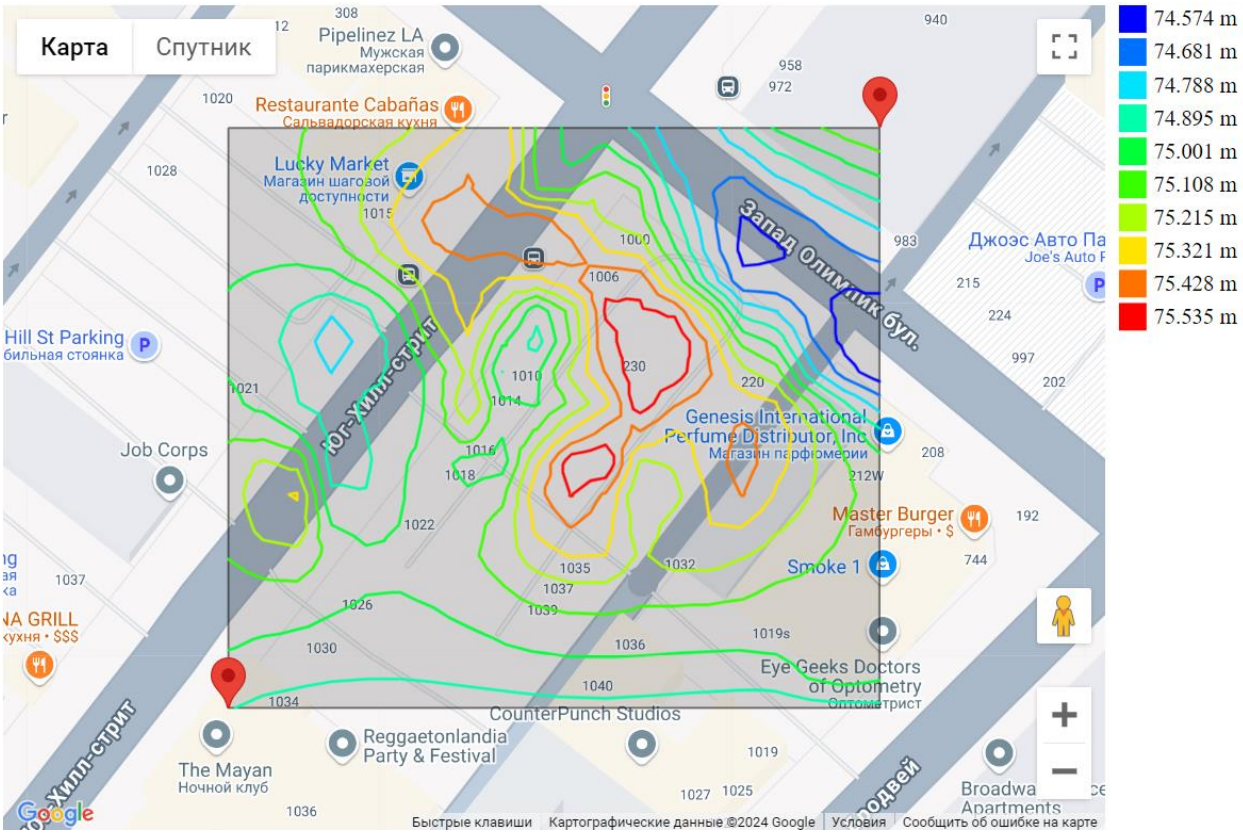

Figure 75. Topographic Map of the Site

As shown in Figure 4.3.1 Topography of the site does not allow runoff to leak to the center from outside. The site's topographic map indicates that the highest points are centrally located within the planned building and parking areas. Runoff will naturally flow from these central points toward the southeast and southwest due to the site's slight inclination. This is totally opposite for idea of using drainage channels around the building to collect all stormwater runoff on the site.

In order to solve this problem, the ground of the site requires grading for the needed directions.

4.4 Grading plan for the site

Grading of the site is required not only for the aesthetics of the site and its usability, but also for the management of proper drainage on the site to prevent it from flooding or pooling.

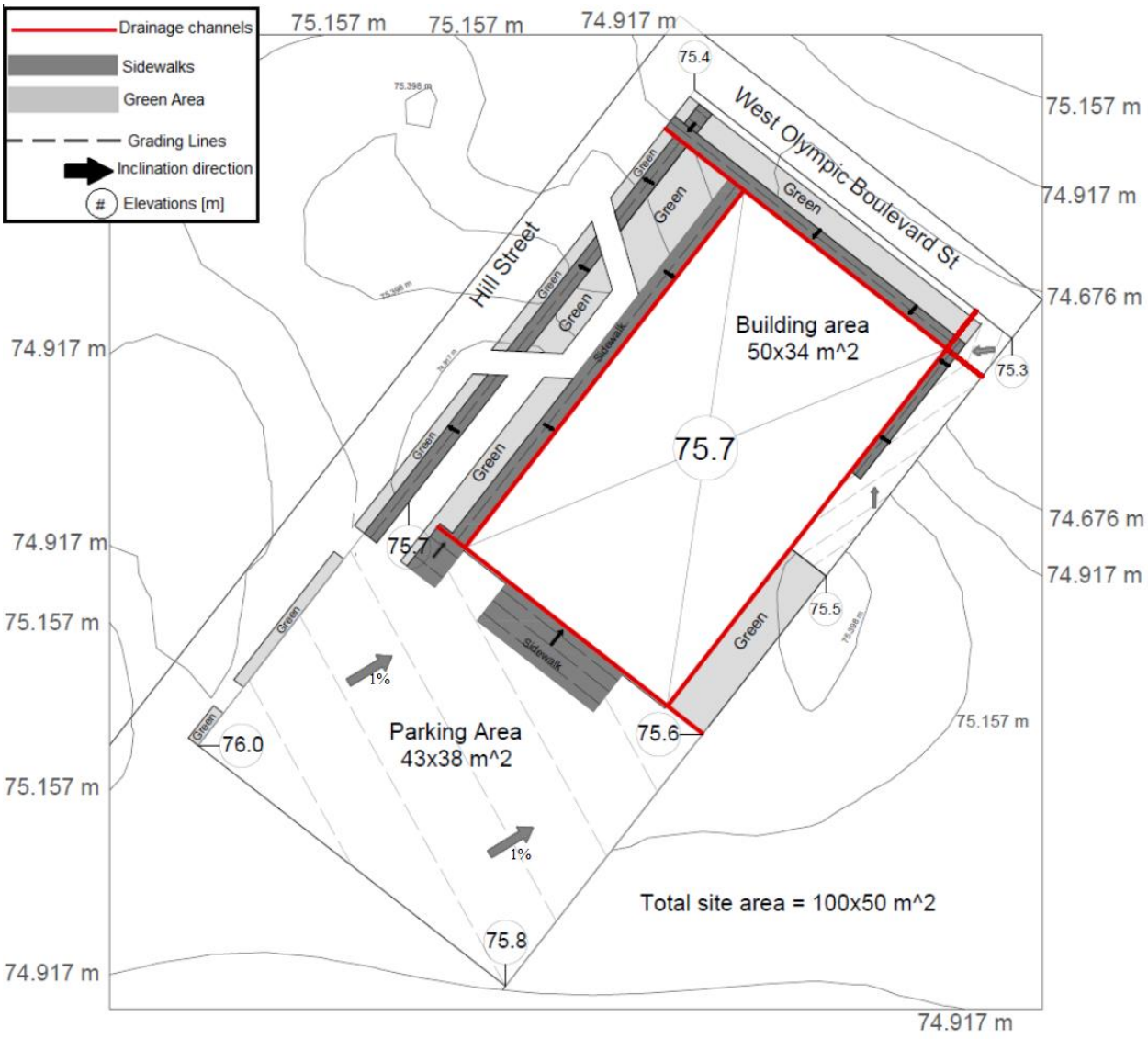

Figure 76. Grading plan for the Site

Grading for the site was implemented with the main purpose of making the inclination to the sides of drainage channels. Generally for grading, the site will be higher than it used to be according to the Topography map. The soil needed for making it elevated will be taken from those which will be dug from the main building area to construct 2 underground storeys used for underground parking.

As the highest point of the topography used to be about 75.5m above sea level, by grading, the highest point located at the South-West corner of the Parking area will be 76.0m. Parking area generally will be flat, however will have a few inclinations enough to direct the stormwater to leak to the North-East corner, to drainage channels located along the South side of the building. Building top itself will have no inclination, as it should be flat and parallel to the ground in which it will be 75.7m above sea level.

The sidewalks area located around the building will have an inclination to the drainage channels (red lines in Figure 38). However, areas of sidewalks far from the main building area and near to Hill street will have an inclination to the side of the Green area.

Green areas will have no gradings in this plan due to very few differences in elevations in topography at the particular areas. In addition, it is expected that Green areas will absorb all the stormwater, considering the climatic and weather conditions of low amounts of rain in LA city, which will not exceed the amount of water for the Green Areas.

Finally, throughout the lowest point of the site which will have an elevation of 75.3m above sea level, rainwater collected by the drainage channels will be connected through underground pipelines to the MS4 Stormwater Sewage system of LA.

4.5 Rainfall Estimation

According to The Los Angeles County Department of Public Works - LACDPW - for the proper design of stormwater drainage systems we should use the **10 years** interval of recurrence of storm with **15 minutes** duration.
By the use of The official data NOAA Atlas 14 - Precipitation-Frequency Atlas we found the precipitation rates for the site. It shows that rainfall amount is **0.639 inches** as the highest/maximum. For the best design we should consider the possibility of the worst case with

the highest amount of rainfall, so we use the 0.639 inches, rather than the given average **0.523 inches** (see the Figure 77).

PDS-based point precipitation frequency estimates with 90% confidence intervals (in inches)[1]										
Duration	Average recurrence interval (years)									
	1	2	5	10	25	50	100	200	500	1000
5-min	0.152 (0.128-0.184)	0.195 (0.163-0.235)	0.252 (0.210-0.306)	0.302 (0.249-0.369)	0.372 (0.297-0.472)	0.430 (0.335-0.557)	0.491 (0.373-0.653)	0.557 (0.410-0.763)	0.651 (0.459-0.932)	0.729 (0.495-1.08)
10-min	0.219 (0.183-0.264)	0.279 (0.233-0.337)	0.362 (0.301-0.439)	0.432 (0.357-0.529)	0.534 (0.425-0.676)	0.616 (0.480-0.798)	0.703 (0.534-0.935)	0.798 (0.588-1.09)	0.933 (0.658-1.34)	1.04 (0.710-1.55)
15-min	0.264 (0.221-0.319)	0.337 (0.282-0.408)	0.438 (0.365-0.530)	0.523 (0.432-0.639)	0.645 (0.514-0.818)	0.745 (0.580-0.965)	0.850 (0.646-1.13)	0.965 (0.711-1.32)	1.13 (0.796-1.62)	1.26 (0.859-1.88)
30-min	0.352 (0.295-0.425)	0.450 (0.376-0.543)	0.583 (0.486-0.707)	0.697 (0.576-0.852)	0.860 (0.686-1.09)	0.993 (0.774-1.29)	1.13 (0.861-1.51)	1.29 (0.948-1.76)	1.50 (1.06-2.15)	1.68 (1.14-2.50)
60-min	0.505 (0.423-0.609)	0.644 (0.539-0.779)	0.836 (0.697-1.01)	0.999 (0.825-1.22)	1.23 (0.983-1.56)	1.42 (1.11-1.84)	1.62 (1.23-2.16)	1.84 (1.36-2.52)	2.16 (1.52-3.09)	2.41 (1.64-3.58)
2-hr	0.723 (0.605-0.873)	0.930 (0.778-1.12)	1.21 (1.01-1.47)	1.45 (1.20-1.77)	1.79 (1.43-2.27)	2.06 (1.60-2.67)	2.35 (1.78-3.12)	2.65 (1.96-3.63)	3.09 (2.18-4.42)	3.44 (2.34-5.11)

Figure 77. PDS-based precipitation rate by NOAA

Then rainfall intensity per hours will be calculated as: $I = 0.639 \times \frac{60}{15} = 2.556\ inches/hour$

4.6 Site planning

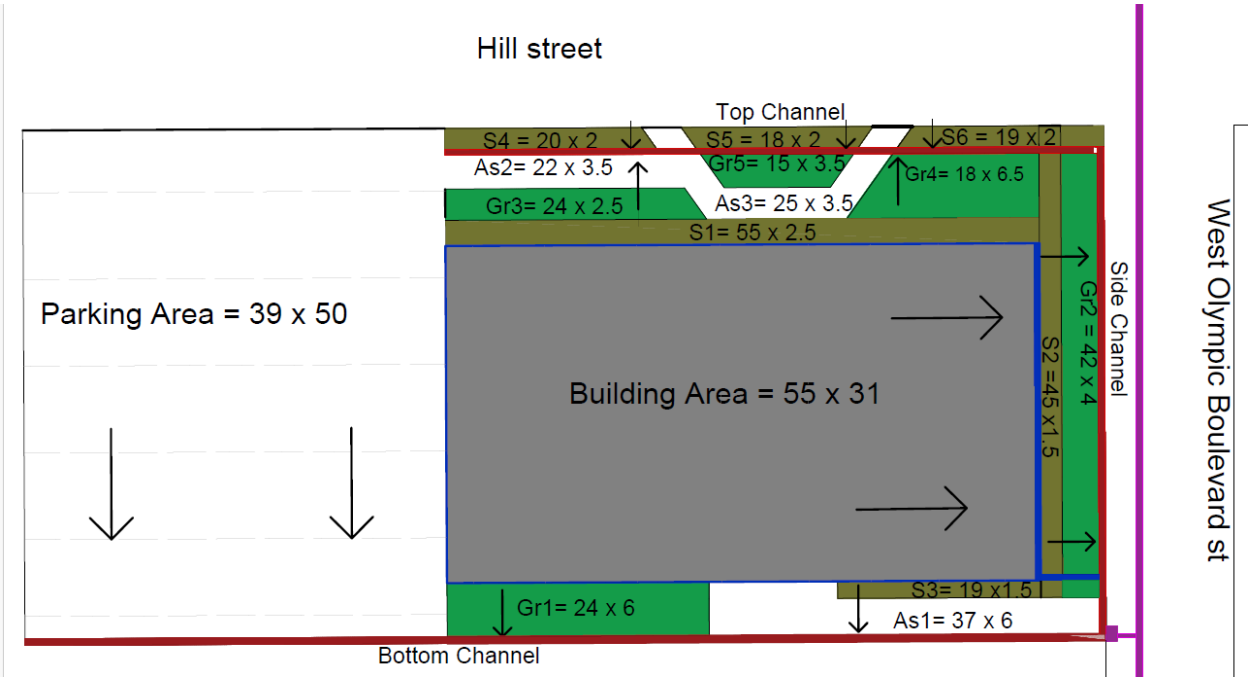

Figure 78. Site plan by sections and dimensions

During the work, it was decided to place all of the channels outside of the building, in order to avoid the possibility of foundation settlement or foundation subsidence. So now the little changes were implemented so the main channels are located far from the building.

The whole area of the site was splitted by sections due to that all of them have different shapes, pavements, directions. It was decided to use three main drainage channels which are shown by red colour on the Figure 4.6.1. Areas for each of the parts of the site is given on the table below.

Table 49. Site section's dimensions and area in meters and acres

Section	Length (m)	Width (m)	**Area (m^2)**	**Area (acres)**
Building Area	55	31	1705	0.4213
Parking Area	39	50	1950	0.4819
Sidewalk 1 (S1)	55	2.5	137.5	0.0340
Sidewalk 2 (S2)	45	1.5	67.5	0.0167
Sidewalk 3 (S3)	19	1.5	28.5	0.0070
Sidewalk 4 (S4)	20	2	40	0.0099
Sidewalk 5 (S5)	18	2	36	0.0089

Sidewalk 6 (S6)	19	2	38	0.0094
Green area 1 (Gr1)	24	6	144	0.0356
Green area 2 (Gr2)	42	4	168	0.0415
Green area 3 (Gr3)	24	2.5	60	0.0148
Green area 4 (Gr4)	18	6.5	117	0.0289
Green area 5 (Gr5)	15	3.5	52.5	0.0130
Asphalt 1 (As1)	37	6	222	0.0549
Asphalt 2 (As2)	22	3.5	77	0.0190
Asphalt 3 (As3)	25	3.5	87.5	0.0216

4.7 Manning's equation, Peak Runoff Calculation

For the calculation of the Flow Rate in channels, we use the Manning's equation:

$$Q = \frac{1.49}{n} \times A \times R^{2/3} \times S^{1/2}$$

Q = flow rate (cubic feet per second, **cfs**)

n = Manning's roughness coefficient (depends on surface roughness)

A = cross-sectional area of flow (square feet)

R = hydraulic radius (feet) = A/P, where P is the wetted perimeter

S= slope of the grade line (dimensionless)

In order to design the sizing of channels, we first should find the Peak Runoff amount of rainfalls so the designed channel's Flow Rate could handle it.

Flow rate: $Q = CIA$

Q = Peak Runoff

C = Runoff coefficient

A = area of surface in square feet

Each of the constants are given below:

Slope for each of the parts was designed to be 1%, which is typical in most of the cases of site plannings for stormwater collection designs.

$$S=1\%=0.01ft/ft$$

Table 50. Roughness Coefficient

Surface	Roughness Coefficient, n
Smooth asphalt	0.011
Smooth Concrete	0.012
Short grass prairie	0.15
Dense grasses	0.24

Table 51. Intercept Coefficient

Surface	Intercept Coefficient, k
Paved Area	0.619
Unpaved	0.419
Grassed waterway	0.457

Table 52. Runoff Coefficient

Surface	Runoff Coefficient, C
Asphalt	0.9

Concrete sidewalks	0.85
Building roof	0.95
Grass	0.3

4.8 Calculation of Peak Runoff

Section Name	Building Area	Parking Area	S1	S2	S3	S4	S5	S6	Gr1	Gr2	Gr3	Gr4	Gr5	As1	As2	As3
Length (m)	31.0000	39.0000	55.0000	45.0000	19.0000	20.0000	18.0000	19.0000	24.0000	42.0000	24.0000	18.0000	15.0000	37.0000	22.0000	25.0000
Width (m)	55.0000	50.0000	2.5000	1.5000	1.5000	2.0000	2.0000	2.0000	6.0000	4.0000	2.5000	6.5000	3.5000	6.0000	3.5000	3.5000
Area (m²)	1,705.0000	1,950.0000	137.5000	67.5000	28.5000	40.0000	36.0000	38.0000	144.0000	168.0000	60.0000	117.0000	52.5000	222.0000	77.0000	87.5000
Area (acres)	0.4213	0.4819	0.0340	0.0167	0.0070	0.0099	0.0089	0.0094	0.0356	0.0415	0.0148	0.0289	0.0130	0.0549	0.0190	0.0216
Flow Length (length) (L, ft)	101.7110	127.9590	180.4550	147.6450	62.3390	65.6200	59.0580	62.3390	78.7440	137.8020	78.7440	59.0580	49.2150	121.3970	72.1820	82.0250
Flow Length (width)(L, ft)	180.4550	164.0500	8.2025	4.9215	4.9215	6.5620	6.5620	6.5620	19.6860	13.1240	8.2025	21.3265	11.4835	19.6860	11.4835	11.4835
Slope (ft/ft)	0.0100	0.0100	0.0100	0.0100	0.0100	0.0100	0.0100	0.0100	0.0100	0.0100	0.0100	0.0100	0.0100	0.0100	0.0100	0.0100
Roughness coefficient (n)	0.0120	0.0110	0.0130	0.0130	0.0130	0.0130	0.0130	0.0130	0.1500	0.1500	0.1500	0.1500	0.1500	0.0110	0.0110	0.0110
Runoff Coefficient (C)	0.9500	0.9000	0.8500	0.8500	0.8500	0.8500	0.8500	0.8500	0.3000	0.3000	0.3000	0.3000	0.3000	0.9000	0.9000	0.9000
Intercept Coefficient (k)	0.6190	0.6190	0.6190	0.6190	0.6190	0.6190	0.6190	0.6190	0.4570	0.4570	0.4570	0.4570	0.4570	0.6190	0.6190	0.6190
Rainfall Intensity (I) (in/hr)	2.5560	2.5560	2.5560	2.5560	2.5560	2.5560	2.5560	2.5560	2.5560	2.5560	2.5560	2.5560	2.5560	2.5560	2.5560	2.5560
Velocity (V) (ft/sec)	2.0303	2.0303	2.0303	2.0303	2.0303	2.0303	2.0303	2.0303	1.4990	1.4990	1.4990	1.4990	1.4990	2.0303	2.0303	2.0303
Overland flow travel time (T1) (minutes)	4.0568	3.6365	0.6662	0.4903	0.4903	0.5827	0.5827	0.5827	4.8866	3.8313	2.8899	5.1270	3.5364	1.0190	0.7375	0.7375
Conveyance flow travel time (T2)(minutes)	0.8349	1.0504	1.4813	1.2120	0.5117	0.5387	0.4848	0.5117	0.8755	1.5322	0.8755	0.6567	0.5472	0.9965	0.5925	0.6733
Time Concentration (Tc) (minutes)	**4.8918**	**4.6869**	**2.1475**	**1.7023**	**1.0021**	**1.1214**	**1.0675**	**1.0944**	**5.7621**	**5.3635**	**3.7654**	**5.7837**	**4.0836**	**2.0156**	**1.3300**	**1.4108**
Peak Runoff (Q, cfs)	**1.0230**	**1.1085**	**0.0738**	**0.0362**	**0.0153**	**0.0215**	**0.0193**	**0.0204**	**0.0273**	**0.0318**	**0.0114**	**0.0222**	**0.0099**	**0.1262**	**0.0438**	**0.0497**

Figure 79. Table with results

4.9 Design of a channel

For the easy installation and maintenance of the drainage channels, it was decided to use rectangular shaped trench open channels. And firstly for its sizings, the width is chosen to be **0.7 feet** (20-21cm) which is also typical for open channel designs, and which is easy to do maintenance like cleaning etc. Bottom of the channel will be concrete, and for the surface we will use the trench steel.

Figure 80. Trench open channel example

Now by applying the width of 0.7ft and Peak Runoffs for each of the channels (bottom, top and side, as shown in figure 4.2.1) we find the depth for each of three channels.

Calculations for each of channels shows:

Bottom Channel (Length = 100 m)

Contributing Sections: Parking Area, Gr1, As1, S3

Total Peak Runoff: 1.277 cfs

Depth: 0.47 ft (≈ 14.3 cm)

Width: 0.7 ft (≈ 21.3 cm)

Hydraulic Capacity: 1.292 cfs

Top Channel (Length = 61 m)

Contributing Sections: S4, As2, Gr3, S1, As3, Gr5, S5, S6, Gr4

Total Peak Runoff: 0.272 cfs

Depth: 0.16 ft (≈ 4.9 cm)

Width: 0.7 ft (≈ 21.3 cm)

Hydraulic Capacity: 0.294 cfs

Side Channel (Length = 37 m)

Contributing Sections: S2, Gr2, Building Area

Total Peak Runoff: 1.091 cfs

Depth: 0.42 ft (≈ 12.8 cm)

Width: 0.7 ft (≈ 21.3 cm)

Hydraulic Capacity: 1.117 cfs

Highest hydraulic capacity is in the Bottom Channel, which is 1.292 cfs. So this hydraulic capacity will be used for the designing of channels for the whole area, as it is thought to use the same sizings for the channels, rather than making three different sized channels.

So, the calculation for the Bottom Channel shows that the depth will be 0.47ft, which will be rounded to 0.5 ft.

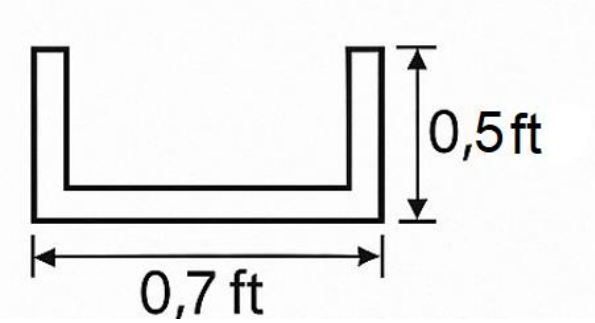

Figure 81. Channel's cross sectional view

5. Construction Management Area

5.1 Project charter

Table 53. Project charter.

General information

<table>
<tr><td>Project title</td><td colspan="3">Design of 15-Storey “South Park” Hotel Building in Los Angeles, California, USA</td></tr>
<tr><td>Project description</td><td colspan="3">The following building is a 15-story hotel with 2-story underground parking. The building will be at 1030 South Hill Street in downtown Los Angeles, California, USA. The 1st floor is the hotel lobby, restaurant, dining room, kitchen, and laundry. The building consists of 7 lifts (5 for commercial use and 2 for working use) and 3 stairs. The following image is a 3D model of the hotel.</td></tr>
<tr><td>3D model</td><td colspan="3">  </td></tr>
<tr><td>Project start date</td><td>August 2024</td><td>Project end date</td><td>January 2026</td></tr>
<tr><td>Problem statement</td><td colspan="3">Los Angeles, a global hub for business and tourism, faces a growing need for premium lodging options in its vibrant South Park District. Our 15-storey hotel project at 1030 S Hill Street aims to meet this demand by</td></tr>
</table>

	overcoming challenges of high construction costs, limited urban space, and sustainability requirements. By integrating innovative design solutions and environmentally conscious construction practices, this hotel will set a new standard for luxury accommodations, enhancing the city's skyline and delivering a profitable and exceptional hospitality experience.
Project objectives	The main objective of the project is to design and build a sustainable, 15-level hotel at 1030 S Hill Street, Los Angeles. The conclusion of this project will be a lushly-appointed accommodation that includes 196 rooms and two high-end restaurants. Following is the list of supplementary project objectives which should be met throughout the project: ● To adhere to local building regulations, seismic safety standards, and environmental guidelines. ● to conduct site and geotechnical analysis to ensure optimal design and regulatory compliance. ● To integrate the hotel's architecture seamlessly with the urban environment of Los Angeles. ● To minimize the environmental footprint through the use of sustainable construction methods and energy-efficient systems. ● to manage costs effectively while maximizing operational efficiency and guest satisfaction. ● To enhance operational efficiency to ensure sustainable profitability.
Project deliverables	1. 15-storey hotel building 2. Parking lots on the ground 3. Underground 2-level parking 4. Restaurants

	5. Courtyard
Estimated budget	$60,131,686
Risks and Possible Issues	• **Regulatory Compliance**: Delays in obtaining permits and meeting local building codes. • **Seismic Risks**: Potential structural vulnerabilities due to earthquakes. • **Cost Overruns**: Unforeseen expenses in materials, labor, or equipment. • **Environmental Impact**: Challenges in meeting sustainability and environmental standards. • **Market Competition**: Difficulty achieving occupancy rates due to nearby hotels. • **Construction Delays**: Weather conditions or supply chain disruptions affecting timelines.
Assumptions	• **Regulatory Approval:** Assuming timely approvals from local authorities for permits and compliance with all building regulations. • **Stable Market Conditions:** Assuming demand for premium lodging remains steady in Los Angeles, supporting projected occupancy rates. • **Qualified Workforce Availabilit**y: Assuming availability of skilled labor and contractors required to meet project timelines. • **Weather Conditions**: Assuming favorable weather conditions to avoid significant construction delays. • **Technology Integration:** Dependence on seamless installation and functioning of energy-efficient systems and hotel management technology.

Team members	Aikelbet Zhumagulova Aruzhan Syndarova Assanali Aldan Bexultan Bazarbayev Nurmukhammed Mukhtarzhanov Yelnur Nurgali

5.2 Feasibility study

A thorough analysis must be done before any construction project is started. A highrise hotel, as a large, complex project, should be preliminarily investigated to duly prove the viability of the project. Below, the project is analysed in terms of each aspect of the future project.

Site Analysis:

The site selected is in downtown Los Angeles, a metropolitan area with world-class shopping malls, restaurants, entertainment venues, corporate offices and everything else one could find. The construction site covers 40,000 square feet so there is plenty of space to perform construction processes, store material stockpiles, as well as achieve the necessary physical separations. Upon completion, its post-construction use will be in outdoor parking and landscaped areas and will be used to augment the whole look and feel of the hotel. The hotel will be located on the south side of the site in a place to allow for safe and efficient vehicular movement and close access to main streets and public transportation centres.

Design and Development Plan:

The stage of preliminary designing of the hotel has also been targeted to modern aesthetics and available functionality, that can be configurable for future adding any of the rooms in case of a sudden need, keeping the maximum amount of fire separation. This product was created in 3D architectural design, in compliance with the California Building Code and the Los

Angeles Building Code, which both demand local authority approvals. Key design features include:

- Structural System: Reinforced Concrete Moment Frame design with C40 grade concrete and Grade 60 rebar, assuring robustness and satisfaction for seismic requirements.
- Floor Layout: The 15 storeys, plus 2 underground levels, will each efficiently serve 196 guest rooms per floor, on average 14 rooms, and have conference and fitness centre facilities for each.
- Sustainability: Energy efficient systems incorporation of LED lighting and sustainable building material aiming towards LEED certification to boost environmental performance.
- Technological Integration: To meet modern guest expectations, advanced technology systems, high-speed Wi-Fi, smart room features and comprehensive security facilities.

Environmental Impact Assessment:

Due to the location of Los Angeles, situated in a seismic zone, the building of a high-rise hotel height comes with compliance with environmental regulations. According to the California Environmental Quality Act, a thorough environmental impact assessment has been conducted:

- Seismic Considerations: The seismic risks are addressed by providing a structured design that includes flexible structural elements and damping systems for enduring earthquakes.
- Soil and Groundwater Analysis: All geotechnical investigations have been carried out concluding soil conditions that the foundation is properly designed for settlement or structural failure.
- Waste Management: Such construction activities there will responsibly manage waste by ensuring that it is recycled and properly disposed of to minimize environmental impact throughout construction.

- Energy Efficiency: The hotel will have post-construction sustainable practices of energy-efficient HVAC systems and water conservation measures to minimise its carbon footprint.

Legal Analysis:

Compliance with all legal requirements is essential to ensure the project's success:

- Permits and Approvals: Early in the project, obtaining needed building permits, zoning clearances, and environmental approvals from operating local government agencies.
- Contracts and Agreements: Committing to establishing clear and comprehensive contracts with contractors, suppliers and service providers, and providing evidence of the project specifications and timelines.
- Regulatory Compliance: Seeking assistance from legal professionals to help you navigate Los Angeles Construction law: the need to stay current with labour law, safety rules, and workers' rights.
- Risk Management: Readily available insurance policies to protect from risks like builder's risk, general liability and worker's compensation insurance on implementation

Based on this feasibility study of the construction project, this project will be successfully finished, with high-quality accommodations and services to the guests. The strategic location of the hotel downtown makes the people meet the needs and demands of both business and leisure travellers. The deliverables and benefits of the project satisfy stakeholders, investors and future guests.

The 15-storey hotel has been well chosen and designed so that it will be a great asset to the local hospitality landscape. The project provided strong financial indicators, as well as positive economic and environmental impacts, thus it is a viable project in every sense.

5.3 Construction site planning

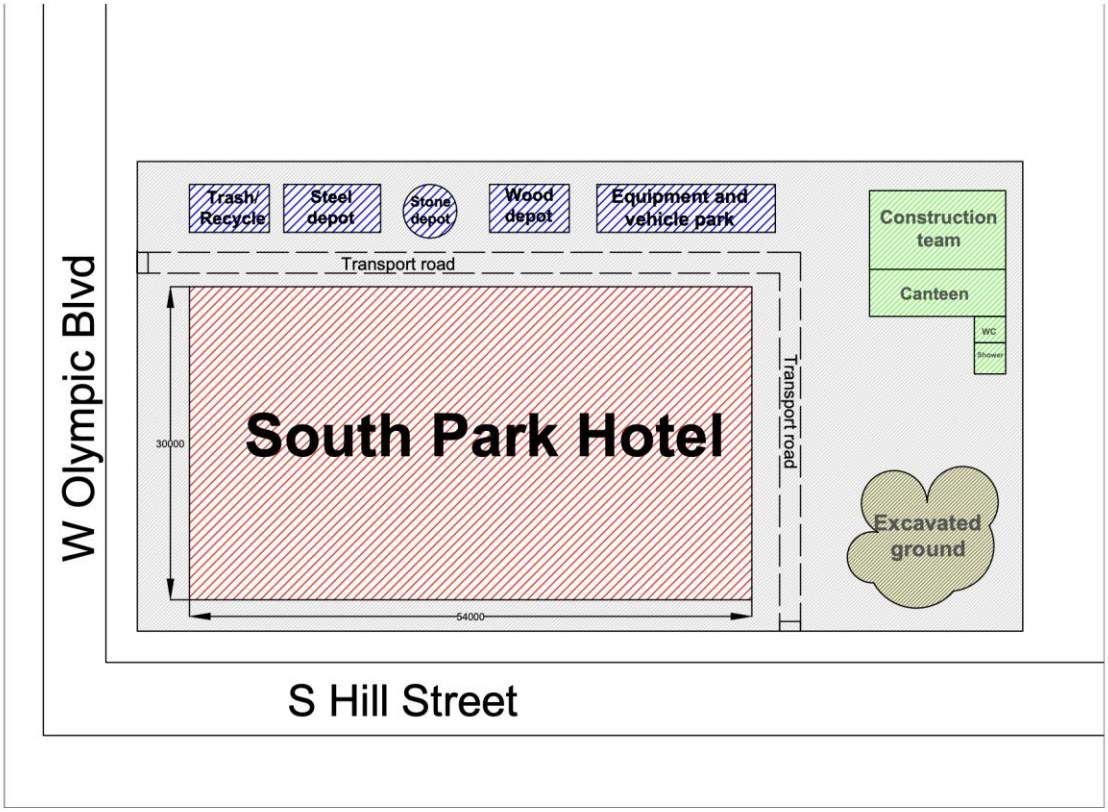

Figure 82.Site planning during construction phase

In a limited urban setting, the South Park Hotel project's construction site plan is made to guarantee effective workflow, safety, and space optimization. Careful site organisation is crucial for both construction operations and minimising disruption to nearby infrastructure, as the project is situated at the intersection of South Hill Street and West Olympic Boulevard.

To increase readability and functionality, the zones on the construction site plan have been marked with different colours:

The red zone indicates the main construction object, access to which is restricted and only is possible with special protective equipment such as glasses, special shoes, helmet.

The green zone is a safe area for engineering personnel and foremen, where it is possible to stay without protective clothing.

The blue zone indicates storages of construction materials and parking of machinery. Only authorised workers are allowed to access these zones. Transport roads were laid out along the building zone and with access to all materials. There are two gates and space for excavated ground is located near the south gate.

Layout and Zoning of the Site:

The building footprint takes up the central portion of the construction site plan (Figure X), with distinct zones surrounding it to facilitate construction logistics.

The trash/recycle area on the north side (top of the plan) guarantees environmentally friendly waste disposal.

Segregated material storage depots, such as steel, stone, and wood depots, reduce contamination and facilitate access for particular trades.

In order to minimise disruptions to the primary transportation route, the Equipment and Vehicle Park is designated for the parking of machinery and service vehicles.

The green zone is located in the East of the construction site which could be shown in Figure X. The largest container was designed for the construction team. Engineering and site managers have their rooms there with their work laptop and all other items. In order to provide better conditions for workers and contractors, a tender for the canteen was held. The winners of the tender moved in temporarily on a 16-month lease basis. There are also restrooms and showers for men and women separately. Temporary engineering networks for the green area were installed, which was also taken into account when calculating the construction budget.

5.4 Work breakdown structure.

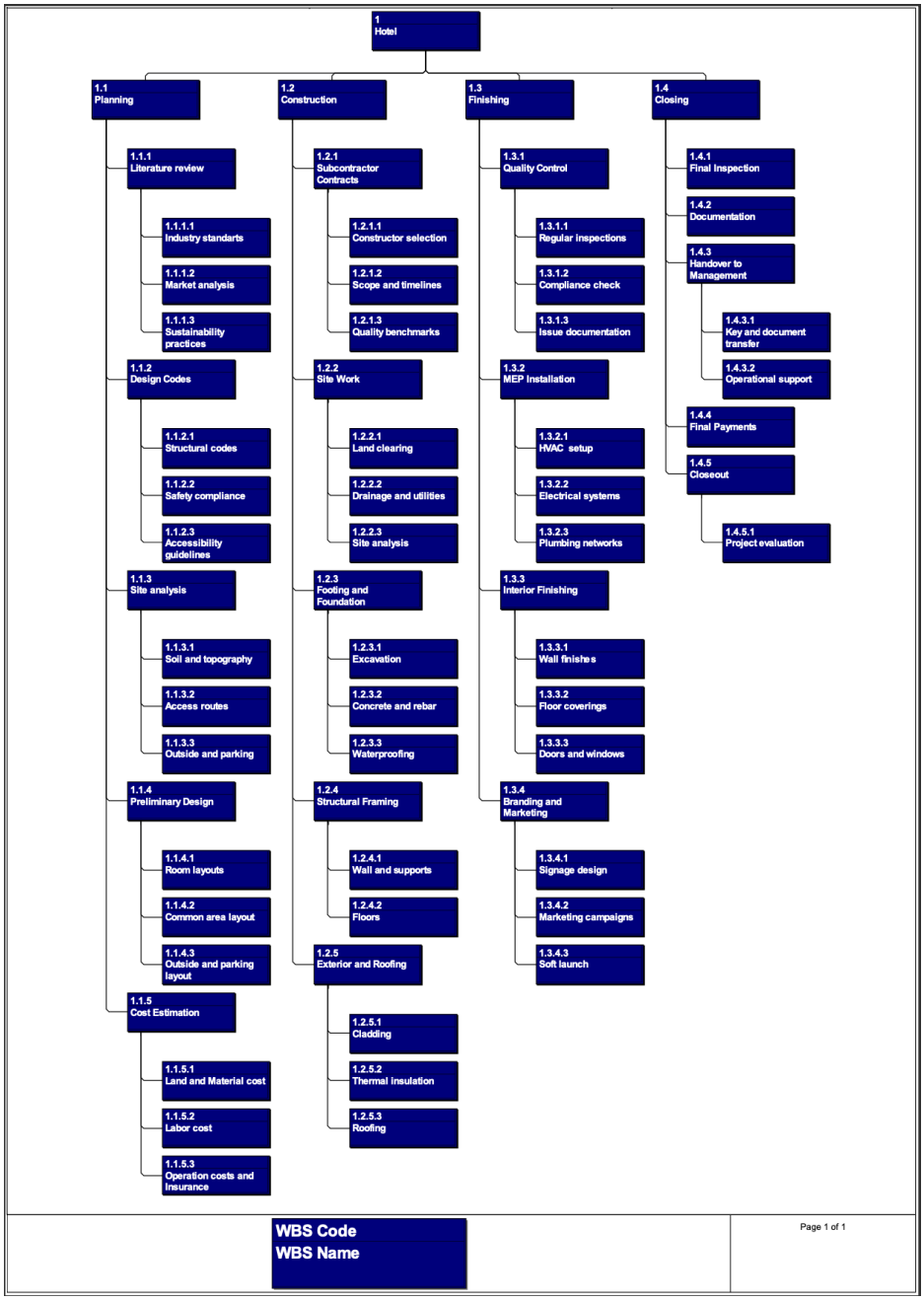

Figure 83. Work breakdown structure (Primavera P6)

The Work Breakdown Structure (WBS) created in the Primavera P6 application for the 15-story hotel project provides a comprehensive framework, dividing the project into key phases: Planning, Construction, Finishing and Closing. Each phase must have certain basic tasks crucial to project success.

In the Planning phase, literature review, market analysis, site analysis, design codes and cost estimation can be done to prepare the project profile structurally and safety-wise as per the standard. During the Construction phase, subcontractor management, site work, foundation, and the structural frame begin to create a stable building and one that works. The Finishing phase includes the interior element, brand, and MEP installations to quality and compliance of the final appearance and functionality. Branding and marketing have also been added to the Work breakdown structure part as a marketing campaign also requires physical work like putting up posters and running hotel advertising campaigns. The Closing phase consists of final inspections, documentation, handing over, and project closeout to ensure a smooth transfer between building operations and a completed project.

The project team might take advantage of the structure in this WBS so that they could effectively manage each stage and allocate their resources, as well as schedule and control the quality of the project at all levels of the project life cycle.

5.5 Scheduling.

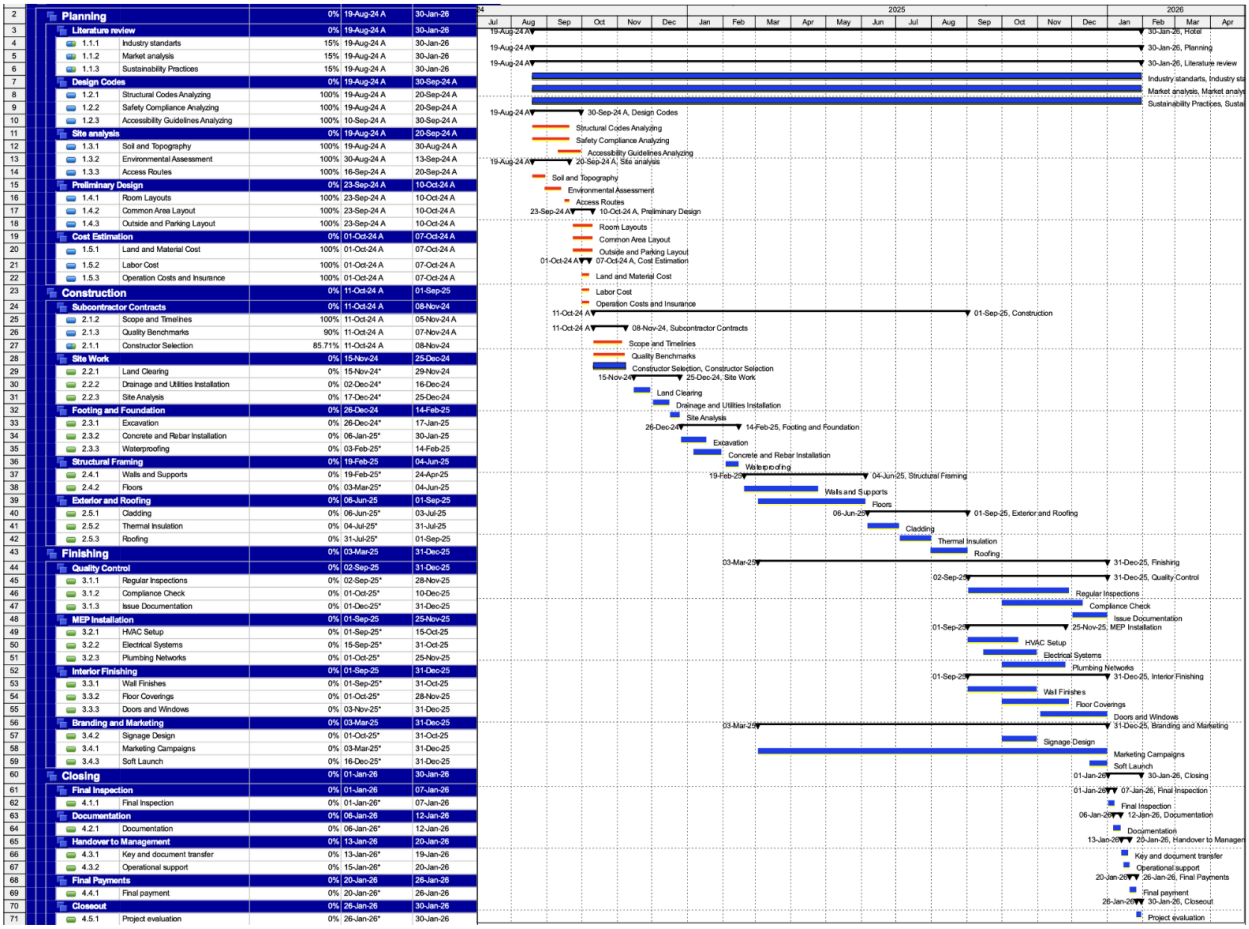

2	Planning		0%	19-Aug-24 A	30-Jan-26
3	Literature review		0%	19-Aug-24 A	30-Jan-26
4	1.1.1	Industry standarts	15%	19-Aug-24 A	30-Jan-26
5	1.1.2	Market analysis	15%	19-Aug-24 A	30-Jan-26
6	1.1.3	Sustainability Practices	15%	19-Aug-24 A	30-Jan-26
7	Design Codes		0%	19-Aug-24 A	30-Sep-24 A
8	1.2.1	Structural Codes Analyzing	100%	19-Aug-24 A	20-Sep-24 A
9	1.2.2	Safety Compliance Analyzing	100%	19-Aug-24 A	20-Sep-24 A
10	1.2.3	Accessibility Guidelines Analyzing	100%	10-Sep-24 A	30-Sep-24 A
11	Site analysis		0%	19-Aug-24 A	20-Sep-24 A
12	1.3.1	Soil and Topography	100%	19-Aug-24 A	30-Aug-24 A
13	1.3.2	Environmental Assessment	100%	30-Aug-24 A	13-Sep-24 A
14	1.3.3	Access Routes	100%	16-Sep-24 A	20-Sep-24 A
15	Preliminary Design		0%	23-Sep-24 A	10-Oct-24 A
16	1.4.1	Room Layouts	100%	23-Sep-24 A	10-Oct-24 A
17	1.4.2	Common Area Layout	100%	23-Sep-24 A	10-Oct-24 A
18	1.4.3	Outside and Parking Layout	100%	23-Sep-24 A	10-Oct-24 A
19	Cost Estimation		0%	01-Oct-24 A	07-Oct-24 A
20	1.5.1	Land and Material Cost	100%	01-Oct-24 A	07-Oct-24 A
21	1.5.2	Labor Cost	100%	01-Oct-24 A	07-Oct-24 A
22	1.5.3	Operation Costs and Insurance	100%	01-Oct-24 A	07-Oct-24 A
23	Construction		0%	11-Oct-24 A	01-Sep-25
24	Subcontractor Contracts		0%	11-Oct-24 A	08-Nov-24
25	2.1.2	Scope and Timelines	100%	11-Oct-24 A	05-Nov-24 A
26	2.1.3	Quality Benchmarks	90%	11-Oct-24 A	07-Nov-24 A
27	2.1.1	Constructor Selection	85.71%	11-Oct-24 A	08-Nov-24
28	Site Work		0%	15-Nov-24	25-Dec-24
29	2.2.1	Land Clearing	0%	15-Nov-24*	29-Nov-24
30	2.2.2	Drainage and Utilities Installation	0%	02-Dec-24*	16-Dec-24
31	2.2.3	Site Analysis	0%	17-Dec-24*	25-Dec-24
32	Footing and Foundation		0%	26-Dec-24	14-Feb-25
33	2.3.1	Excavation	0%	26-Dec-24*	17-Jan-25
34	2.3.2	Concrete and Rebar Installation	0%	06-Jan-25*	30-Jan-25
35	2.3.3	Waterproofing	0%	03-Feb-25*	14-Feb-25
36	Structural Framing		0%	19-Feb-25	04-Jun-25
37	2.4.1	Walls and Supports	0%	19-Feb-25*	24-Apr-25
38	2.4.2	Floors	0%	03-Mar-25*	04-Jun-25
39	Exterior and Roofing		0%	06-Jun-25	01-Sep-25
40	2.5.1	Cladding	0%	06-Jun-25*	03-Jul-25
41	2.5.2	Thermal Insulation	0%	04-Jul-25*	31-Jul-25
42	2.5.3	Roofing	0%	31-Jul-25*	01-Sep-25
43	Finishing		0%	03-Mar-25	31-Dec-25
44	Quality Control		0%	02-Sep-25	31-Dec-25
45	3.1.1	Regular Inspections	0%	02-Sep-25*	28-Nov-25
46	3.1.2	Compliance Check	0%	01-Oct-25*	10-Dec-25
47	3.1.3	Issue Documentation	0%	01-Dec-25*	31-Dec-25
48	MEP Installation		0%	01-Sep-25	25-Nov-25
49	3.2.1	HVAC Setup	0%	01-Sep-25*	15-Oct-25
50	3.2.2	Electrical Systems	0%	15-Sep-25*	31-Oct-25
51	3.2.3	Plumbing Networks	0%	01-Oct-25*	25-Nov-25
52	Interior Finishing		0%	01-Sep-25	31-Dec-25
53	3.3.1	Wall Finishes	0%	01-Sep-25*	31-Oct-25
54	3.3.2	Floor Coverings	0%	01-Oct-25*	28-Nov-25
55	3.3.3	Doors and Windows	0%	03-Nov-25*	31-Dec-25
56	Branding and Marketing		0%	03-Mar-25	31-Dec-25
57	3.4.2	Signage Design	0%	01-Oct-25*	31-Oct-25
58	3.4.1	Marketing Campaigns	0%	03-Mar-25*	31-Dec-25
59	3.4.3	Soft Launch	0%	16-Dec-25*	31-Dec-25
60	Closing		0%	01-Jan-26	30-Jan-26
61	Final Inspection		0%	01-Jan-26	07-Jan-26
62	4.1.1	Final Inspection	0%	01-Jan-26*	07-Jan-26
63	Documentation		0%	06-Jan-26	12-Jan-26
64	4.2.1	Documentation	0%	06-Jan-26*	12-Jan-26
65	Handover to Management		0%	13-Jan-26	20-Jan-26
66	4.3.1	Key and document transfer	0%	13-Jan-26*	19-Jan-26
67	4.3.2	Operational support	0%	15-Jan-26*	20-Jan-26
68	Final Payments		0%	20-Jan-26	26-Jan-26
69	4.4.1	Final payment	0%	20-Jan-26*	26-Jan-26
70	Closeout		0%	26-Jan-26	30-Jan-26
71	4.5.1	Project evaluation	0%	26-Jan-26*	30-Jan-26

Figure 84. Gantt chart (Primavera P6).

The Gantt chart was also created in the Primavera P6 Professional, a powerful project management software, to have very accurate scheduling and task allocation. In planning for the holidays, the holidays of the State of California were chosen as non-working days, as were Saturdays and Sundays, to incorporate realistic working conditions. The project allows for a balanced workload for the team and still maintains efficiency, assuming a 8-hour workday. However, overtime can be allowed for certain critical tasks to help get key milestones in hand without delay.

The chart is a detailed design with a timeline of 15 levels of hotel construction from August 2024 to January 2026 in the Planning, Construction, Finishing and Closing phases respectively. Other tasks run concurrently with the Planning phase of the project, which is the base on which the project rests. This includes things like a literature review, showing how we look at industry standards, market trends and sustainable practices, and the site analyses (soil, topography, access route). This is followed by cost estimation and preliminary design to determine if the project is financially viable and has what might be considered 'actionable blueprints.'

Structural Framing can be considered the longest task and is estimated at approximately 200 days. That duration is a representation of how complex and important the project was, in that it required erecting walls, supports, and floors that make up the core of the hotel. It also extends due to the need to coordinate meticulously, collect high-quality materials and execute with precision. Both exterior work (cladding, thermal insulation, roofing) are overlapping tasks that optimise resources, and minimise downtime plans. For this stage of the process, overtime can sometimes be used to complete these big-ticket items if critical deadlines are important such as framing or foundation work that takes longer than anticipated.

The hotel goes from being under construction, to ready for operation, which is done in the Finishing phase, from March 2025 through to December 2025. Key activities include Quality Control, with regular inspections and compliance checks to maintain safety and functionality standards. Interior finishing includes wall treatments, flooring and the doors-windows installation transforming the structural shell into a shiny neat space. This phase is extremely important and branding and marketing efforts are key including signage design, marketing campaigns and a soft launch.

The Closing phase (January 2026) consists of a final inspection and contract requirements to verify all work to the required regulator and contract standards. Documentation involves all the project records provided as one to make sure there is a smooth handover to management. The project ends with final payments and evaluation of the project so as to serve as a guide in

future improvements. With its precise scheduling features and ability to integrate overtime in critical tasks, the use of Primavera P6 Professional ensures that the project is under control, taking into account the real hours of work and non working days ensuring a high quality hotel ready for use.

5.6 Cost estimation

Table 54. Cost estimation.

Costs	**Description**	**Amount**
Land cost	The cost of the 40,000-square-foot land	$24,000,000
Site preparation	Grading the site	$500,000
Foundation Works	Construction of the foundation, including excavation, formwork, reinforcement, and concrete pouring for the building's foundation.	$1,500,000
Geotechnical Investigations	Soil testing, environmental surveys, and assessments	$300,000
Concrete material cost	Construction of slabs, beams, and columns using reinforced concrete moment frames with updated specifications.	$1,765,850
Steel Reinforcement	Supply and installation of Grade 60 rebar used in the concrete superstructure to meet structural requirements.	$2,160,000

Exterior Walls	Multi-layered walls with architectural precast panels, insulation, vapour barriers, and interior finishes for energy efficiency and aesthetic appeal.	$2,907,342
Interior Walls	Construction of interior partition walls using lightweight steel framing, insulation, and gypsum board to create rooms and internal spaces.	$8,748,000
Elevator cost	Supply and installation of 7 elevators (4 large, 3 small) for passenger movement throughout the building's floors.	$1,150,000
Labor cost	Labor cost for the construction period	$5,028,504
Equipment cost	Contains equipment and machine rental cost	$335,234
Insurance	Insurance of workers and construction site	$1,021,802
Property and sales tax	1.25% of land cost and 9.5% of the material cost	$1,892,437
Technology and IT systems	Hotel Management Software, Networking, Guest Wi-Fi, and Security Systems.	$200,000
Marketing cost	Cost for marketing campaigns	$150,000
Interior Furnishings	Procurement and installation of furniture, fixtures, and equipment for guest rooms, lobbies, restaurants, and other interior spaces.	$2,916,000

Contingency (10%)	A reserve fund to cover unforeseen expenses or cost overruns during the construction process (10% of subtotal)	$5,466,517
TOTAL BUDGET		**$60,131,686**

Cost estimates for the construction of a 15-story five-star hotel at 1030 S. Hill Street in Los Angeles were carefully calculated. This results in a total projected budget of $57,323,102. This budget includes all important elements required for the success and operation of the project. Land acquisition costs are the most significant costs. This is estimated at $24,006,255, which is roughly $600 per square foot. This reflects the high value of land in Los Angeles' South Park district.

Area preparation including land grading was budgeted at $500,000. This will ensure that the construction foundation will be stable. Foundation work, which includes digging, placing rebar, and pouring concrete, is expected to cost $1,500,000 for the project. We used about 5,000 cubic meters of reinforced concrete for the foundation, 60 piles with 0.8 m diameter and 6.225 metres in depth. Because of its exceptional fire resistance, durability, and compressive strength, reinforced concrete was selected for high-performance structural applications. The concrete is reinforced with structural steel to increase its tensile strength and sustain the building's vertical loads.

The entire 15-story building has about 1,000 reinforced columns, with 60 columns on each floor. The main structural system of the hotel is made up of these columns, beams, and concrete slabs. With a density of about 2,400 kg/m³, reinforced concrete also offers thermal resistance, which lowers energy use and boosts building efficiency in general. Strategic steel reinforcement helps to mitigate its low ductility, which necessitates careful engineering.

The concrete superstructure consists of the C40-grade concrete construction of the slabs, beams and columns. At an updated cost of $1,765,859, about 8,369 cubic meters of concrete are

used. Two-way slabs that are 6 by 6 meters and 0.15 meters thick are used in this design. They are held up by beams that are 6 meters long, 0.3 meters wide, and 0.6 meters high.

A total of $2,160,000 is spent on steel because 1,088 metric tonnes of Grade 60 rebar—which is currently valued at $2 per kilogram—are used for reinforcement. Steel is especially well-suited for construction in seismically active areas like Los Angeles due to its compressive and tensile strengths, toughness, and exceptional earthquake resistance. Steel and reinforced concrete combine to create a strong, flexible structure that can withstand lateral forces as well as vertical loads.

The total cost of exterior walls is $2,907,342. Architectural precast panels of thickness 40 mm, synthetic stucco, vapour barrier, spray foam insulation and reinforced lightweight concrete and fire-rated gypsum board. By combining a multiple-layered design, the resulting product delivers improved insulation, reduced cost of the operation and better guest comfort.

The cost of building the interior walls is $8,748,000. Lightweight steel framed with drywall, spray foam insulation and gypsum board finish. By creating these walls, the hotel's internal spaces can occur, as these walls insulate the sound, resist the fire, and are also factors in the overall hotel's structural integrity.

The hotel includes seven elevators – four large and three smaller ones for efficient vertical transportation throughout the 15 floors and two underground levels. The total cost of supplying and installing these elevators is $1,150,000. Modern elevators enhance guest convenience, improve accessibility, and are vital for the operational efficiency of a high-rise hotel.

The estimated construction labour costs total $5,028,504. This includes wages for a skilled workforce, such as engineers, supervisors, foremen, skilled labourers, and unskilled labourers. These costs are necessary for keeping the quality and speed of construction at a high level, and all work has to be carried out complying with the safety requirements.

$335,234 worth of equipment was rented to secure cranes, excavators, concrete mixers and generators. The right equipment is a key factor for executing construction tasks and keeping to the project schedule.

Insurance costs are calculated at $1,021,802, covering builder's risk insurance, general liability insurance, and worker's compensation insurance. These policies protect the project from potential risks, liabilities, and unforeseen events during the construction phase.

The land is subject to property tax and construction materials to sales tax at a total of $1,892,437. There are 1.25% of land cost and 9.5% of the material cost in the State of California. Owing taxes produces compliant forms which will prevent you from paying penalties or delays.

Technology systems and IT systems share $200,000 in investment. These include hotel management software, networking infrastructure, guest Wi-Fi systems and access controls as well as security systems, such as CCTV. Without these systems in place, the hotel would not function properly and would not offer the consumers much in the way of a guest experience or be able to remain safe.

As such, marketing costs are picked up at $150,000 which are marketing campaigns on both the digital and offline front to market the hotel before it opens. With the way things are, it's essential the hotel builds brand awareness, brings guests, and makes the hotel's presence known in a competitive market.

The procurement and installation of interior furnishings are estimated at $2,916,000. This includes high-quality furniture, fixtures, and equipment (FF&E) for guest rooms, the lobby, restaurants, and other public areas. These furnishings play a significant role in defining the hotel's ambiance and guest experience, directly impacting customer satisfaction and repeat business.

The total project cost before contingency amounts to $54,665,169 (10% of the project cost). In covering unforeseen expenses or cost overruns on construction, such as unexpected site

conditions, price fluctuations for materials and design changes, this fund is crucial. It provides financial flexibility for the project, while keeping the project on track.

Overall, the project cost is **$60,131,686**, encompassing all aspects from land acquisition to interior furnishings. This comprehensive cost estimate provides a clear view of the financial requirements of building a hotel. It meets the expectations of modern hospitality standards. This gave the company a clearer picture of what the project involves, from the basic geotechnical studies to the final touches inside. The use of reinforced concrete and steel makes the overall structure safe and even meets some of the seismic challenges common to the region. Just as energy efficiency and sustainability in material selection helps achieve long-term operational savings and environmental responsibility.

Allocating resources for labour, equipment, contingency plans and insurance is proof of intent to manage contingencies and deliver projects on time. Along with guest expectations and industry standards, the hotel will be able to compete when it opens by incorporating state-of-the-art amenities and area-specific technology systems.

5.7 Annual cash inflow

Table 55. Net profit in a year.

Item	Amount
Room Revenue	**$19,286,400**
Restaurant Revenue	**$3,832,500**
Operating expenses	**$15,027,285**
Net profit	**$8,091,615**

Annual room profit was calculated by taking into account seasonal variations in occupancy and an average rate of $400 per night. For the calculations, the year was roughly divided into three seasons: high, medium, and low. In the high season, which lasts 4 months and includes such periods as summer and holidays, it is assumed that the hotel occupancy is 80%. With this utilization and the current rate, the total room revenue for this period is $7,526,400. During the mid-season, which covers 5 months of the year, the expected occupancy drops to 70%, which corresponds to stable but not peak demand. This generates revenue of $8,232,000. During the low season, which spans 3 months, hotel occupancy is estimated at 50%, reflecting quieter periods of demand. Under these conditions, room revenue during this period would be $3,528,000. Combining these figures for all seasons, we arrive at a total annualized room revenue of $19,286,400.

Profit from the two restaurants located in the hotel lobby was calculated based on an average check of $100 and a total capacity of 150 seats. This assumes an average utilization rate

of approximately 70% throughout the year due to the attractive location in downtown Los Angeles and high traffic. At this rate, the total annual revenue from the restaurants will be $3,832,500. This calculation takes into account the daily flow of guests from both hotel guests and outside visitors attracted by the high level of service and quality cuisine.

Together, these calculations provide a realistic view of the hotel's revenue potential, taking into account seasonal fluctuations in demand and the average check-in of restaurants. The total payback period is about 7,5 years which could be considered adequate for the hotel business. This approach allows one to see the full picture of the project's financial efficiency and contributes to further successful management of the hotel in the competitive Los Angeles market.

5.8 Risk management

Effective risk management is essential for ensuring projects are completed on time, within budget, and to stakeholder satisfaction. It does not hurt to have strategies for risk identification, assessment and continuous monitoring so that risks like material shortages due of labour strikes or configuration of materials due to weather disruptions can have a higher cost and impede progress. The research recommends that a risk matrix can be used to help prioritise risks by likelihood and impact, and on the basis of such probability and impact, it can be decided what targeted response, for example, risk avoidance, transfer or mitigation, should be implemented (Kovacevic et al, 2019).

By integrating qualitative and quantitative assessments within a given risk framework, a comprehensive risk register can be developed that details potential risks. This promotes best practice and allows for dynamic planning aimed at minimizing losses when time and cost and risks are exceeded, as well as ensuring the project's ability to recover in times of change.

Our hotel project has been using a 5x5 risk matrix (MIL-STD-882B) instead of a 3x3 or 4x4 matrix for more precise control of construction risks. In this matrix, risks are categorized according to a score that is based on a combination of Severity Level and Probability Level. The steps that this grid provides are not to create a risk management plan but to provide a level of

fearless analyzed risk, in five steps the level of impact and probability of the risks are very likely, likely, possible, unlikely, and very unlikely. In the colour grid, the severity of the risks rises from dark green to red colour. This method helps to visually assess risks and allows the team to determine which risks deserve more resources on mitigation methods

The 5x5 risk matrix (MIL-STD-882B) was formed for risk assessment in the U.S. military, and the mentioned matrix is implemented in the American Military Standard (American Military Standard or abbreviation MIL-STD) (Kovacevic et al., 2019). The effectiveness of that method makes it valuable in providing clear guidelines on risk categorization which always allows both administrative and on-ground teams to understand, interpret and manage risks correctly. Through systematic risk organising, the project team can appropriately use decisions to address high-priority risks to improve project resilience and schedule completion in a timely fashion.

Table 56. 5x5 risk matrix

Likelihood \ Impact	Negligible	Minor	Moderate	Significant	Severe
Very Likely	Low Med	Medium	Med Hi	High	High
Likely	Low	Low Med	Medium	Med Hi	High
Possible	Low	Low Med	Medium	Med Hi	Med Hi
Unlikely	Low	Low Med	Low Med	Medium	Med Hi
Very Unlikely	Low	Low	Low Med	Medium	Medium

The risk score is shown in the brackets in the Risk matrix table. It is calculated by multiplying probability by the result of the event:

□□□□ □□□□□

= □□□□□□□□□□□ □□ □h□ □□□□ × □□□□□□ □□ □h□ □□□□□

Table 57. The risk score table.

Risk category	Severity (1-5)	Probability (1-5)	Risk score	Risk mitigation
Shortage of skilled labour	4	3	12	Contract with reliable local agencies to find labour.
Design Changes and Approval Delays	4	4	16	Scheduling projects in an organized manner and accelerating design change request approvals.
Violation of building codes and regulations	5	2	10	Ensure compliance through regular audits, qualified labour, training, and strict documentation.
Project cost overrun	5	4	20	Regularly track costs, implement cost control measures and negotiate discounts with suppliers.
Safety hazards and non-compliance with PPE rules.	5	3	15	Mitigate safety hazards by ensuring PPE use, regular inspections, and worker training.

Unsatisfied quality of materials	3	5	15	Preliminary inspection of materials upon arrival and quality control throughout the project.
Unexpected soil issues	5	2	10	Conduct detailed geotechnical investigations in the early stages of the project
High seismicity	5	5	25	Use seismic-resistant design, reinforced structures, and strict adherence to building codes.
Structural collapse	5	3	15	Ensure proper design, quality materials, regular inspections, and adherence to safety standards.
Cost inflation	5	3	15	Set fixed prices with suppliers for basic materials and keep extra funds for unexpected expenses.
Geopolitical risks	3	2	6	Identify alternative suppliers in different regions to minimize dependence on one region.
Machine errors	1	3	3	Schedule regular maintenance and have rental options in case equipment breaks down.

Table 58. Risk matrix.

Likelihood	Impact of a dangerous event					
		Negligible	Minor	Moderate	Significant	Severe
	Very likely			Unsatisfied quality of materials;		High seismicity
	Likely				Design Changes and Approval Delays	Project cost overrun
	Possible	Machine errors			Shortage of skilled labor	Cost inflation; Structural collapse; Safety hazards and Non-compliance with PPE rules.
	Unlikely			Geopolitical risks		Unexpected soil issues; Violation of building codes and regulations
	Very					

	unlikely					

The typology of risks found when the risk assessment of this construction project is organised on a detailed table and risk matrix with mentioning both probability and severity basis for potential problems. For example, high probability risk (critical risk) such as cost overruns and high seismicity are marked in red and immediately prioritised for action with immediate contingency plans and structural precautions. Regular monitoring is needed for moderate risks, for design changes and project delays, while low risk, machine issues and equipment errors, are covered by standard safeguards. Such a structure allows a focused approach where the main threats to project stability and efficiency as much as possible are addressed to ensure project stability and efficiency present.

5.9 Quality control checklist

Quality control checklist

Project Information:

- Project name: "South Park" Hotel
- Project team: "Rolling Stones"
- Location: 1030 South Hill St., Los Angeles, California
- Inspection Date: October 11th, 2024

Pre-Construction Phase:

- ☐ Check site boundaries, excavation plans, and land grading compliance;
- ☐ Design review;
- ☐ Confirm soil testing aligns with design specifications;
- ☐ Ensure proper compaction of soil;
- ☐ Check for compliance for environmental and sustainability requirements;
- ☐ Material Inspection.

Construction Phase:

- ☐ Structural framework inspection;
- ☐ Reinforcement and concrete quality checks;
- ☐ Fire safety and emergency systems assessment;
- ☐ HVAC system installation review;
- ☐ Waterproofing and insulation validation;
- ☐ Compliance with seismic and wind load standards.

Post-Construction Phase:

- ☐ Punch list review and defect corrections
- ☐ Handover documentation and as-built drawings submission
- ☐ Walkthrough and approval

Project Manager Signature: _____

Structural Engineer Signature: _____

Geotechnical Engineer Signature: _____

Notes and Comments: _____

Figure 85. Quality control checklist

A quality control checklist was developed to ensure the South Park Hotel construction project meets all required standards, specifications, and legal requirements. There are three phases of the checklist: preconstruction, construction, and post construction, allowing for methodical verification and action should it be deemed necessary.

Quality assurance during the pre construction stage was aimed at preparing the site for ground work, mainly in terms of confirming site boundaries, approved excavation plan, and grading compliance. A thorough design review was carried out to validate that all planned works followed the engineering and architectural intentions. Compatibility of soil testing with design specifications was checked and further compaction was confirmed on site. All incoming construction materials were visually and technically inspected for physical compliance, environmental compliance and material sustainability were examined.

In the Construction Phase, continuous inspections were carried out on the structural framework to detect any design deviation early. Regular checks were made on reinforcement detailing and quality of concrete mix for strength and durability. Inspections of fire safety systems and HVAC installations were done with regard to performance and code compliance. Special emphasis was put on testing waterproofing and insulation systems to ascertain their thermal efficiency and moisture intrusion resistance. Seismic and wind load standards were strictly followed due to the high-rise classification of this building and due to the fact that it is located in seismic zones.

The Post-Construction Phase consisted of final walk-throughs and defect detection. A list of work that had been completed prior to final closure was compiled. Final documentation including as-built drawings and system manuals was prepared and submitted. Approval and acceptance were to be made but were contingent on the fulfillment of all contract, technical, and safety conditions.

5.10 Procurement planning

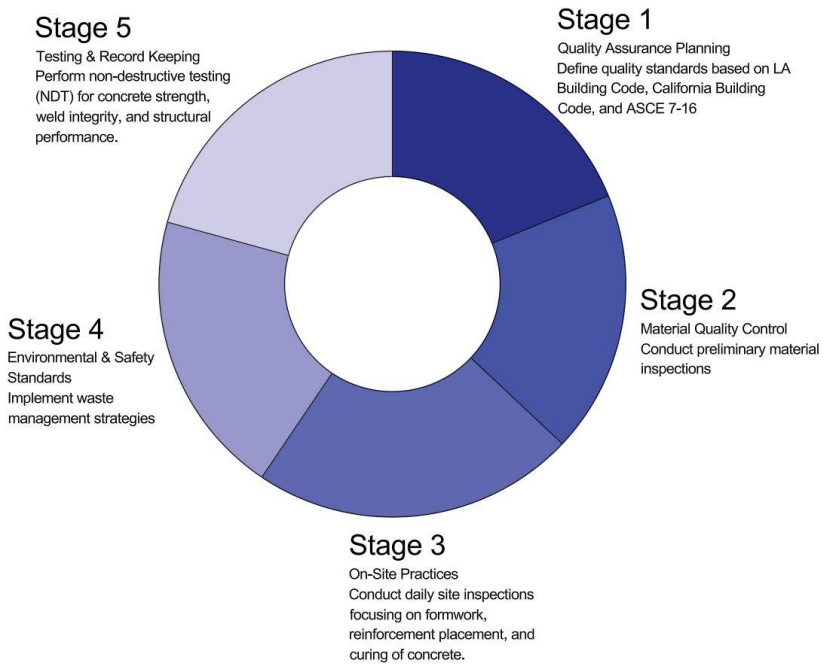

Figure 86. Quality control measures.

Procurement for the high-rise hotel follows a structured process to ensure efficiency, cost-effectiveness, and quality. The procurement planning is divided into five key stages:

- **Stage 1:** Quality Assurance Planning – Define quality standards based on LA Building Code, California Building Code, and ASCE 7-16 to establish procurement requirements.
- **Stage 2:** Material Quality Control – Conduct preliminary material inspections to ensure compliance with safety and performance standards.
- **Stage 3:** On-Site Practices – Daily site inspections focusing on formwork, reinforcement placement, and concrete curing to ensure materials are utilized as per procurement specifications.
- **Stage 4:** Environmental & Safety Standards – Implement waste management strategies and ensure materials meet sustainability standards.

- **Stage 5:** Testing & Record Keeping – Perform non-destructive testing (NDT) for concrete strength, weld integrity, and structural performance to validate material quality post-procurement.

Supplier and Contractor Selection

- **Competitive Bidding**: Selection of suppliers and contractors through a transparent bidding process.
- **Prequalification of Vendors**: Ensuring vendors meet quality, delivery, and cost standards.
- **Long-Term Supplier Agreements**: Establishing contracts with key suppliers for essential materials to minimize procurement delays and cost fluctuations.

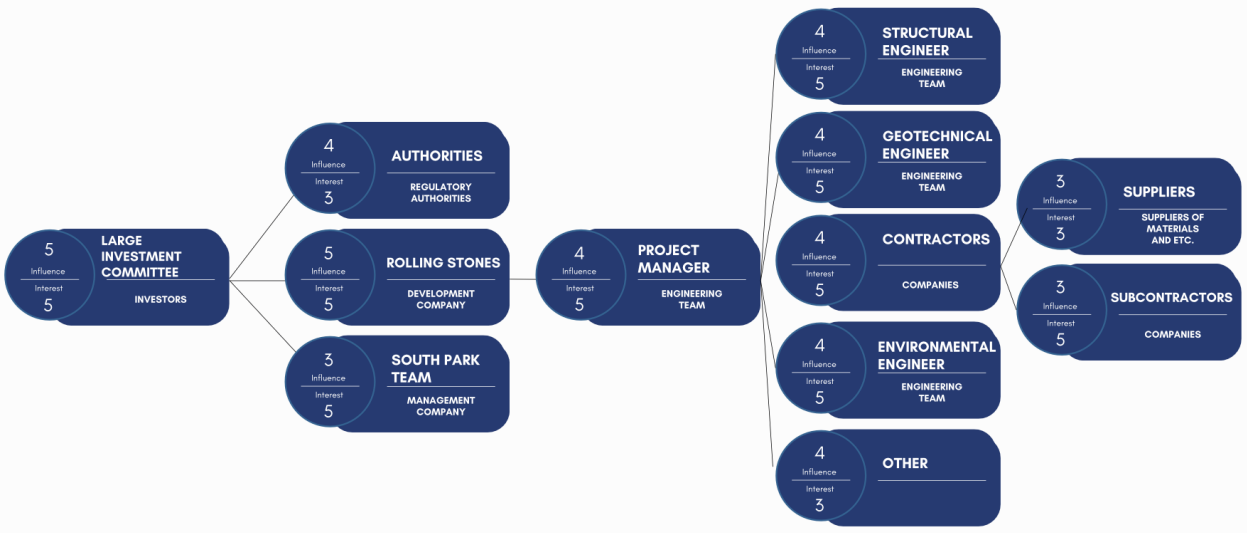

Figure 87. Stakeholder matrix

Implementation of the project depends on successful management of stakeholders. Investors, regulatory agencies, contractors, engineers, suppliers, and subcontractors are key stakeholders. Financial support and viability of the project are assured by the Large Investment Committee, and compliance with the law and safety standards rests with Regulatory Authorities.

Development and management companies, such as Rolling Stones and South Park Team, are also part of the planning and execution process. The Project Manager coordinates with engineering teams, contractors, and environmental specialists to ensure project sustainability and quality. Suppliers and subcontractors, less powerful but extremely interested, ensure the delivery of quality materials and timely completion of work. By open communication and coordinated collaboration among all the stakeholders, the project can effectively and efficiently achieve its objectives.

5.11 Hierarchy of controls

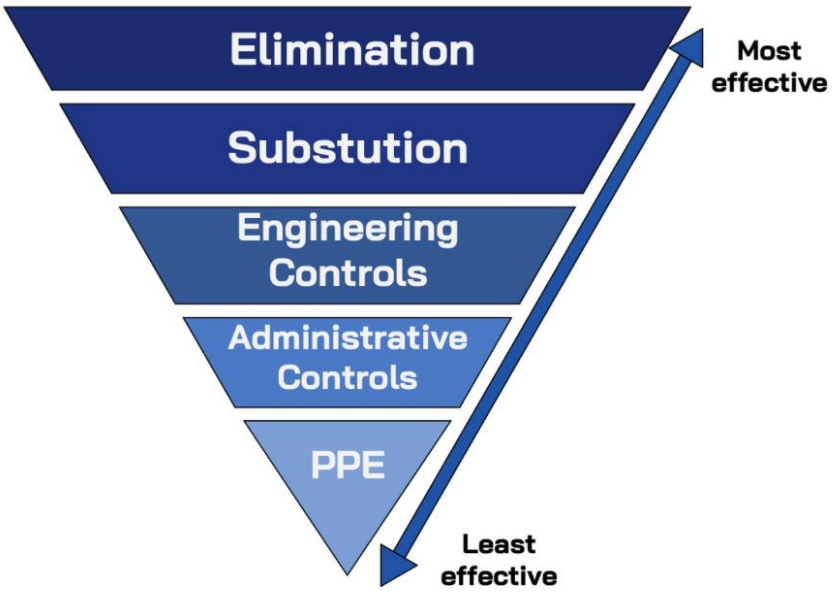

Figure 88. Hierarchy of controls

In Figure 88, control hierarchy could be seen which was applied to safety planning at the South Park Hotel construction site. This model organises the hazard control method from the most to the least. Elimination, which involves the complete elimination of the hazards, was taken into consideration during the design stage to reduce the amount of high risk activities that took place on the construction site. Substitution was carried out by replacing potentially hazardous materials

with safer materials, such as low VOC adhesives. By installing edge protection systems, scaffolding built-in rails and noise reduction barriers, engineering controls were implemented. Scheduled shift rotations, safety training sessions and zone-based site access were examples of administrative controls. The last layer of protection is PPE (Personal Protective Equipment). The Figure 88 underlines the structured safety approach adopted throughout the project.

5.12 Green Building Certification

The 15-storey hotel project (1030 South Hill Street, Los Angeles, CA) is designed to incorporate sustainability and environmentally conscious practises, in compliance with Leadership in Energy and Environmental Design (LEED) certification standards throughout the construction management process. The project follows the U.S. Green Building Council's criteria through which it hopes to achieve a certification that showcases its commitment towards reducing environmental impact and maximising energy efficiency and sustainability.

Table 59. Green building practices

Category	Strategy	Implementation
Sustainable Site Development	Minimize land disturbance and use the urban site effectively.	Break up existing flat topography and connect catch basins and pipes to storm drainage systems.
	Leverage natural ventilation and sunlight.	Building orientation to accept breezes off the Pacific Ocean and control shadows from nearby structures.
Water Efficiency	Reduce potable water usage through efficient plumbing and recycling.	The installation of low flow fixtures and sewage recycling systems for irrigation and flushing will be installed.
Energy Optimization	Incorporate energy-efficient lighting and HVAC systems.	Use LED lighting in all rooms and optimize HVAC performance

	Maximize thermal efficiency	Use reinforced concrete and insulated materials to reduce heating and cooling demands
Materials and Resources	Use locally sourced and recycled materials.	Integrate recycled steel beams and low-emission cement into the construction.
	An effective waste management plan amounts to minimising construction waste.	Recycle materials such as steel, concrete, and wood during construction.
Indoor Environmental Quality	Enhance air quality and natural lighting.	Install large windows exceeding IBC 2024 standards and use low-VOC materials like paints and adhesives.
	Provide healthy indoor environments for occupants	Incorporate natural ventilation
Construction Management Practices	Design efficient parking and traffic flow.	Implement two-way traffic systems in parking areas to minimize congestion.

Throughout the construction phase the construction is monitored and documented tightly, to be certain that The LEED standard is met. The implementation of sustainable practises along with their compliance with certification requirements will be validated by independent third party evaluations.

Although the 15 storey hotel project integrates these strategies into the construction management process, the goal of achieving LEED certification while providing an example of how environmentally and contextually sensitive development can be pursued in the South Los Angeles area. This approach aligns with the city's vision of enhancing urban infrastructure while promoting environmental stewardship.

Conclusion

The South Park Hotel project, located at 1030 South Hill Street in Downtown Los Angeles, was designed to meet the growing demand for high-quality accommodation in the heart of the city. The design of the 15-storey high-rise building with two levels of underground car parking was focused on safety, durability, sustainability and operational efficiency.

Already in the early planning stages, the project team made efforts to ensure compliance with the latest codes and design standards, ACI 318-22 and ASCE 7-16, which guaranteed that the structure could withstand the seismic and wind loads typical of the Los Angeles region. Therefore, the structural system was analysed using SAP2000 software and validated by manual calculations to ensure sufficient performance under lateral and vertical forces.

Soil conditions, liquefaction potential and groundwater conditions were investigated as part of a comprehensive geotechnical study. Based on the results, shallow and deep foundation systems were designed and optimised; the behaviour of the pile group was modelled in a long-term stability and serviceability analysis using Plaxis 3D and GEO5 to account for serviceability under operational loads.

The architecture and environmental design primarily emphasise functionality, energy efficiency and occupant comfort. To achieve LEED certification, a sustainable approach was used throughout all phases of the project: installation of water-saving systems, energy-saving mechanical systems, use of sustainable materials, and stormwater management planning. The hotel was sited and oriented to optimize natural ventilation and reduce environmental impact, in line with the citywide sustainability goals of Los Angeles.

The construction site planning was detailed to a high degree, which optimizes logistics, material flow, and safety. There is proper zoning within the construction site-separating danger zones from administrative and storage zones that were able to minimize incidents while maximizing

operational efficiency. The firm maintained the construction quality through a structured checklist and inspection system across every critical stage.

Safety management on site followed the Hierarchy of Controls model which favors the elimination of hazards before engineering controls and the strict enforcement of PPE. Regular risk assessments were done and as the conditions changed mitigation strategies were updated.

Financial planning with elaborate estimation of cost and prediction of cash flows proved the economic viability of the project by ensuring that everything was carried out in line with the planned budget without compromising on quality during construction and at material standards.

The South Park Hotel project shows a modern realization of best practices in high-rise construction management and engineering with an emphasis on multidisciplinary approaches to structural integrity, sustainability, and efficient execution. It is anticipated that, once completed, the hotel will significantly enhance urban development within Downtown Los Angeles by providing luxury hospitality services based on strong safety attributes concerning environmental responsibility and operational excellence.

Appendix

Table 58. Portal Frame Method for Internal Forces analysis (Part 1)

Story	h,m	Fxi (kN)	Fx (kN)	V (kN)	a (m)	b (m)	1 (kN)	2 (kN)	3 (kN)
15	3.3	17.36	17.36	1.74	1.65	3	-0.95	-15.62	0.95
14	3.3	17.12	34.48	3.45	1.65	3	-3.81	-15.41	2.85
13	3.3	16.87	51.36	5.14	1.65	3	-8.53	-15.19	4.72
12	3.3	16.61	67.97	6.80	1.65	3	-15.09	-14.95	6.56
11	3.3	16.33	84.30	8.43	1.65	3	-23.46	-14.70	8.37
10	3.3	16.04	100.34	10.03	1.65	3	-33.62	-14.44	10.16
9	3.3	15.73	116.06	11.61	1.65	3	-45.52	-14.15	11.90
8	3.3	15.39	131.45	13.15	1.65	3	-59.14	-13.85	13.61
7	3.3	15.02	146.47	14.65	1.65	3	-74.42	-13.52	15.29
6	3.3	14.62	161.10	16.11	1.65	3	-91.34	-13.16	16.92
5	3.3	14.18	175.28	17.53	1.65	3	-109.84	-12.76	18.50
4	3.3	13.68	188.95	18.90	1.65	3	-129.87	-12.31	20.03
3	3.3	13.10	202.05	20.21	1.65	3	-151.38	-11.79	21.51
2	3.3	12.75	214.80	21.48	1.65	3	-174.30	-11.47	22.93
1	5	15.98	230.78	23.08	2.5	3	-211.43	-14.38	37.13
0 (Ground)	**Ax (kN)**	**Ay (kN)**	**Ma (kN-m)**	**Bx (kN)**	**By (kN)**	**Mb (kN-m)**	**Cx (kN)**	**Cy (kN)**	**Mc (kN-m)**
	-23.08	-211.43	57.69	-46.16	0.00	115.39	-46.16	0.00	115.39

Table 60. Portal Frame Method for Internal Forces analysis (Part 2)

4 (kN)	5 (kN)	6 (kN)	7 (kN)	8 (kN)	9 (kN)
0.00	-12.15	0.95	0.00	-8.68	0.95
0.00	-11.99	2.85	0.00	-8.56	2.85
0.00	-11.81	4.72	0.00	-8.44	4.72
0.00	-11.63	6.56	0.00	-8.31	6.56
0.00	-11.43	8.37	0.00	-8.17	8.37
0.00	-11.23	10.16	0.00	-8.02	10.16
0.00	-11.01	11.90	0.00	-7.86	11.90
0.00	-10.77	13.61	0.00	-7.69	13.61

0.00	-10.52	15.29	0.00	-7.51	15.29
0.00	-10.24	16.92	0.00	-7.31	16.92
0.00	-9.93	18.50	0.00	-7.09	18.50
0.00	-9.58	20.03	0.00	-6.84	20.03
0.00	-9.17	21.51	0.00	-6.55	21.51
0.00	-8.92	22.93	0.00	-6.37	22.93
0.00	-11.18	37.13	0.00	-7.99	37.13
Dx (kN)	**Dy (kN)**	**Md (kN-m)**	**Ex (kN)**	**Ey (kN)**	**Me (kN-m)**
-46.16	0.00	115.39	-46.16	0.00	115.39

Table 61. Portal Frame Method for Internal Forces analysis (Part 3)

10 (kN)	**11 (kN)**	**12 (kN)**	**13 (kN)**	**14 (kN)**	**15 (kN)**	**16 (kN)**
0.00	-5.21	0.95	0.00	-1.74	0.95	0.95
0.00	-5.14	2.85	0.00	-1.71	2.85	3.81
0.00	-5.06	4.72	0.00	-1.69	4.72	8.53
0.00	-4.98	6.56	0.00	-1.66	6.56	15.09
0.00	-4.90	8.37	0.00	-1.63	8.37	23.46
0.00	-4.81	10.16	0.00	-1.60	10.16	33.62
0.00	-4.72	11.90	0.00	-1.57	11.90	45.52
0.00	-4.62	13.61	0.00	-1.54	13.61	59.14
0.00	-4.51	15.29	0.00	-1.50	15.29	74.42
0.00	-4.39	16.92	0.00	-1.46	16.92	91.34
0.00	-4.25	18.50	0.00	-1.42	18.50	109.84
0.00	-4.10	20.03	0.00	-1.37	20.03	129.87
0.00	-3.93	21.51	0.00	-1.31	21.51	151.38
0.00	-3.82	22.93	0.00	-1.27	22.93	174.30
0.00	-4.79	37.13	0.00	-1.60	37.13	211.43
Fx (kN)	**Fy (kN)**	**Mf (kN-m)**				
-23.08	211.43	57.69				

Table 62. Wind and seismic drifts in hand calculations for Frame G (transverse)

	Total drift under wind load,	**Total drift under seismic load, mm**

	mm							
Level	**Inter-story displacement, mm**	**Absolute displacement, mm**	**Inter-story drift, %**	**Inter-story displacement, mm**	**Absolute displacement, mm**	**Inter-story drift, %**	**Amplified inter-story deflection, mm**	**Allowable limit, mm**
15	1.26	52.32	0.038	9.71	352.34	0.324	53.40	60
14	2.13	51.06	0.065	19.89	342.63	0.663	109.37	60
13	2.80	48.93	0.085	25.12	322.75	0.837	138.16	60
12	2.86	46.13	0.087	24.58	297.63	0.819	135.18	60
11	2.76	43.27	0.084	22.73	273.05	0.758	125.03	60
10	2.78	40.51	0.084	21.94	250.32	0.731	120.68	60
9	2.89	37.73	0.087	21.76	228.38	0.725	119.67	60
8	3.04	34.84	0.092	21.90	206.62	0.730	120.43	60
7	3.26	31.80	0.099	22.39	184.72	0.746	123.15	60
6	3.51	28.54	0.106	23.01	162.33	0.767	126.56	60
5	3.76	25.03	0.114	23.44	139.32	0.781	128.92	60
4	4.00	21.27	0.121	23.71	115.88	0.790	130.41	60
3	4.23	17.27	0.128	23.84	92.17	0.795	131.10	60
2	7.61	13.05	0.231	40.14	68.33	1.338	220.75	60
1	5.44	5.44	1.088	28.20	28.20	0.854	155.09	66

Table 62. Wind and seismic drifts in 2D SAP2000 for Frame G (transverse)

	Total drift under wind load, mm			**Total drift under seismic load, mm**				
Level	**Inter-story displacement, mm**	**Absolute displacement, mm**	**Inter-story drift, %**	**Inter-story displacement, mm**	**Absolute displacement, mm**	**Inter-story drift, %**	**Amplified inter-story deflection, mm**	**Allowable limit, mm**
15	1.10	45.66	0.033	10.56	319.68	0.352	58.10	60
14	2.07	44.55	0.063	19.27	309.12	0.642	105.97	60
13	3.03	42.48	0.092	27.10	289.85	0.903	149.07	60
12	2.84	39.45	0.086	24.28	262.75	0.809	133.54	60
11	2.79	36.62	0.084	22.82	238.47	0.761	125.52	60

10	2.85	33.83	0.086	22.27	215.65	0.742	122.51	60
9	2.97	30.99	0.090	22.22	193.37	0.741	122.22	60
8	3.14	28.01	0.095	22.39	171.15	0.746	123.15	60
7	3.32	24.87	0.101	22.62	148.76	0.754	124.39	60
6	3.60	21.55	0.109	23.43	126.14	0.781	128.89	60
5	3.75	17.95	0.114	23.27	102.71	0.776	127.97	60
4	3.90	14.20	0.118	23.13	79.44	0.771	127.22	60
3	3.82	10.30	0.116	21.70	56.31	0.723	119.36	60
2	3.49	6.47	0.106	19.03	34.61	0.634	104.68	60
1	2.98	2.98	0.597	15.58	15.58	0.472	85.68	66

Table 63. Wind and seismic drifts in 3D SAP2000 for Frame G (transverse)

	Total drift under wind load, mm			**Total drift under seismic load, mm**				
Level	**Inter-story displacement, mm**	**Absolute displacement, mm**	**Inter-story drift, %**	**Inter-story displacement, mm**	**Absolute displacement, mm**	**Inter-story drift, %**	**Amplified inter-story deflection, mm**	**Allowable limit, mm**
15	1.40	49.20	0.042	16.50	376.10	0.550	90.75	60
14	2.30	47.80	0.070	25.50	359.60	0.850	140.25	60
13	3.40	45.50	0.103	33.20	334.10	1.107	182.60	60
12	3.10	42.10	0.094	29.71	300.90	0.990	163.41	60
11	3.00	39.00	0.091	25.89	271.19	0.863	142.40	60
10	3.00	36.00	0.091	25.70	245.30	0.857	141.35	60
9	3.20	33.00	0.097	25.40	219.60	0.847	139.70	60
8	3.30	29.80	0.100	25.40	194.20	0.847	139.70	60
7	3.50	26.50	0.106	25.70	168.80	0.857	141.35	60
6	3.90	23.00	0.118	26.50	143.10	0.883	145.75	60
5	3.90	19.10	0.118	26.30	116.60	0.877	144.65	60
4	4.20	15.20	0.127	26.10	90.30	0.870	143.55	60
3	4.10	11.00	0.124	24.60	64.20	0.820	135.30	60
2	3.70	6.90	0.112	21.70	39.60	0.723	119.35	60
1	3.20	3.20	0.640	17.90	17.90	0.542	98.45	66

Table 64. Stability coefficient calculations for Frame G (tranverse)

	Shear		Flexural		Total			
Story	**Interstory**	**Absolute**	**Interstory**	**Absolute**	**Interstory**	**Absolute**	**Vu**	**Pu**
15	9.71	352.34	0.21	2.032	9.91	354.37	1877.9	64930.0
14	19.89	342.63	0.20	1.827	20.09	344.46	3571.1	76455.8
13	25.12	322.75	0.20	1.623	25.32	324.37	5086.3	87981.7
12	24.58	297.63	0.19	1.424	24.77	299.05	6445.1	99507.6
11	22.73	273.05	0.18	1.234	22.91	274.28	7653.2	111033.5
10	21.94	250.32	0.17	1.055	22.11	251.37	8716.3	122559.4
9	21.76	228.38	0.16	0.887	21.91	229.26	9639.9	134085.2
8	21.90	206.62	0.14	0.731	22.04	207.35	10429.7	145611.1
7	22.39	184.72	0.13	0.589	22.52	185.31	11091.4	157137.0
6	23.01	162.33	0.12	0.459	23.13	162.79	11621.4	168662.9
5	23.44	139.32	0.10	0.344	23.54	139.66	12038.0	180188.8
4	23.71	115.88	0.08	0.244	23.79	116.12	12339.8	191714.6
3	23.84	92.17	0.07	0.160	23.90	92.33	12550.7	203240.5
2	40.14	68.33	0.05	0.093	40.18	68.43	12676.1	214766.4
1	28.20	28.20	0.04	0.045	28.24	28.24	12739.0	230522.2

Table 65. Stability coefficient calculation for Frame G (longitudinal)

	Shear		Flexural		Total		Vu	Pu
Story	**Interstory**	**Absolute**	**Interstory**	**Absolute**	**Interstory**	**Absolute**		
15	10.87	328.12	0.34	3.386	11.21	331.51	1138.1	64930.0
14	18.41	317.25	0.34	3.045	18.75	320.30	2164.3	76455.8
13	23.26	298.84	0.33	2.706	23.59	301.55	3082.6	87981.7
12	22.76	275.58	0.32	2.374	23.07	277.96	3906.1	99507.6
11	21.05	252.82	0.30	2.057	21.35	254.88	4638.3	111033.5

10	20.32	231.78	0.28	1.758	20.60	233.53	5282.6	122559.4
9	20.15	211.46	0.26	1.478	20.41	212.94	5842.4	134085.2
8	20.27	191.31	0.24	1.219	20.51	192.53	6321.0	145611.1
7	20.73	171.04	0.22	0.981	20.95	172.02	6722.1	157137.0
6	21.31	150.31	0.19	0.766	21.50	151.07	7043.2	168662.9
5	21.70	129.00	0.17	0.573	21.87	129.57	7295.7	180188.8
4	21.95	107.30	0.14	0.406	22.09	107.70	7478.7	191714.6
3	22.07	85.34	0.11	0.266	22.18	85.61	7606.5	203240.5
2	37.16	63.27	0.08	0.156	37.24	63.43	7682.5	214766.4
1	26.11	26.11	0.07	0.074	26.18	26.18	7720.6	230522.2

References

APPLIED TECHNOLOGY COUNCIL, Hortacsu, A., Moresco, J., Molina Hutt, C., Kakoty, P., Hulsey, A. M., Eksir Monfared, A., Rattie, M., Yen, W.-Y., Haley, M. X., Walton, W., Hooper, J. D., Bonowitz, D., Deierlein, G., Vahdani, S., Kelly, N., Carroll, M. E., How, K., Hui, T., . . . Heintz, J. (2018). *San Francisco Tall Buildings study*.

ACI. (2022). *Building Code Requirements for Structural Concrete (ACI 318-22).* American Concrete Institute. https://www.concrete.org/store/productdetail.aspx?ItemID=31822

Applied Technology Council, Hortacsu, A., Moresco, J., Molina Hutt, C., Kakoty, P., Hulsey, A. M., Eksir Monfared, A., Rattie, M., Yen, W.-Y., Haley, M. X., Walton, W., Hooper, J. D., Bonowitz, D., Deierlein, G., Vahdani, S., Kelly, N., Carroll, M. E., How, K., Hui, T., … Heintz, J. (2018).

ASCE. (2016). *Minimum Design Loads and Associated Criteria for Buildings and Other Structures (ASCE/SEI 7-16).* American Society of Civil Engineers. https://ascelibrary.org/doi/book/10.1061/9780784414248

Bassioni, H., Mostafa, T. M., Estaitieh, M. A., & Arab Academy for Science, Technology and Maritime Transport. (2024). The appropriate pile diameter and penetration distance through the bearing layer corresponding to minimum cost of piled foundations. In 9th International Conference on The Role Of Engineering Towards A Better Environment.

Das, B. M., & Sivakugan, N. (2019). Principles of foundation engineering (9th ed.). Cengage Learning.

Fine Software. (n.d.). GEO5 – Geotechnical Software Package. https://www.finesoftware.eu/

GeoPentech. (2024). Geotechnical report on chloride levels and pH of the soil for the South Park Hotel project.

Geocon West, Inc. (2017). Geotechnical investigation: Proposed high-rise development "Olympic and Hill," 1000-1034 Hill Street and 220 & 226 West Olympic Boulevard, Los Angeles, California. Prepared for Onni Contracting (California) Inc. https://www.geoconinc.com/

Kovačević, N., Stojiljković, A., & Kovač, M. (2019). Application of the matrix approach in risk assessment. Operational Research in Engineering Sciences: Theory and Applications, 2(3), 55–64. https://doi.org/10.31181/oresta1903055k

LEED (U.S. Green Building Council). (n.d.). Leadership in Energy and Environmental Design. https://www.usgbc.org/leed

Life365. (n.d.). Service life modeling software for concrete durability. https://www.life365co.com/

Martin, G. R., Lew, M., Arulmoli, K., Baez, J. I., Blake, T. F., Earnest, J., Gharib, F., Goldhammer, J., Hsu, D., Kupferman, S., O'Tousa, J., Real, C. R., Reeder, W., Simantob, E., Youd, T. L., Southern California Earthquake Center, & University of Southern California. (1999). Recommended procedures for implementation of DMG Special Publication 117 guidelines for analyzing and mitigating liquefaction hazards in

California. Southern California Earthquake Center. http://scecinfo.usc.edu/resources/catalog/LiquefactionproceduresJun99.pdf

Plaxis. (n.d.). Plaxis 3D – 3D Geotechnical Finite Element Software. Bentley Systems. https://www.plaxis.com/

Sharp, R. (2024). Urban architecture integration and redevelopment in Downtown LA.

U.S. Department of Commerce. (2024). Los Angeles Climate Summary 2024. National Weather Service. https://www.weather.gov/

U.S. Geological Survey. (2020, January 16). What is liquefaction?. https://www.usgs.gov/faqs/what-liquefaction

Western Regional Climate Center. (2024). Climate data summary: Downtown Los Angeles station. https://wrcc.dri.edu/